Austrian Journal of Technical and Natural Sciences

№ 5–6 2016
May–June

«East West» Association for Advanced Studies and Higher Education GmbH

Vienna
2016

Austrian Journal of Technical and Natural Sciences

Scientific journal

№ 5–6 2016 (May–June)

ISSN 2310-5607

Editorial office European Science Review
"East West" Association for Advanced Studies
and Higher Education GmbH, Am Gestade 1
1010 Vienna, Austria

Email: info@ew-a.org

Homepage: www.ew-a.org

Austrian Journal of Technical and Natural Sciences is an international, German/English/Russian language, peer-reviewed journal. It is published bimonthly with circulation of 1000 copies.

The decisive criterion for accepting a manuscript for publication is scientific quality. All research articles published in this journal have undergone a rigorous peer review. Based on initial screening by the editors, each paper is anonymized and reviewed by at least two anonymous referees. Recommending the articles for publishing, the reviewers confirm that in their opinion the submitted article contains important or new scientific results.

East West Association GmbH is not responsible for the stylistic content of the article. The responsibility for the stylistic content lies on an author of an article.

Instructions for authors

Full instructions for manuscript preparation and submission can be found through the "East West" Association GmbH home page at: http://www.ew-a.org.

Material disclaimer

The opinions expressed in the conference proceedings do not necessarily reflect those of the «East West» Association for Advanced Studies and Higher Education GmbH, the editor, the editorial board, or the organization to which the authors are affiliated.

East West Association GmbH is not responsible for the stylistic content of the article. The responsibility for the stylistic content lies on an author of an article.

Typeset in Berling by Ziegler Buchdruckerei, Linz, Austria.
Printed by «East West» Association for Advanced Studies and Higher Education GmbH, Vienna, Austria on acid-free paper.

Section 1. Mathematics

Drushinin Victor Vladimirovich
Holushkin Vladimir Semenovich
National research nuclear University "MEPHI"
Sarov physical-technical Institute
E mail: vvdr@newmail.ru

Cubic the Fermat's amounts

Abstract: The formulas for the sum of three or four natural numbers in the third degree, which equal to the number in a cube, are a generalization of the classical sum of the Fermat. Such calculated amounts received for four and five numbers not exceeding "100". The application are in the examples.

Keywords*:* Fermat's last theorem, sums of cubes of integers.

Under the amount of Fermat we understand this constriction

$$F(n,m)=\sum_{k=1}^{m}\beta_k a_k^n. \qquad (1)$$

In (1) β_k integers and a_k and n a natural numbers. The name " Fermat " dates back to the famous (great) the Fermat's last theorem $a^n+b^n\neq c^n$, if $n>2$. This theorem is proved in 1995 by Wiles [1]. The question arises which properties are more complicated in that amounts of Fermat? It has a number of outstanding tasks. For example, Euler assumed that it is always inequality $a^4+b^4+c^4\neq d^4$, which was analytically proved in 1951 [2]. However, in 1988 it was discovered numeric equality [3]

$$2682440^4+15365639^4+18796760^4=20615673^4, \qquad (2)$$

refuting the hypothesis of Euler and the proof of 1951. In 1994, it was discovered another four quartets Fermat

$$95800^4+217519^4+414560^4=422481^4. \qquad (3)$$

In [4] that this equality is called the sensation without reference to the equation above and the previously obtained.

In this paper, we analyze the Fermat's amount type ($m\geq 3$)

$$\sum_{k=1}^{m}a_k^3=a_1^3+a_2^3+a_3^3+\ldots a_m^3=b^3. \qquad (4)$$

The analysis of these equations allows, for example, to solve the problem of a complete filling of the vessel the cubic form cubic capacities smaller volumes. There is also such a problem. Let the set of objects is quantized by distance, all objects have a cubic shape and fill the volume void. What is the highest construction will arise in such a world? There are also non-linear Diophantine equations of the form (4) and the problem of their solution.

When solving equation (4) we proceed with the generalization of the small Fermat's theorem described Druzhinin [5, 6]. From this theorem there is equality

$$n^3=C_n\cdot 7+\delta_n, \qquad (5)$$

where $\delta_n=\pm 1$, if $(n\perp 7)$ — mutual simplicity numbers, $\delta_n=0$ if $(n\vdots 7)$. Sign δ_n is given by $\delta_n=\left(sign(\mu)\right)\left(3|\mu|-\mu^2-1\right)$. Here μ is the deduction comparison $n\equiv\mu(mod\,7)$ from the full set of the smallest module of deductions. This means that $\mu=\{-3;-2;-1;0;1;2;3\}$. For example, $18\equiv(-3)(mod\,7)$, i. e. $\delta_n=1$. Do, $18^3=833\cdot 7+1$. For C_n calculation we obtained the recurrence relation $C_n=C_{n-1}+A_{n-2}$, where $A_m=\sum_{k=0}^{m}a_k$. $m=7s+r,$. s takes all integers non-negative values, a r — the remainder when m divided by "7". For example, $a_0=1,\quad a_1=a_2=2, a_3=a_4=4, a_5=5;$ $3^3=27=4\cdot 7-1;\ 4^3=64=9\cdot 7+1$; $A_2=5;9=4+5.$ These formulas allow you to quickly calculate the internal structure of the cube of an integer (5).

Knowledge of deductions δ_n and private C_n in (5) allows us to formulate a necessary and sufficient condition of equality of the sum of the Fermat (4).

$$\sum_{k=1}^{m}\delta_k=\delta_b; C_b=\sum_{k=1}^{m}C_k. \qquad (6)$$

From (6) immediately implies Fermat's last theorem for a,b,c is not a multiple of "7". As $\delta_n=\pm 1$, then three of these numbers to zero is impossible. Search numbers satisfying (4) is conducted according to the equations (6), after which there are a specific number. We received a huge number of equations (4) with different m.

Table 1. – Sets of numbers, giving the equality $a^3+b^3+c^3=d^3$

a	b	c	d	a	b	c	d	a	b	c	d	a	b	c	d
1	6	8	9	12	19	53	54	21	43	84	88	31	33	72	76
2	17	40	41	14	23	70	71	22	51	54	67	32	54	85	93
3	4	5	6	15	42	49	58	25	31	86	88	34	39	63	72
3	10	18	19	16	23	41	44	25	38	87	90	36	38	61	69
3	36	37	46	17	40	86	89	25	48	74	81	38	43	66	75
4	17	22	25	18	19	21	28	26	55	78	87	38	48	79	87
7	14	17	20	19	53	90	96	27	30	37	46	45	69	79	97
7	54	57	70	19	60	69	82	28	53	75	84	50	61	64	85
11	15	27	29	20	54	79	87	29	34	44	53	58	59	69	90

When $m=3$ and the numbers $\{a;b;c;d\}$ is not in excess of "100" in the block form are relatively simplicity to "36" sets $a^3+b^3+c^3=d^3$ (see table. № 1).

Single formula the receipt of such amounts, the same amounts to the square of Fermat [7], we have not found, but for some cases are the formula. For example, if $d=c+1$, then $a^3+b^3=3c(c+1)+1$. Indeed, the first line of the table. №. 1 gives $217=3\cdot 8\cdot 9+1$. From the bundles tab. №. 1 you can create a new equality multiplying them by any n^3, and a longer numeric design, if instead of d^3 and substitute four numbers, where $d=90$ is the first number. For example, $a^3+b^3+c^3+d^3=e^3$ or $4^3+17^3+22^3+48^3+74^3=81^3$. If d^3 in the bundles are the same, there is, for example, at $d=90$ equality $25^3+38^3+87^3-58^3-59^3-69^3=0$. The same applies to $d=87$, there are three ligaments.

Cubic Fermat's sums of five numbers of the form $a^3+b^3+c^3+d^3=e^3$ in the block are mutually simplicity and numbers not exceeding "100" we found 189. In table. № 2 shows the first 30 ligaments.

Table 2. – Sets of numbers giving the equality $a^3+b^3+c^3+d^3=e^3$

a	b	c	d	e	a	b	c	d	e	a	b	c	d	e
1	5	7	12	13	2	15	27	61	63	3	18	29	70	72
1	10	15	26	28	2	24	67	76	91	3	22	42	60	67
2	3	8	13	14	2	34	57	63	78	3	28	35	57	63
2	4	13	27	28	2	35	52	69	80	3	30	45	78	84
2	5	37	91	93	2	41	42	79	86	3	32	34	88	91
2	7	16	38	39	3	5	28	32	38	3	35	36	39	53
2	7	44	73	78	3	14	15	31	33	4	5	29	63	65
2	10	14	24	26	3	15	17	21	26	4	7	8	17	18
2	13	33	43	49	3	16	63	87	97	4	7	41	74	78
2	13	60	62	77	3	18	26	37	42	4	12	15	41	42

Table. № 2 extends more cubic long amounts of Fermat. For example, taking $e=28$ from the table. № 2 and $a=28$ from the table № 1, we learn the same amount of Fermat $2^3+4^3+13^3+27^3+53^3+75^3=84^3$.

Here for example are two problems to be solved using the amounts of Farm. 1. There are four plasticize balls with radius $\{3;5;28;32\}$ and $\{4;7;15;18\}$. You can blind from them the ball with a integer radius? Answers: "yes" and "no". 2. There is the linear homogeneous differential equations

$$\frac{\partial^3\varphi}{\partial x^3}+\frac{\partial^3\varphi}{\partial y^3}+\frac{\partial^3\varphi}{\partial z^3}+\frac{\partial^3\varphi}{\partial u^3}=0.$$

Need to find the quotient of a non-trivial solution with integer coefficients in the exponents. Looking for a solution in the form $\varphi(x,y,z,u)=exp(ax+by+cz-du)$. This approach gives the characteristic equation of the form $a^3+b^3+c^3=d^3$ and any set of numbers from the table. № 1.

References:

1. Wails A. Annals of Mathematics. 141 (1995) P. 443–551.
2. Serpinski V. The solution of equations in integers. FML. M. 1961, P. 60.
3. Alvarez L. F. A. Fermat, M., De Agostini, M. 2015, P. 52.
4. Graham R., Knuth D., Patashnik O. Concrete mathematics, M. Mir, 1998, P. 155.

5. Drushinin V. V., Lazarev A. A. Austrian Journal of Technical and Natural Science, No. 9–10, 18–20, 2015.
6. Drushinin V. V. NTVP, N. 5, 28–29, 2015.
7. Drushinin V. V. NTVP, N. 1, 19–24, 2013.

Section 2. Machinery construction

Vasenin Valery Ivanovich,
Perm National Research Polytechnic University,
associate professor, candidate of technical sciences,
department "Materials, technologies and design of machinary"
E-mail: vaseninvaleriy@mail.ru

Investigation of the work of the gating system with two sprues

Abstract: The results of theoretical and experimental study of gating system with two sprues are given. This is part of ring-shaped system with four sprues. When there is odd number of feeders in every half of the system, the filling of only one half of form with metal is calculated. When there is even number of feeders in every half of the system, the filling of only quarter of form with metal is calculated. The time of form filling with metal equals the filling time for half or quarter of form correspondingly. The sprues work independently, these are separate hydraulic systems. For the purposes of calculation zero point position is specified, calculation by successive approximation method is performed and zero point position is changed when required. A good agreement between the calculated and the experimental data is obtained.

Keywords: pouring basin, sprue, collector, feeder, pressure head, zero point, resistance coefficient, mass-flow coefficient, flow rate, fluid consumption.

Introduction

L-shaped, branched, combined, cross-gate, step-gate, ring-shaped (horizontal and vertical) gating systems (GS) have been studied previously, including *L*-shaped system with variable cross-section collector. The difference between the calculated and the experimental values of flow rates and consumption amounted 1–6%, although the Bernoulli's equation (BE) for the variable consumption (mass) fluid flow was used. This equation is derived for the **particular** case — for the constant consumption (mass) fluid flow where there is no fluid dispensing on feeders [1, P. 205; 2, P. 10], i. e. the equation is derived for the gating system with one feeder. It follows that the Bernoulli's equation works with the variable consumption flow but it is difficult to explain why the equation works. And the possibility of usage of BE for GS calculations when consumption in the collector (skim gate) changes from maximum to zero *is not proven theoretically*. Only one sprue is used in all the GS mentioned above. But a few sprues are also used in gating systems. As we know, these systems have not been subjected to calculations. The present article deals with theoretical and experimental study of such systems.

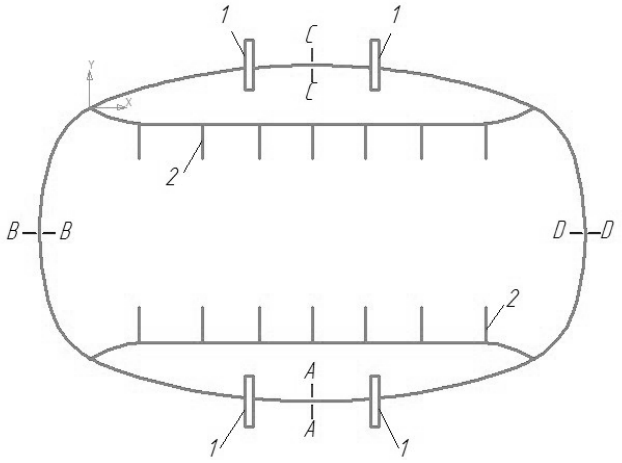

Fig. 1. The diagram of the ring-shaped gating system with four sprues: 1 — sprue, 2 — feeder

Ring-shaped GSs with four sprues (fig. 1) are widely used in industry for example for magnesium alloys casting. There is common pouring basin over sprues. Fluid flow rate in the basin can be taken as 0. It seems that it is impossible to make calculations for such GS. But in the cross sections *A–A*, *B–B*, *D–D* and *C–C* of the collector there is no movement of metal. It means that filling of only half of the form is calculated, the second half is filled within the same time. The time for filling of the whole form with liquid metal equals the time for filling of the half of the form.

When there is even number of feeders for every half, for example 6, it is allowed to calculate filling with metal of only ¼ of the molding. It is standard *L*-shaped GS which is well studied both theoretically and experimentally. And the time for filling of the whole form with liquid metal equals the time for filling of the quarter of molding, because all sprues work independently. That is why it is quite interesting to perform calculation and experiment with ring-shaped GS having odd number of feeders — in industry they use 7 feeders for every half of the form. It is incomprehensible for explanation but it seems that this fact has been established in practice.

Studying procedure

Operation of the half of the ring-shaped GS shown in fig. 1 is studied in the present work. Calculation consists in determination of fluid flow rates and consumption in GS with 7 feeders fed with fluid from two sides. The collector can be "unbent" and this fact will not reflect on the calculation procedure, just pressure head losses related to friction will be reduced along the length and in local resistances but calculations and experiments will be more accurate. The system (fig. 2) consists of 2 pouring basins, 2 sprues, collector and 7 feeders. Fluid level *H* is the vertical distance from the cross sections *1–1* and *15–15* in pouring basins to horizontal axis of collectors. This level has been held constant due to continuous addition of water to the basins and discharge of excessive water through special gaps in the basins: $H = 0.361$ m. Fluid is poured out the feeders to buckets. There are piezometers — glass tubes 400 mm in length and with internal diameter of 4.5 mm, in the collector cross sections *5–5,.., 12–12*. Time of fluid discharge from every feeder amounted 35–75 s — depending on the number of simultaneously operating feeders, and volume of the discharged water was approximately 8 l. These limitations on time and weight have provided deviations from the average flow rate ± 0.005 m/s maximum. Fluid consumption from every feeder has been determined minimum 6 times.

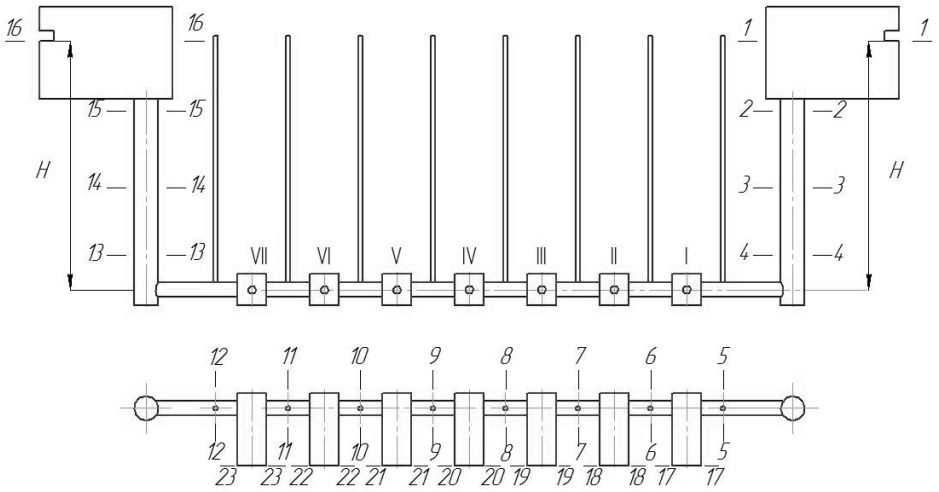

Fig. 2. Gating system with two sprues

Body

First we shall calculate the GS characteristics when only one feeder I is operating when hydraulic system is opened in the cross section *6–6*. The Bernoulli's equation (BE) for the sections *1–1* and *17–17* of GS shall be compiled:

$$\frac{p_1}{\gamma} + \alpha \frac{v_1^2}{2g} + H = \frac{p_{17}}{\gamma} + \alpha \frac{v_{17}^2}{2g} + h_{1-17}, \qquad (1)$$

where p_1 and p_{17} — pressure in the cross sections *1–1* and *17–17*, N/m² (equals atmospheric pressure: $p_1 = p_{17} = p_a$); α — coefficient of the flow rate distribution irregularity along the flow cross section (Coriolis coefficient); is taken as $\alpha = 1.1$ [1, P. 108]; g — gravity acceleration; $g = 9.81$ m/s²; v_1 and v_{17} — metal velocities in the cross sections *1–1* and *17–17*, m/s (due to big difference of the area of the basin S_1 in the cross section *1–1* and the feeder S_n in the cross section *17–17* can be taken as $v_1 = 0$); γ — liquid metal density, N/m³; h_{1-17} — pressure head losses when fluid goes from the cross section *1–1* to the cross section *17–17*, m. These pressure head losses is

$$h_{1-17} = \left(\zeta_{cm} + \lambda\frac{l_{cm}}{d_{cm}}\right)\alpha\frac{v_3^2}{2g} + \left(\zeta_{\kappa} + \lambda\frac{l_0}{d_{\kappa}}\right)\alpha\frac{v_5^2}{2g} + \left(\zeta_n + \lambda\frac{l_n}{d_n}\right)\alpha\frac{v_{17}^2}{2g}, \quad (2)$$

where ζ_{cm}, ζ_{κ} and ζ_n — coefficient of local resistances for metal entering from the basin to the sprue, turning from the sprue to the collector and turning from the collector to the feeder I; v_3 and v_5 — fluid flow rates in the section *3–3* of the sprue and in the cross section *5–5* of the collector, m/s; l_{cm} — the sprue length (height), m; d_{cm}, d_{κ} and d_n — hydraulic diameters of the sprue, collector and feeder I, m; λ — friction losses coefficient; l_0 — the distance from the sprue to the feeder I, m; l_n — length of the feeder, m. Consumption in GS when top discharge is used is determined by metal velocity v_{17} in exit cross section *17–17* of the feeder I and its cross section area S_n:

$$Q_{17} = v_{17}S_n. \quad (3)$$

Remaining fluid flow rates in GS channels are determined by the flow continuity equation:

$$Q_{17} = v_3S_{cm} = v_5S_{\kappa} = v_{17}S_n, \quad (4)$$

where S_{cm} and S_{κ} — cross section areas of the sprue and the collector, m^2. All metal velocities (2) can be expressed via v_{17}, using the flow continuity equation (4):

$$h_{1-17(17)} = \alpha\frac{v_{17}^2}{2g}\left[\left(\zeta_{cm} + \lambda\frac{l_{cm}}{d_{cm}}\right)\left(\frac{S_n}{S_{cm}}\right)^2 + \left(\zeta_{\kappa} + \lambda\frac{l_0}{d_{\kappa}}\right)\left(\frac{S_n}{S_{\kappa}}\right)^2 + \zeta_n + \lambda\frac{l_n}{d_n}\right]. \quad (5)$$

The expression in square brackets can be defined as $\zeta_{1-17(17)}$ — the coefficient of the system resistance from the cross section *1–1* to the cross section *17–17*, reduced to fluid flow rate in this section:

$$\zeta_{1-17(17)} = \left(\zeta_{cm} + \lambda\frac{l_{cm}}{d_{cm}}\right)\left(\frac{S_n}{S_{cm}}\right)^2 + \left(\zeta_{\kappa} + \lambda\frac{l_0}{d_{\kappa}}\right)\left(\frac{S_n}{S_{\kappa}}\right)^2 + \zeta_n + \lambda\frac{l_n}{d_n}. \quad (6)$$

Then (1) can be written down the following way:

$$H = \alpha v_{17}^2(1 + \zeta_{1-17(17)})/2g. \quad (7)$$

And coefficient of the system consumption from the cross section *1–1* to the cross section *17–17*, reduced to the flow rate v_{17},

$$\mu_{1-17(17)} = \left(1 + \zeta_{1-17(17)}\right)^{-1/2}. \quad (8)$$

Flow rate

$$v_{17} = \mu_{1-17(17)}\sqrt{2gH/\alpha}. \quad (9)$$

The consumption Q_{17} can be determined by the expression (3). For this GS the sprue length (height) $l_{cm} = 0.2675$ m, the length of each feeder $l_n = 0.0495$ m, the distance between feeders $l = 0.1190$ m, the distance from the sprue to the first feeder $l_0 = 0.1220$ m. Diameters of feeders, collector and sprues: $d_n = 0.00903$ m, $d_{\kappa} = d_5 = ... = d_{12} = 0.01603$ m, $d_{cm} = d_3 = d_{14} = 0.02408$ m. Let us take coefficient of friction losses $\lambda = 0.03$, as in the works [3; 4]. Coefficient of local resistance for entering from the basin to the sprue, depending on rounding radius of the leading edge can be determined from the reference book [5, P. 126]: $\zeta_{cm} = 0.12$. Coefficient of local resistance for turning from the sprue to the collector by 90° and change of the flow cross section area $\zeta_{\kappa} = 0.396$ [6]. Coefficient of local resistance for turning from the collector to the feeder by 90° (with change of cross section areas) $\zeta_n = 0.334$ [6]. The results of calculations by ratios (6), (8), (9) and (3): $\zeta_{1-17(17)} = 0.570283$, $\mu_{1-17(17)} = 0.798015$, $v_{17} = 2.02496$ m/s, $Q_{17} = 129.683044 \cdot 10^{-6}$ m^3/s.

When both sprues are used fluid goes to the feeder I from the left from the cross section *6–6* and from the right from the cross section *5–5*, from parallel pipelines. BE for the cross sections *1–1* and *17–17* has already been written down — it is the expression (1). BE for the cross sections *16–16* and *17–17*:

$$\frac{p_{16}}{\gamma} + \alpha\frac{v_{16}^2}{2g} + H = \frac{p_{17}}{\gamma} + \alpha\frac{v_{17}^2}{2g} + h_{1-17}. \quad (10)$$

$p_{16} = p_1 = p_{17} = p_a$, $v_{16} = v_1 = 0$. Pressure head losses when fluid goes from the cross section *16–16* to the cross section *17–17*

$$h_{16-17} = \left(\zeta_{cm} + \lambda\frac{l_{cm}}{d_{cm}}\right)\alpha\frac{v_{14}^2}{2g} + \left(\zeta_{\kappa} + \lambda\frac{l_0 + 6l}{d_{\kappa}}\right)\alpha\frac{v_{12}^2}{2g} + \left(\zeta_n + \lambda\frac{l_n}{d_n}\right)\alpha\frac{v_{17}^2}{2g}. \quad (11)$$

The left parts of the equations (2) and (11) are equal. Let us set equal their right parts and after conversion we obtain the following: $v_5 = 1.695061v_{12}$, $v_{12} = 0.589949v_5$.

Flow rate in the section *17–17* of the feeder I $Q_{17} = v_{17}S_n = (v_5 + v_{12})S_n = (v_5 + 0.589949v_5)S_n = 1.589949v_5S_{\kappa}$, and $v_5 = v_{17}S_n / 1.589949S_{\kappa}$. The same way we determine that $v_{12} = v_{17}S_n / 2.695061S_{\kappa}$.

When we substitute these ratios between v_5 and v_{12} into the equations (2) and (11) and, keeping in view that $v_3 = v_5S_{\kappa} / S_{cm}$, and $v_{14} = v_{12}S_{\kappa} / S_{cm}$, we determine that $\zeta_{1-17(17)} = \zeta_{16-17(17)} = 0.526867$ — which is to be expected, because these are parallel pipelines. The results of calculations and experiments (in denominator) — are given in the table 1.

For operation of the feeder IV $v_5 = v_{12}$, $v_5 = v_{17}S_n / 2S_{\kappa}$, a $v_{12} = v_{17}S_n / 2S_{\kappa}$.

Table 1. – GS performance indicators with two sprues and one feeder

Indicators	Operating feeders			
	I*	I	IV**	IV
ζ	0.570	0.527	0.638	0.533
μ	0.798	0.809	0.781	0.808
v	2.024 / 2.10	2.054 / 2.12	1.983 / 1.97	2.049 / 2.13
Q	129.68 / 134.49	131.51 / 135.77	126.99 / 126.16	131.24 / 136.41

* *The system is opened in the cross section 6–6*

** *The system is opened in the cross section 9–9*

Let us consider operation of the system consisting of two feeders, I and II. It is clear that in one of the feeders there shall be the point of flows junction (or watershed point, or zero point). Fluid to this point shall go from two sides. It seems that in the system consisting of two feeders zero point is located in the feeder II. Pressure head losses from the cross section *16–16* to the cross section *18–18:*

$$h_{16-18} = \left(\zeta_{cm} + \lambda\frac{l_{cm}}{d_{cm}}\right)\alpha\frac{v_{14}^2}{2g} + \\ + \left(\zeta_{\kappa} + \lambda\frac{l_0 + 5l}{d_{\kappa}}\right)\alpha\frac{v_{12}^2}{2g} + \left(\zeta_n + \lambda\frac{l_n}{d_n}\right)\alpha\frac{v_{18}^2}{2g}, \quad (12)$$

Pressure head losses from the cross section *1–1* to the cross section *18–18*

$$h_{1-18} = \left(\zeta_{cm} + \lambda\frac{l_{cm}}{d_{cm}}\right)\alpha\frac{v_3^2}{2g} + \left(\zeta_{\kappa} + \lambda\frac{l_0}{d_{\kappa}}\right)\alpha\frac{v_5^2}{2g} + \\ + \left(\zeta_6 + \lambda\frac{l}{d_{\kappa}}\right)\alpha\frac{v_6^2}{2g} + \left(\zeta_n + \lambda\frac{l_n}{d_n}\right)\alpha\frac{v_{18}^2}{2g}, \quad (13)$$

Pressure head losses from the cross section *1–1* to the cross section *17–17*

$$h_{1-17} = \left(\zeta_{cm} + \lambda\frac{l_{cm}}{d_{cm}}\right)\alpha\frac{v_3^2}{2g} + \\ + \left(\zeta_{\kappa} + \lambda\frac{l_0}{d_{\kappa}}\right)\alpha\frac{v_5^2}{2g} + \left(\zeta_{17} + \lambda\frac{l_n}{d_n}\right)\alpha\frac{v_{17}^2}{2g}. \quad (14)$$

In the equations (13) and (14) ζ_6 is the resistance coefficient for fluid passage from the cross section *5–5* to the cross section *6–6* when the part of the flow is branched out the collector to the feeder I; ζ_{17} — is the resistance coefficient for branching out of the part of the flow from the collector to the feeder I with the exit cross section *17–17*. Resistance coefficients related to the flow separation from the collector to the feeder will be calculated by the equations for T-pipes [2, 112–115]. The resistance coefficient for passage in the collector when the part of the flow is branched out the collector to the feeder

$$\zeta_{np} = 0{,}4\left(1 - v_{np}/v_{\kappa}\right)^2 / \left(v_{np}/v_{\kappa}\right)^2, \quad (15)$$

and the resistance coefficient for branching out of the part of the flow to the feeder

$$\zeta_{отв} = \left[1 + \tau\left(v_n/v_{\kappa}\right)^2\right] / \left(v_n/v_{\kappa}\right)^2, \quad (16)$$

where v_{κ} and v_{np} are metal velocities in the collector before and after branching out of the part of the flow to the feeder, m/s; v_n — fluid flow rate in the feeder, m/s; τ — coefficient. In our case when $S_n / S_{\kappa} = 0.317$ then $\tau = 0.15$ [7]. The obtained coefficient ζ_{np} is reduced to the flow rate of the passing flow v_{np}, and $\zeta_{отв}$ — to the flow rate in the feeder v_n.

The value of the part of the flow separated to the feeder I from the cross section *5–5* is unknown. Let's take the following definitions: $v_{6/5} = v_6 / v_5$. $Q_6 = v_{6/5} \cdot Q_5$. Consumption in the feeder I $Q_{17} = v_{17}S_n = \\ = \left(1 - v_{6/5}\right)Q_5 = \left(1 - v_{6/5}\right)v_5 S_{\kappa}$, and $v_{17}/v_5 = \\ = \left(1 - v_{6/5}\right)S_{\kappa}/S_n$ — is the ratio v_n / v_{κ} in the equation (16). Let us assume that $v_{6/5} = 0{,}5$. Based on the ration (15) we may find that $\zeta_6 = 0.4$; when $v_{6/5} = 0.5$ $v_{17}/v_5 = 1.575657$, and $\zeta_{17} = 0.552788$ — by the expression (16).

It is obvious that $v_3 = v_5 S_{\kappa}/S_{cm}$, $v_6 = v_{6/5} \cdot v_5$, $v_{14} = v_{12}S_{\kappa}/S_{cm}$. The left parts of the equations (12) and (13) are equal. Let us set equal their right parts and after conversion we obtain the following: $v_6 = 0.724955 v_{12}$, $v_{12} = 1.379396 v_6$.

Consumption in the cross section *18–18* of the feeder II $Q_{18} = v_{18}S_n = \left(v_6 + v_{12}\right)S_{\kappa} = \left(v_6 + 1{,}379396 v_6\right)S_{\kappa} = \\ = 2{,}379396 v_6 S_{\kappa}$, a $v_6 = v_{18}S_n / 2{,}379396 S_{\kappa}$.

The same way we find that $v_{12} = v_{18}S_n / 1.724955 S_{\kappa}$.

When we substitute these ratios to the equations (12) and (13), we determine that $\zeta_{1-18(18)} = \zeta_{16-18(18)} = 0.569278$. $\mu_{1-18(18)} = 0.800570$, $v_{18} = 2.031448$ m/s, $Q_{18} = 130.098141 \cdot 10^{-6}$ m³/s.

Fluid consumption in the feeder I $Q_{17} = v_{17}S_n = (1-v_{6/5})v_5 S_к = (1-v_{6/5})v_3 S_{cm}$. It follows that: $v_3 = v_{17}S_n / (1-v_{6/5})S_{cm}$, $v_5 = v_{17}S_n / (1-v_{6/5})S_к$. When we substitute these ratios to the equations (14), (8), (9) and (3), we determine: $\zeta_{1-17(17)} = 1.004563$, $\mu_{1-17(17)} = 0.706301$, $v_{17} = 1.792242$ m/s, $Q_{17} = 114.778868 \cdot 10^{-6}$ m^3/s.

$Q_6 = v_{18}S_n / 2.379396 = 54.676977 \cdot 10^{-6}$ m^3/s. The ratio $v_{6/5} = Q_6 / Q_5 = Q_6 / (Q_6 + Q_{17}) = 0.322622$. We have set $v_{6/5} = 0.5$. Let's take $v_{6/5} = 0.322622$, we perform calculations again and we obtain $v_{6/5} = 0.244003$. By means of the similar approximations with the specified ratio $v_{6/5} = 0.10917352$ we obtain $v_{6/5} = 0.109173519$. Thereon calculation of the ratio v_6 / v_5 can be finished, as the obtained value differs from the set value only by 0.000000001. Let's take $v_{6/5} = 0.10917352$. The results of calculations and experiments are given in the table 2.

For the purposes of calculation of the feeders I and IV performance it is required to substitute $\left(\zeta_к + \lambda\frac{l_0+5l}{d_к}\right)\alpha\frac{v_{12}^2}{2g}$ with $\left(\zeta_к + \lambda\frac{l_0+3l}{d_к}\right)\alpha\frac{v_{12}^2}{2g}$ in the equation (12). From calculation we obtain $v_{6/5} = 0{,}038084$. It means that from the cross section *5–5* to the cross section *6–6* to the feeder IV goes only 3.8% of fluid. For the feeders I and II this value amounted 10.9%. It is likely to be true, as the feeder II has been located closer to the feeder I, than the feeder IV.

Operation of the feeders I and VII $v_{17} = v_{23} = 2.024$ m/s — as well as operation of the feeder I in the open cross section 6–6 in the gating system. Left and right parts of the system work independently and flow rate of fluid in the section between the feeders I and VII equals zero.

For the system consisting of three feeders (I–III) let's assume that zero point is located in the feeder III. Pressure head losses will be the following:

$$h_{1-17} = \left(\zeta_{cm} + \lambda\frac{l_{cm}}{d_{cm}}\right)\alpha\frac{v_3^2}{2g} + \left(\zeta_к + \lambda\frac{l_0}{d_к}\right)\alpha\frac{v_5^2}{2g} + \left(\zeta_{17} + \lambda\frac{l_n}{d_n}\right)\alpha\frac{v_{17}^2}{2g}, \quad (17)$$

$$h_{1-18} = \left(\zeta_{cm} + \lambda\frac{l_{cm}}{d_{cm}}\right)\alpha\frac{v_3^2}{2g} + \left(\zeta_к + \lambda\frac{l_0}{d_к}\right)\alpha\frac{v_5^2}{2g} + \left(\zeta_6 + \lambda\frac{l}{d_к}\right)\alpha\frac{v_6^2}{2g} + \left(\zeta_{18} + \lambda\frac{l_n}{d_n}\right)\alpha\frac{v_{18}^2}{2g}, \quad (18)$$

$$h_{1-19} = \left(\zeta_{cm} + \lambda\frac{l_{cm}}{d_{cm}}\right)\alpha\frac{v_3^2}{2g} + \left(\zeta_к + \lambda\frac{l_0}{d_к}\right)\alpha\frac{v_5^2}{2g} + \left(\zeta_6 + \lambda\frac{l}{d_к}\right)\alpha\frac{v_6^2}{2g} + \left(\zeta_7 + \lambda\frac{l}{d_к}\right)\alpha\frac{v_7^2}{2g} + \left(\zeta_n + \lambda\frac{l_n}{d_n}\right)\alpha\frac{v_{19}^2}{2g}, \quad (19)$$

$$h_{16-19} = \left(\zeta_{cm} + \lambda\frac{l_{cm}}{d_{cm}}\right)\alpha\frac{v_{14}^2}{2g} + \left(\zeta_к + \lambda\frac{l_0+4l}{d_к}\right)\alpha\frac{v_{12}^2}{2g} + \left(\zeta_n + \lambda\frac{l_n}{d_n}\right)\alpha\frac{v_{19}^2}{2g}. \quad (20)$$

In addition to the value $v_{6/5} = v_6 / v_5$, one more unknown value $v_{7/6} = v_7 / v_6$ appears. Let us set $v_{6/5} = 0.5$, $v_{7/6} = 0.5$ and find that $v_7 = 0.332306v_{12}$, and $v_{12} = 3.009276v_7$ by the equations (19) and (20).

Consumption in the cross section *19–19* of the feeder III: $Q_{19} = v_{19}S_n = (v_7 + v_{12})S_n = (v_7 + 4{,}009276v_6)S_n = 4{,}009276v_7 S_к$, a $v_7 = v_{19}S_n / 4{,}009276S_к$.

The same way we find that $v_{12} = v_{19}S_n / 1.332306S_к$.

When we substitute these ratios into the equation (19), we obtain $\zeta_{1-19(19)} = 0.589455$. $\mu_{1-19(19)} = 0.793187$, $v_{19} = 2.012716$ m/s, $Q_{19} = 128.898526 \cdot 10^{-6}$ m^3/s.

Fluid consumption in the feeder I for $v_{6/5} = 0.5$ has been determined previously: $Q_{17} = 114.778868 \cdot \cdot 10^{-6}$ m^3/s.

Resistance coefficient for the feeder II can be found using the equation (18): $\zeta_{1-18(18)} = 2.117353$. $\mu_{1-18(18)} = 0.566379$, $v_{18} = 1.437188$ m/s, $Q_{18} = = 114.778868 \cdot$ m^3/s.

$Q_7 = v_{19}S_n / 4.009277 = 32.150074 \cdot 10^{-6}$ m^3/s. The ratio of the velocities will be the following: $v_{7/6} = Q_7 / Q_6 = Q_7 / (Q_7 + Q_{18}) = 0.258877$, $v_{6/5} = = Q_6 / Q_5 = (Q_7 + Q_{18}) / (Q_7 + Q_{18} + Q_{17}) = 0.519692$. We have set $v_{6/5} = v_{7/6} = 0{,}5$. Let's take $v_{6/5} = 0.519692$, $v_{7/6} = 0.258877$, we perform calculations again and we obtain: $v_{6/5} = 0.540024$, $v_{7/6} = 0.152973$. But subsequent calculations have shown that $v_{6/5} = 0.522040$, and $v_{7/6} = 7.45 \cdot 10^{-8}$, it means that water does not go from the cross section *6–6* to the cross section *7–7*. It is required to change zero point, in this system only the feeder II may be used for this purpose.

For calculations the equation (17) is used, in the equation (18) we substitute ζ_{18} with ζ_n. We have two equations for the feeders III and II:

$$h_{16-19} = \left(\zeta_{cm} + \lambda\frac{l_{cm}}{d_{cm}}\right)\alpha\frac{v_{14}^2}{2g} + \left(\zeta_к + \lambda\frac{l_0+4l}{d_к}\right)\alpha\frac{v_{12}^2}{2g} + \left(\zeta_{19} + \lambda\frac{l_n}{d_n}\right)\alpha\frac{v_{19}^2}{2g},$$

$$h_{16-18} = \left(\zeta_{cm} + \lambda\frac{l_{cm}}{d_{cm}}\right)\alpha\frac{v_{14}^2}{2g} + \left(\zeta_{к} + \lambda\frac{l_0 + 4l}{d_{к}}\right)\alpha\frac{v_{12}^2}{2g} +$$
$$+\left(\zeta_7 + \lambda\frac{l}{d_{к}}\right)\alpha\frac{v_7^2}{2g} + \left(\zeta_n + \lambda\frac{l_n}{d_n}\right)\alpha\frac{v_{18}^2}{2g}.$$

In addition to $\nu_{6/5} = \nu_6 / \nu_5$, instead of $\nu_{7/6}$ the value $\nu_{7/8}$ appears — fluid to the feeder II goes from the left and from the right. When we solve the system according to aforesaid we obtain: $\nu_{6/5} = 0.455519$, $\nu_{7/8} = 0.151874$.

For operation of the feeders I–IV and I–V zero point is located in the feeder III, for the feeders I–VI and I–VII — in the feeder IV. Note that the ratio $\nu_{6/5}$ increases from 0.109 to 0.757 when the number of operating feeders is increased from two to seven.

The results of calculations and experiments are given in the table 2.

The results of the studies and discussions

First, let us discuss concerning the feeder IV. It seems that as it consists of two sprues, fluid consumption will be greater than with one sprue. But calculations and experiments have demonstrated that the effect of this on fluid flow rate and consumption caused small changes: 1.983 and 2.049 m/s, by 3.2%. It is strange, because flow rates in every sprue and collector have reduced by 2 times and pressure head losses decreased by 4 times. It is likely that meet of two flows from the collectors 16.03 mm in diameter, their joining and turning by 90 degrees in the feeder 9.03 mm in diameter is energy-consuming process. The same situation is observed for the feeder I, flow rate increase is even smaller — only 1.4%. Note that according to the calculations flow rate (and fluid consumption) in the feeder I is slightly greater than in the feeder IV (located further from the sprues) — by 0.2%.

When only the feeder IV works increase of the number of sprues from 1 to 2 does not reflected on fluid flow rate and consumption. But when the number of feeders has increased the influence of the second sprue comes out. Consumption equals 650.22 cm^3/s when 7 feeders work in the system with two sprues and 377.68 cm^3/s in the system with one sprue [8]. It means that consumption has increased by 1.72 times — quite considerably. That is the influence of two sprues on GS operation.

It is impossible to identify location of zero point precisely when there are several feeders. We have to set its position and calculate it using successive approximation method. When required zero point position is changed.

In general we can conclude that a good agreement between the calculated and the experimental data is obtained. And the Bernoulli's equation derived for the particular case — for one feeder system — works also for the gating system with a few feeders even for the GS which is the most complex for GS calculations — ring-shaped with four sprues.

Conclusion

It is the first time when the gating system with 2 sprues being the part of the system with 4 sprues has been studied. When there is odd number of feeders in every half of the system, the filling of only one half of form with metal is calculated. The time for filling of the whole form with liquid metal equals the time for filling of the half of the form. When there is even number of feeders in every half of the system, the filling of only quarter of form with metal is calculated. The time of form filling with metal equals the filling time for half or quarter of form. The sprues work independently; these are separate hydraulic systems. Taking into consideration the data obtained in the process of studying of L-shaped, branched, combined, cross-gate, step-gate, ring-shaped (horizontal and vertical) gating systems and L-shaped system with variable cross-section collector it may be concluded that the Bernoulli's equation is proven to be used for cross sections of flow with different consumption rates, i. e. for calculations of multi-fed gating systems. Although it is not proven theoretically.

Table 2. – Characteristics in the gating system

Indicators	Operating feeders						
	I, II	I, IV	I–III	I–IV	I–V	I–VI	I–VII
1	*2*	*3*	*4*	*5*	*6*	*7*	*8*
ν_{17}	2.050 / 2.04	2.071 / 2.04	1.848 / 1.93	1.608 / 1.59	1.439 / 1.46	1.361 / 1.36	1.231 / 1.30
ν_{18}	1.982 / 2.06		1.897 / 1.92	1.793 / 1.72	1.640 / 1.71	1.566 / 1.64	1.435 / 1.46
ν_{19}			1.959 / 2.03	1.838 / 1.90	1.747 / 1.82	1.720 / 1.81	1.608 / 1.68

1	*2*	*3*	*4*	*5*	*6*	*7*	*8*
v_{20}		1.990 2.08		1.983 2.06	1.808 1.89	1.657 1.63	1.606 1.65
v_{21}					1.649 1.72	1.590 1.67	1.608 1.71
v_{22}						1.393 1.46	1.435 1.52
v_{23}						1.361 1.35	1.231 1.25
Q	258.25 262.57	260.07 263.85	365.34 376.57	462.53 465.59	530.35 550.76	594.70 612.88	650.22 676.92

Список литературы:

1. Чугаев Р. Р. Гидравлика. – М.: изд-во "Бастет", 2008. – 672 с.
2. Меерович И. Г., Мучник Г. Ф. Гидродинамика коллекторных систем. – М.: Наука, 1986. – 144 с.
3. Токарев Ж. В. К вопросу о гидравлическом сопротивлении отдельных элементов незамкнутых литниковых систем//Улучшение технологии изготовления отливок. – Свердловск: изд-во УПИ, 1966. – С. 32–40.
4. Jonekura Koji (et al.) Calculation of amount of flow in gating systems for some automotive castings//The Journal of the Japan Foundrymen's Society. – 1988. – Vol. 60. – № 8. – P. 326–331.
5. Идельчик И. Е. Справочник по гидравлическим сопротивлениям. – М.: Машиностроение, 1992. – 672 с.
6. Васенин В. И., Васенин Д. В., Богомягков А. В., Шаров К. В. Исследование местных сопротивлений литниковой системы//Вестник Пермского национального исследовательского политехнического университета. Машиностроение, материаловедение. – 2012. – Т. 14. – № 2. – С. 46–53.
7. Васенин В. И., Богомягков А. В., Шаров К. В. Исследования L-образных литниковых систем//Вестник Пермского национального исследовательского политехнического университета. Машиностроение, материаловедение. – 2012. – Т. 14. – № 4. – С. 108–122.
8. Vasenin V. I., Bogomyagkov A. V., Sharov K. V. Investigation into a *L*-type gating system//Austrian Journal of Technical and Natural Sciences. – 2015. – № 1–2. – P. 45–55.

Section 3. Medical science

Boychuk Alexandra Gregoryvna,
PhD, assistant of the Department of Obstetrics,
Gynecology and Reproduction,
Shupik National Medical Academy
of Postgraduate Education, Kyiv, Ukraine,
E-mail: tanyakolom@gmail.com

Management system for women with infertility and non-alcoholic fatty liver disease

Abstract: The application of the management system for the women with infertility and NAFLD, which includes forecasting of inefficiency of the assisted reproductive technologies (ART) and additional therapeutic and preventive measures with hepatoprotectors, ursodeoxycholic acid preparations, L-arginine, ω-3 polyunsaturated fatty acids and probiotics improves the overall condition of women, liver status, cardiovascular regulation, reduces the dysbiosis symptoms, hormonal status of reproductive system, and, as a result, increases the effectiveness of ART programs up to population-wide level (pregnancy occurred in 36.7% women).

Keywords: infertility, assisted reproductive technologies, non-alcoholic fatty liver disease, treatments.

Introduction. Nonalcoholic fatty liver disease (NAFLD) — the most common cause of chronic liver disease in Europe. In the common population the part of NAFLD is nearly 20–40% [1]. In recent years there is growing evidences that NAFLD is multisystem disease that increases the risk of type 2 diabetes, cardiovascular diseases, chronic kidney disease, osteoporosis and hormonal disorders [2].

Current approaches to treating of NAFLD aimed mainly at eliminating or alleviating the factors that lead to the development of this disease [3]. NAFLD treatment includes gradual decrease of body weight, control blood glucose levels, correction of blood lipid profile by hypocholesterolemic agents [4]. Advantages provided by: essential phospholipids, mechanisms of action of which includes a such effects as repair of enzyme systems of hepatocytes, stabilization and renewal of cell membranes; preparations of ursodeoxycholic acid (UDCA), which has a hepatoprotective and independent lipid-lowering effect; agents that normalized the oxidative stress, apoptosis, excessive bacterial growth etc. [5]. It was established that gradual weight loss, normalization of carbohydrate metabolism in conjunction with moderate exercise is accompanied by positive dynamics in clinical and laboratory parameters [6].

We established new links in the pathogenesis of reproductive losses among women with functional diseases of the liver, which includes genetically conditionality, autoimmune and prothrombotic status, violations of microbiota and vascular regulation. The results creates a theoretical background for the development of complex of the medical and organizational measures for women with infertility and NAFLD at the stage of preparation to the ART program.

Objective: To evaluate the effectiveness of complex of the therapeutic and preventive measures for women with non-alcoholic fatty liver disease at the stage of preparation to the ART programs.

Materials and methods. To evaluate the effectiveness of therapeutic and preventive measures based on the forecasting algorithm it was selected 60 women with a high risk of ART inefficiencies. The participants were randomized into: main group — 30 women on a recommended complex of preparation to the ART, and the comparison group — 30 women with preparation to the ART according to the Ministry of Health's protocols.

The including criteria of this study were following: women who are seeking treatment for infertility and were included to the ART program; NAFLD diagnosed by required examinations; high risk of ART inefficiencies

established by the forecasting. For women of the main group in addition was administered the recommended course of treatment (duration of 1 month) with the following agents: L-arginine, ω-3 polyunsaturated fatty acids, probiotics and differentially hepatoprotectors for the detected abnormalities of severe cytolysis, and/or ursodeoxycholic acid preparations for the expressed signs of cholestasis.

The analysis of blood biochemical parameters were carried out according to the standard procedures: bilirubin, ALT, AST, γ-glutamyl transpeptidase (GGTP) alkaline phosphatase (AP). The analysis of total cholesterol (TC), high-density lipoprotein cholesterol (HDL–C) and triglycerides (TG) were performed by enzymatic colorimetric methods. Low-density lipoprotein (LDL–C) and very-low-density (VLDL–C) lipoprotein cholesterol, atherogenic index (AI) were calculated according to the common formulas.

The levels of pituitary hormones and steroid in peripheral blood serum were determined by radioimmunoassay methods. Hormonal colpocytologic study was conducted by the conventional procedure. The hemostasis parameters investigated by biochemical analyzer.

The content of L-arginine in the blood was measured by a photometric method, based on the reaction of L-naphthol with hypobromide reagent. The level of homocysteine was determined by a cyclic enzymatic reaction.

Results and discussion

After a pathogenetic treatment in women of the main group the biochemical indices were improved: decreased the bilirubin level, and nearly 2-fold decreased the levels of transaminases (ALT from 47,8 ± 6,4 to 25,2 ± 5,3 U/L, AST from 42,7 ± 4,9 to 28,3 ± 5,2 U/L, p <0,05) and AP from 110,1 ± 15,2 to 74,8 ± 9,4 U/L (p <0, 05). Cholesterol, low-density lipoprotein and very-low-density lipoprotein cholesterol also decreased significantly — from 1,1 ± 0,14 to 0,6 ± 0,12 mmol/L, and also triglycerides; this resulted in reducing of the atherogenic index from 3,3 ± 0,24 to 1,0 ± 0,32 (p <0,05). Such changes show positive effects of the recommended treatment of liver enzymatic function, cholesterol and lipid metabolism. In contrast, among women of comparison group was not mentioned improving of biochemical parameters, but on the contrary, during preparation therapy to the ART procedure without a "cover up" of liver the transaminase levels significantly increased (ALT from 49,1 ± 5,3 to 69,4 ± 6.8 U/L, p <0,05) and a few raised the level of AP and GGT.

As a result of the normalization of the hepatobiliary system (GBS) in the main group improved the general status of women, reduced the number of complaints from the gastrointestinal tract side; before treatment such complaints was fixed in 14 (46.7%) women, and after the treatment — in 8 (26.7%) women (p <0,05). During study period in the comparison group only one woman of 13 (43.3%) ceased to complain on discomfort, in 12 (40.0%) the complaints persisted (p> 0,05).

The positive impact of the recommended treatment on the GBS condition was confirmed by the results of ultrasound examination: decreased the number of women with the enlarged liver, with hyperechogenic liver, irregularity of vascular pattern. The 2-fold decrease in the percentage of women with signs of intrahepatic cholestasis (16.7% versus 8.0% in the control group, p> 0,05) was noted. In contrast, in the comparison group of women the US-signs demonstrated the tendency to deterioration of the GBS; the percentage of women with signs of intrahepatic cholestasis (40.0%) was significantly higher than in the study group (p <0,05).

After recommended therapy complex among women of the main group the improvement in intestinal microbiocenosis was noted: increasing of dominated flora (bifidobacteria and lactobacilli) and decreasing concentrations of the pathological pathogenic microflora (*Klebsiellapneumonial, Proteusvulgaris, Staphylococcusaureus* and fungi of the genus *Candida*). After treatment intestinal dysbiosis of different severity was observed in 13.3% of women with NAFLD versus 43.3% in the comparison group (p <0,05).

Complex effect of the recommended treatment improves the condition of the vascular homeostasis in women of the main group (see table). It was noted the positive changes in platelet (platelet count was significantly increased and reduced their ability to aggregation), as well as in coagulation level of hemostasis (D-dimer and fibrinogen levels decreased, APTT and INR increased, p <0,05). This evidenced about decline the risk of thrombosis and hypercoagulability. In the comparison group of women, on the contrary, there was a slight tendency to deterioration, which could be a result of preparation therapy to the ART. On the improvement of endothelial condition indicated the growth of NO-donator L-arginine from 41,7 ± 1,8 to 48,6 ± 1,1 mmol/L (p <0,05) and the reduction of damaging factor homocysteine from 6,9 ± 0,32 to 6,0 ± 0,31 mmol/L (p <0,05).

After a course of recommended treatment among women of the main group it was noted a marked improvement of the reproductive system, as indicated by a decrease of the imbalance in gonadotropic and sex hormones (which was confirmed by the blood hormone

analysis), and colpocytologic studies of vaginal discharges. According to a derived results a resumption of the ovulatory cycles was observed in 23,3% women of the main group vs. 6.7% in the comparison group (p <0,05).

As a result of the combined effect of the recommended treatment the efficiency of ART programs improved up to population-wide level: pregnancy occurred in 11 (36.7%) women of the main group and in 7 (23.3%) female from the comparison group.

Conclusions

The application of the management system for the women with infertility and NAFLD, which includes forecasting of inefficiency of the assisted reproductive technologies (ART) and additional therapeutic and preventive measures with hepatoprotectors, ursodeoxycholic acid preparations, L-arginine, ω-3 polyunsaturated fatty acids and probiotics improves the overall status of women, liver condition, cardiovascular regulation, reduces the dysbiosis symptoms, hormonal status of reproductive system, and, as a result, increases the effectiveness of ART programs up to population-wide level (pregnancy occurred in 36.7% women). This complex of the therapeutic and preventive measures with proven safety and high efficiency can be recommended for introduction in the practice of reproductive clinics. This will improve the effectiveness of ART and preserve the health of women.

Table 1. – Indicators biochemical examination examination of women in the dynamics of treatment

Indicator	Main group, n = 30		Comparison group, n = 30		Control group, n = 50
	Before treatment	After treatment	Before treatment	After treatment	
Total bilirubin mmol/L	23,1±2,65*	15,2±2,02*^#	25,2±3,81*	29,6±4,54*	8,2±1,34
ALT, U/L	47,8±6,4*	25,2±5,3*^#	49,1±5,3*	69,4±6,8*#	12,4±3,7
AST, U/L	42,7±4,9*	28,3±5,2*^#	40,2±4,7*	60,4±7,1*#	15,8±3,6
Coefficient de Rytis	0,88±0,32	1,12±0,31	0,85±0,39	0,86±0,31	1,4±0,31
AP, U/L	110,1±15,2*	74,8±9,4*^#	102,7±12,3*	118,4±16,5*	42,3±7,4
GGTP, U/L	44,2±6,7*	27,4±5,7^#	43,2±5,6*	49,4±7,1*	17,3±4,2
Cholesterol, mmol/L	5,98±0,41*	4,1±0,54*^#	5,94±0,51*	5,82±0,52*	3,7±0,25
LDL – C, ммоль/л	3,87±0,32*	2,7±0,26*^#	4,00±0,32*	4,02±0,31*	2,1±0,18
HDL – C, ммоль/л	1,0±0,25*	1,4±0,30	1,1±0,13*	1,1±0,21*	1,8±0,12
IA	3,3±0,24*	1,9±0,25*^#	3,0±0,25*	3,1±0,22*	1,1±0,18
TG, mmol/l	2,3±0,22*	1,0±0,32^#	2,1±0,20*	2,1±0,24*	1,1±0,18
VLDL – C, mmol/l	1,1±0,14*	0,6±0,12^#	1,0±0,18*	1,2±0,16*	0,5±0,11

*Notes: * — significant difference regarding the rate of women in the control group (p <0,05); ^ — significant difference regarding the rate of women comparison group (p <0,05); # — significant difference regarding the rate of women before treatment (p <0,05).*

Table 2. – Indicators vascular hemostasis women surveyed in the dynamics of treatment

Indicator	Main group, n = 30		Comparison group, n = 30	
	Before treatment	After treatment	Before treatment	After treatment
Platelet count, 10^9/L	180,2±13,1	212,3±14,1*^	178,4±12,7	180,6±12,5
Index of ADP-induced aggregation,%	78,1±4,3	65,0±3,9*^	79,2±4,5	84,5±4,8
Fibrinogen, g/L	3,8±0,25	3,1±0,27*^	3,7±0,21	3,9±0,22
Prothrombin index,%	99,2±4,1	93,2±4,5	98,4±4,1	99,5±5,2
INR, CU	0,85±0,05	0,97±0,03*^	0,84±0,05	0,81±0,04
APTT, s	23,4±0,51	28,7±0,62*^	22,9±0,38	21,1±0,47
D – dimer,, mg/L	220,8±11,5	195,5±12,1*^	223,6±10,8	220,8±11,5
L – arginine, mmol/L	41,7±1,8	48,6±1,1*^	40,9±1,6	38,1±1,5
Homocysteine, mkmol/L	6,9±0,32	6,0±0,31*^	7,2±0,31	7,5±0,35

*Notes: * — significant difference regarding the rate of women before treatment (p <0,05); ^ — significant difference regarding the rate of women comparison group (p <0,05).*

References:

1. Blachier M., Leleu H., Peck-Radosavljevic M., Valla D.C., Roudot-Thoraval F. (2013). The burden of liver disease in Europe: a review of available epidemiological data. J. Hepatol.; 58 (3): 593–608.
2. Byrne C.D., Targher G. (2015). NAFLD: a multisystem disease. J. Hepatol; 62 (1): S47–64.
3. Miyake T., Kumagi T., Furukawa S., Tokumoto Y., Hirooka M., Abe M., Hiasa Y., Matsuura B., Onji M. (2013). Non-alcoholic fatty liver disease: Factors associated with its presence and onset. J. Gastroenterol Hepatol; 28 (4): 71–8.
4. Ratziu V., Goodman Z., Sanyal A. (2015) Current efforts and trends in the treatment of NASH. J. Hepatol; 62 (1): S65–75.
5. Prosolenko K.O. (2012) Current approaches to the treatment of nonalcoholic fatty liver disease on the background of metabolic syndrome. Liki Ukraini; 3–4 (1): 30–4.
6. Loomba R., Cortez-Pinto H. (2015). Exercise and improvement of NAFLD: practical recommendations. J. Hepatol; 63 (1):10–2.

Utyuzh Anatolij Sergeevich,
Ph. D., Associate Professor, MD,
Head of Department of Prosthetic Dentistry
I. M. Sechenov First Moscow State Medical University,
E-mail: rinairis777@yandex.ru

Samusenkov Vadim Olegovich,
Ph. D., Assistant of Department of Prosthetic Dentistry,
I. M. Sechenov First Moscow State Medical University,

Yumashev Aleksej Valerievich,
Ph. D., Professor, Department of Prosthetic Dentistry,
I. M. Sechenov First Moscow State Medical University,

Nefedova Irina Valerievna,
doctor-intern in the department of Prosthetic Dentistry,
I. M. Sechenov First Moscow State Medical University,

Tsareva Tatiana Viktorovna,
PhD., Senior Researcher NIMSI A. E. Evdokimov
Moscow State University
of Medicine and Dentistry

Analysis of osseointegration adequacy and examination of stability of dental implants after sinus lift operation

Abstract: Based on the experience of 59 performed operations of "balloon" sinus lift in 51 patient, there was performed estimation of adequacy of osseointegration of dental implants mounted in distal parts of upper jaw after carrying out of different variants of sinus lift operation.

Keywords: balloon sinus lift, dental implants, mesodiencephalic modulation.

In our view, estimation of stability of dental implants mounted in distal parts of upper jaw is a crucial point that determines quality of performance of sinus lift operation. Reliable estimation of the osseointegration degree of endosseous implants has fundamental significance for selection of prosthetic construction, technique of functional load of implants, prediction of efficacy of orthopedic treatment. Primary stability is a crucial point for integration of implants, and stability of an implant in different periods of the process of osseointegration and after its fulfillment is reflection of reliability of osseointegration [4, 560].

There are known several possibilities of indirect estimation of the osseointegration degree and stability of implants: clinical (percussion, manual control of implant stability); roentgenological (including determination of bone tissue density around an implant); echoosteometry; periotestometry; gnathodynamometry; torque-test with the use of a torque wrench [3, 150]. In recent times, new method of estimation of implants stability with the use of method of Resonance Frequency Analysis (RFA) has drawn attention of clinicists and researchers.

The method is based on registration of resonance electromagnetic waves of implants and surrounding bone when they are affected by electromagnetic field by means of magnetized peg [1, 128–129; 2, 22; 8, 257–265; 10, 26].

It is of prime importance, in our view, to perform estimation of implants osseointegration during their insertion while performing sinus lift and during implantation after performance of sinus lift. Implants stability would be an indirect sign of adequacy of performed augmentation.

Estimation of osseointegration adequacy of dental implants mounted in distal parts of upper jaw after performance of different variants of sinus lift operation was the **objective of the work.**

Materials and methods

Estimation of 59 operations of "balloon" sinus lift in 51 patients was performed (in 8 patients bilateral sinus lift was performed). Technique of "balloon" sinus lift was carried out with the use of the BALLOON-LIFT CONTROL complex (produced by the company Hager&Meisinger, Germany). "Open" sinus lift according to Tatum's method was performed in 27 patients.

In overall, 314 dental implants (including implants mounted during "close" sinus lift) were mounted in the area of reconstruction of maxillary sinus bottom directly during performance of sinus lift (194 implants) or postponed (after 6–9 months — 120 implants).

Following implants systems were used during the work: Impla (Schutz DENTAL GROUP, Germany), Semados, Bego Implant Systems (Germany), Replace Groovy (Nobel Biocare, Sweden), BTI (Spain).

Mixture of domestic osteotropic preparation Osteomatrix and Plasma Rich Growth Factor (PRGF) was used as augmentatum. Such combination allowed to obtain homogenous material allowing to fill cavity and, in case of small perforation of Schneider membrane, serve a purpose of a membrane.

Selection of the material was determined by the fact that biocompositional material Osteomatrix is a highly-purified bone matrix with preserved collagen and mineral components and natural architectonics of spongy bone. It contains in 1 cm^3 not less than 1.5 mg of affinely connected bone Sulfated Glycosaminoglycans (sGAG).

We used combination of crisps and chips of preparation in a ratio of 2:1. Addition of chips allows to fill to the maximum extent spaces between separate chips by smaller particles.

Technique of obtaining of Plasma Rich Growth Factor (PRGF) and its high efficacy are presented in works of the author of this method — doctor Anitua [5, 65; 6, 23–31; 7, 93].

Blood, from 10 to 20 ml, was collected from ulnar veins into vacuum tube with citral, then it was mixed and centrifuged during 8 minutes with 400 g. Plasma divided into 4 fractions was collected separately. Two lower fractions of platelet rich plasma were put into vessel where 10% solution of calcium chloride was added to, on the basis of 5 drops in 1 ml of plasma. After that, 1–2 cm^3 of crisps and chips of Osteomatrix were put into the vessel. Contents were thoroughly mixed and placed into thermostat under 37 °C for 10 minutes. Formed clot with osteotropic material was used for filling the sinus during sinus lift.

For improving of osseointegration, in a separate group of patients, sessions of mesodiencephalic modulation (MDM) were carried out. Device MDM 2000\1 was used. [9, 19].

Determination of stability of dental implants was carried out by magnetic resonance method with the use of the equipment Osstell mentor (ISQ). Operational principle of the Osstell ISQ is based on indirect determination of attachment rigidity of implant in the jaw bone with the use of resonance frequency analysis of induced vibrations, which are agitated in an implant by means of alternating magnetic field of the radiant device.

In the system of Osstell ISQ, special magnetic peg called SmartPeg is used, which is attached to a dental implant or abutment by screw connection.

Peg is agitated by magnetic impulse sent from measuring probe of the equipment. On the basis of signal response, resonance frequency is calculated, which is rate of attachment rigidity of a dental implant in the bone tissue of the jaw. Results are represented on the display of the equipment in form of ISQ (Implant Stability Quotient) within the range from 1 to100. The higher the value the higher the attachment rigidity of the implant. Minimal value amounts to 55.

SmartPegs are individual for each system of implants (due to different screw thread) and available for all main implant systems. In our work we used SmartPegs

for Nobel Biocare implant system, Sweden, for implants with diameter 3.5 mm type 12, for diameter 4.3 mm and 5 mm — type 13, for the system Semados — type 26, for BTI — type 27. They are not manufactured for the Impla system.

ISQ measurement was carried out in strict compliance with instruction from the manufacturer of the Ostell ISQ equipment. For that purpose SmartPeg was attached to implant using torque wrench with the force 4–5 N/cm. After that, the equipment probe was mounted so that its tip was pointed to a small magnet on the top of the SmartPeg, at the distance of 2–3 mm without touching it. During measurement the probe was hold immovable. If the measurement had successful result, equipment produced audio signal and displayed ISQ value on the screen.

In overall, there was performed estimation of fixation of 35 implants mounted in distal parts of upper jaw after operation of balloon sinus lift (19 patients) and 22 implants after operation of open sinus lift (9 patients). For all studied cases, dental implantation had postponed character and was performed 6–9 months after sinus lift. Examinations were carried out twice: during mounting of implants and 6 months after implantation before start of prosthesis. In overall, 114 measurements were performed.

Examination results

It is worth noting that performing of postponed dental implantation after carrying out of open or balloon sinus lift is rather individual; thus, 6 months after operation, we failed to mount dental implants in 11 patients due to insufficient density of regenerate. For those patients it was necessary to carry out the dental implantation operation after 2 months, i. e. waiting period after sinus lift amounted to 8 months.

Signs of filling of formed space under the Schneider membrane by osteoplastic material were detected for all patients after sinus lift operation; result of lack of bone tissue growth for that period in those groups was not determined. After operation of open sinus lift the volume of inserted osteoplastic material ranged from 1.5 to 2.7 cm^3 (at average 2.1 + 0.3 cm^3) and the height of membrane lift amounted to average 14.0+1.2 mm.

After half a year (based on the CT data), volume of formed bone tissue amounted to 1.8 + 0.3 cm^3 and the height to 12.6 + 1.2 mm.

At an average, after operation of "balloon" sinus lift (based on the data of 17 CT), volume of added bone amounted from 1.5 to 2.4 cm^3 (at average 1.95 + 0.3 cm^3). The height for which it was possible to lift the sinus was from 10 to 17 mm (at averate 13.2 + 1.5 mm).

CT performed 6 months after operation showed that at average the volume of newly formed bone tissue after balloon sinus lift amounted to 1.8 + 0.3 cm^3, and it corresponded to open sinus lift ($p>0.5$). Total height (from the edge of alveolar bone to newly formed maxillary sinus bottom) ranged from 10 to 16 mm and amounted to average 12.3 + 1.1 mm.

Results of measurements performed with the use of the Osstell equipment of attachment rigidity (stability) of dental implants are presented in the Table 1.

Primary stability of dental implants mounted simultaneously with sinus lift depends largely on bicortical position of the implant body. In this regard, for enhancement of certainty of forming of bone tissue after sinus lift, we considered it reasonable to divide measurements results for subgroups. First subgroup — implants mounted in distal part of the jaw with primary (before sinus lift) distance from the edge of alveolar bone to the maxillary sinus bottom from 1 to 3 mm, the second one — at the distance from 4 to 6 mm as fixation of dental implant in own bone have a bigger thickness.

As it is seen in the presented table, there is no difference in implants stability mounted after performing of traditional "open" and "balloon" sinus lift ($p>0.5$), besides, there was also no fundamental significant difference for implantation with different primal height of alveolar bone of the jaw. It corresponds to results of roentgenologic examination and indicates both adequate fixation of dental implants during their mounting and adequate osseointegration.

Table 1. – Results of determination of attachment rigidity of dental implants using the equipment Ostell ISQ (in ISQ units)

Sinus lift type	**During implant mounting**		**After 6 months**	
	Height 1–3 mm	Height 4–6 mm	Height 1–3 mm	Height 4–6 mm
Open lift type n=22	60.64 ±4.1	64.55 ±3.25	63.35 ±4.14	65.65 ± 3.15
Balloon lift type n=35	60.29 ±2.72	64.75 ±2.9	61.4 ± 3.25	68.12 ± 3.45

Histogram (Figure 1) shows distributions of ISQ individual values obtained during implants mounting. As seen, neither of indicators both in group with open sinus lift and in group with balloon sinus lift exceeded the limits of minimal permissible ISQ value (below 55).

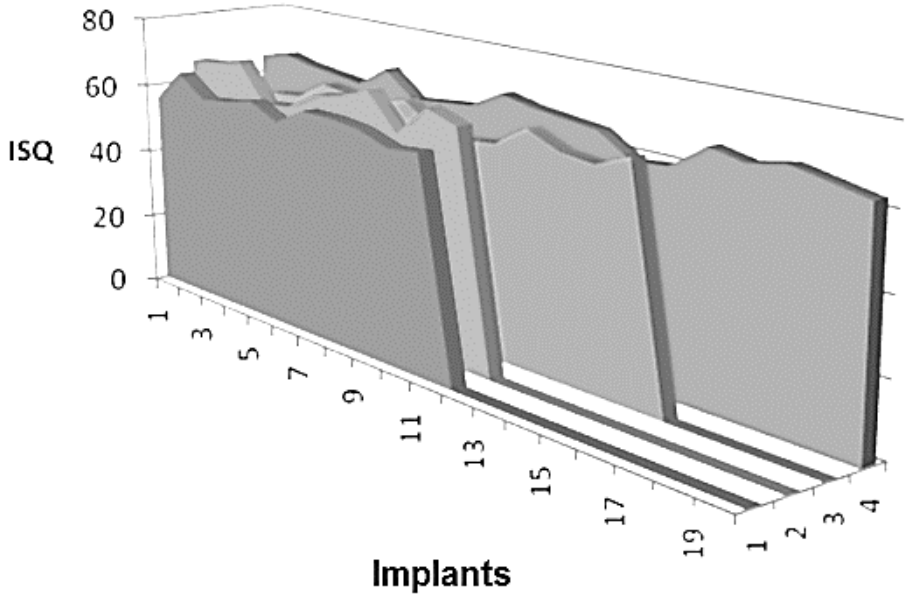

Figure 1. ISQ Values distribution during implants mounting after sinus lift
(1 — open sinus lift, height — 1–3 mm; 2 — open sinus lift, height — 4–6 mm;
3 — balloon sinus lift, height — 1–3 mm; 4 — balloon sinus lift, height — 4–6 mm)

It should be noted that ISQ values with different primary thickness of alveolar bone had no significant difference ($p>0.5$). It signifies of high degree of implants primary fixation after their mounting and of adequate forming of bone tissue after sinus lift. Similar data were also obtained during control of dental implants osseointegration.

Therefore, according to final results of provided therapy, both methods of sinus lift are highly effective. Obtained data also indicates (together with histological data) forming of adequate bone with the use of combination of Ostematrix (crisps and chips) and PRGF as osteoplastic material.

At the same time, in summary, it should be noted that according to majority of clinical indicators characterizing effectiveness of operation "balloon" sinus lift appears to be more favourable comparing to traditional "open" method.

References:

1. Drobyshev A. Y., Dronov M. V. Estimation of stability and osseointegration of dental implants with the use of the resonance frequency method. M.: Stomatology institute 2007. – 2007. – No. 1. – P. 128–129.
2. Dronov M. V. Using of resonance frequency method for estimation of stability and osseointegration of dental implants: Author's abstract of the candidate of medical sciences. – M., 2007. – 22 p.
3. Kulakov A. A., Losev F. F., Gvetadze R.Sh. Dental implantation. – Moscow.: MIA, 2006. – 150 p.
4. Robustova T. G. Implantation of teeth. Surgical aspects/M.: Medicine, 2003. – 560 p.
5. Anitua E., Orive G., Pla R., Roman P., Serrano V, Andia I. The effects of PRGF on bone regeneration and on titanium implant osseointegration in goats: a histologic and histomorphometric study. J Biomed Mater Res A. 2009 Oct; 91 (1): 158–65.
6. Anitua E., Prado R., Orive G. A lateral approach for sinus elevation using PRGF technology. Clin Implant Dent Relat Res. 2009 Oct;11 Suppl 1: e23–31.
7. Anitua E. The use of plasma-rich growth factors (PRGF) in oral surgery. Pract Proced Aesthet Dent. 2001 Aug;13 (6): 487–93.
8. Rabel A., Kohler S. G., Schmidt-Westhausen A. M. Clinical study on the primary stability of two dental implant systems with resonance frequency analysis. Clin Oral Investig. 2007; 11: 257–265.
9. Yumashev A. V., Gorobets T. N., Admakin O. I., Kuzminov G. G., Nefedova I. V. Key Aspects of Adaptation Syndrome Development and Anti-Stress Effect of Mesodiencephalic Modulation//Indian Journal of Science and Technology, Vol 9 (19), DOI: 10.17485/ijst/2016/v9i19/93911, May 2016.
10. Samiotis A., Batnidji M., Galiyardo-Lopes L., Steveling H. G. Clinical control of resonance analysis Frequancy (FRA) implant Astra. Int J Oral Maxillofac Implant 2003; 5: 4.26

Section 4. Food processing industry

Kurbanova Madina,
Tashkent institute of chemical technology (Uzbekistan),
Junior assistant, Department of Food Safety
E-mail: sherzod_mamatov@mail.ru
Dodaev Kuchkor,
Tashkent institute of chemical technology (Uzbekistan),
Professor, Department of Food Safety,
Kurbanov Jamshed,
Samarkand Institute of economics
and service (Uzbekistan) Professor,
Department of International Tourism and Touristic Service

Thermochemical techniques of processing the initial impulse in technology of drying fruits and vegetables

Abstract: The paper describes the results of research on thermochemical techniques of processing the initial impulse in technology of drying fruits and vegetables. Also a summarized information about the technology of drying fruits, vegetables and grapes using the initial impulse was presented.

Keywords: fruits, vegetables, processing, blanching, sulfuration.

Introduction

In accordance with the principle of intensification linearity of processing fruits and vegetables can be achieved both by increasing the kinetic coefficients that characterize the relaxation properties of the products (it includes diffusion coefficients and molar transfer of moisture), and by enhancing the driving forces of the process (which are the corresponding gradients of thermo chemical — mass, temperature, pressure, etc.).

Analysis of research results devoted to the technology and techniques of food processing show that to enhance the driving forces, there are certain technology limits, then to increase the kinetic coefficients significant reserves are available. For example, preheating the material before drying promotes sharp increase of the diffusion coefficient of moisture in the product [1].

Until recently, in food processing, heat and mass transfer has been mainly studied as a macro process and the objects were considered as a continuous model in which the individual phases are presented in the form of a continuous medium, uniformly distributed in body volume and accordingly the analysis of transport processes in them was based on the phenomenological representations. At present, in connection with the significant achievements of molecular physics, as well as with widespread use of new physical effects under the influence of external fields, it is advisable to study the essence of macro-processes and examine processing objects as a corpuscular model, the physical properties of that are stipulated by the molecular structure of bodies and the interaction forces between the generators of wet materials by molecules, atoms and ions [2, 3].

Materials and methods

When analyzing the phenomena developed in a material under interaction of moisture with dry body framework, formation of various types of connection of moisture of the surfactants effects on the wet material, as well as in exposure of the specific features of the effect of different methods of energy supply to the drying objects.

In this connection, at the present stage of drying development it should be considered as a separation process of phases in heterogeneous systems under interaction of external and internal fields, and a determination influence has the initial stage of this interaction, which is called an initial impulse.

The concept "impulse" has been loan worded of mechanics; extending this analogy, it is advisable to also use the concept "impulse of a force", which is a product of the driving force of the process on the time of its impact. An impulse of initial interaction to the object takes into account both the initial acting force of the process, and the duration and the application. In accordance with universal physical principle of Le Chatelier — Braun, the stronger external influence on the process object at the initial moment, the more intense the proceed of internal processes, trying to attain to bring the system back to equilibrium. As a number of studies have shown that the theory of the initial impulse was applied to many processes of heat and mass transfer (drying, baking, extraction, adsorption, desorption, and others.)

In connection with the significant thermolability and moisture inertia of wet material it is necessary to prepare it for the perception of the initial impulse, therefore are especially important the different technological ways of pre-preparation of materials for drying (centrifuging, evaporation, dispersion, vibrational processing, preheating, foaming effect of surfactants, etc.), as well as the combination of drying with other technological operations (moving inside the material of water-soluble mineral substances, enzymes, oxidation, burning, etc.).

Proceeding from above stated we have experimentally investigated and summarized the results of processing fruits and vegetables by thermo-chemical methods of the initial impulse.

In order to intensify and improve the quality in technology of drying fruits and vegetables tentatively before the main drying process the various thermo-chemical methods of the initial impulse is used. In this case, depending on the type of fruits and vegetables, and the methods of drying fruits is subjected to sulfuration (apples, apricots, pears, peaches), processing with alkali solvents (grapes, plums), vegetables are subjected to blanching (potatoes, beets, carrots, cabbage), and washing with water or by boiling.

Results of research

The results of studying fruits with various thermo-chemical methods and the method of initial impulse are presented in Table 1, and the results of research for the main types of vegetables are presented in Table 2.

Table 1. – Drying green-stuffs and fruits using thermo-chemical methods of initial impulse

№	Material	Shape cutting	Processing before drying		Maximal temperature, °C.	Duration of drying, hour.
			Type of processing	Duration, min.		
1	Apples	Peeled, cored, sliced, diced	Sulfuration	15–30	60–71	6–10
2	Apricots	Halves, without stones		15–15	57–68	10–20
3	Cherry	Whole		0–2	57–74	8–12
4	Grapes	Without stems	Alkali	1/13–1/2	65–82	20–30
5	Peaches	Peeled halves	Sulfuration	15–30	63–68	15–24
6	Pear	Peeled, cored, halves		15–30	60–65	15–24
7	Plum	Whole	Alkali	1/60–3/4	63–71	20–30

Table 2. – Drying vegetables using thermo-chemical methods of initial impulse

№	Name of vegetables	Type and size of cutting	Processing before drying		Maximal temperature, °C.	Duration of drying, hour.
			Type of processing	Duration, min.		
1	*2*	*3*	*4*	*5*	*6*	*7*
1	Potatoes	Bars (noodles) up to 7 mm or circles 4 mm	Blanching by boiling water or steam	2–3	85–90 80	5–6 (1) 5–6 (2)
2	Beets	Chips 5–7 mm thick	The same	2–3	90 80	5–6 (1) (2)
3	Carrot	Chips 5–7 mm		2	80–86 75–80	4–5 (1) (2)
4	Cabbage	Chips 3–5 mm	Blanching. Steam pressure not more than 1,5 atmosphere	3–5	70–75 65–70	4–5 (1) (2)

1	*2*	*3*	*4*	*5*	*6*	*7*
5	White core fruits (parsnip, parsley, celery)	Chips 3–5 mm	Washing with water or in 2–3% — solution of caustic soda or in 0,5–1% solution of sodium hydroxide	2–3	60–80 60–65	4–5 (1) (2)
6	Onions	Circles 3–6 mm	—		65–70 65	6 (1) (2)

It is shown from the data in tables that the main types of fruits and vegetables are tentatively processed before drying by different thermochemical methods of the initial impulse.

The main method of initial impulse is blanching or partial scalding in order to intensify the process of drying and preserving the natural color of the product, reduction of the hygroscopicity and give greater stability during storage. Blanching is conducted in steam or in boiling water in special containers (baskets) for a short time.

In this case blanching is carried out at a temperature 95–100 °C with the duration, onions, plums, apricots for 1–2 minutes; apples for 2–3 minutes, cherry for 2–8 minutes, pears for 15–30 minutes. The drying time depending on the type of the products dried at various temperatures is different.

It is advisable to specify that certain types of fruits and vegetables after cutting prior to blanching to avoid darkening during drying they are preliminary bleached in a solution of salt or citric acid (5–10 g per 1 liter of water) [5].

Some fruits, especially light-colored, it is better to boil them in sugar syrup. It retains their color and accelerates drying. Sour fruits or berries are sugared before drying, at the same time, they become more viscous and sweet, preserve the natural color better and are well-kept. To do this, the berries prepared for drying are poured with 50% hot syrup and kept in a cool place for 6–8 hours, after that are put in a colander, the syrup is heated and pour the berries again. 100–200 grams of sugar are added to per liter of syrup. After 6–8 hours the syrup with berries is brought to boil and once again put in a colander. Then, the fruits spread in a thin layer, at the beginning dried and then dried until it is ready.

Blanching can be carried out in various variants. For example, mature roots first are boiled up to 20 minutes after the water boils, then dried and cut at 70–80 °C.

For drying beets, after cutting-off rootlets and heads they are cooked for 20–40 minutes. Further they are immersed in cold water for 10–20 minutes. Then remove the peel, cut into chips 2–5 mm thick and rinsing transferred to drying. Or they are cut into noodles, blanched for 2–3 minutes using water containing 4–5 g of salt per 1 liter of water. After cooling in a clean cold water beets are sent for drying at temperature 80–85 °C with the duration of 5–6 hours. Qualitative dried beets differed with their color, having pink or purple tint. The product yield is from 12 to 15%.

Drying carrots is similar to beets, but the duration of boiling thoroughly shortened to 15–20 minutes. In order to get dried product with better quality another method of preliminary preparation is used. Carrots are cleaned of all skins and cut into circles of 2–3 mm thick or strips. They are blanched in salted water (4–5 grams of salt per 1 liter of water) for 2–3 minutes, thereafter cooled in cold water. Then they are put on a sieve dryer (4–5 kg/m^2) in thin layers and dried for 5–6 hours at a temperature of 70–80 °C. To accelerate the drying process, onions are preliminary blanched for 1–2 minutes in boiling water and dried at 70 °C. Chopped onion as slices 3–4 mm thick are not blanched preventing their adhesion on the sieve, instead of blanching a chopped onion is kept in cold salted water containing 50 g of salt per 1 liter of water for 3–5 minutes. For drying they spread at the rate of 4 kg per 1 m^2 at temperature 60–65 °C with the duration of 4–6 hours. The product yield is from 12 to 16%.

Preliminary processing of fruits by blanching is carried out with steam or boiling water. For example, apples of early-ripening varieties are dried with skin. The core is taken out with a tube specially made of tin or sharp spoon. Prepared apples are cut across the circles into slices 4–7 mm thick, so that the sliced apples are not darkened during drying due to the action of oxidative enzymes. They are immediately immersed in cold salted water (10–15 g of salt per 1 liter of water) or acidic (2–5 g citric or tartaric acid per 1 liter of water) water.

For partial destroy of enzymes and acceleration of the drying process the sliced apples can be blanched for a few minutes in boiling water, and then immediately cooled in cold water.

Instead of blanching the sliced apples can be kept for 10 minutes on a sieve in boiling water steam, and then

cooled in cold water. The apples prepared by this way are intensively dried at a temperature from 70–75 °C to 80–85 °C. When approximately 2/3 of the water evaporates, the temperature is lowered to 50–55 °C. The entire drying process lasts 6–10 hours. Properly dried apples have yellowish-brown color, are not broken under compression and do not release juice, contain approximately 20% moisture.

Blanching by boiling water method and cooling can be used for plums, cherries, cherry. To do this the fruit is let in boiling water for 1–2 minutes, and then immediately cooled in cold water, by that the drying process is accelerated and enzymes are destroyed. In this case the waxen coating dissolves from the surface of fruits. To speed up this process baking soda (10–15 g per 1 liter of water) is added into boiling water. In this case, the blanching time is reduced to 5–20 seconds. The fruits of plum varieties with thin skin are blanched in hot water at 90–95 °C, a dense and thick-skinned ones in soda solution.

The chilled fruits spread on a sieve in one layer and dried for the first 3–4 hours at 40–45 °C. When the plum is dry and the skin is wrinkled, the drying is interrupted and the content in the sieve is kept for 4–6 hours at 18–22 °C. Then, it is re-dried during 4–5 hours at high temperature of 50–60 °C. Again drying is interrupted. It is thoroughly dried for 12–15 hours up to bluish tint of color, when they are light-colored grade-storm with a brown tint of color. They should be shiny, evenly wrinkled, bone is well separated from the pulp.

In the same way, pears are processed. Small fruits can be dried as a whole, the average ones are cut in half, and the big ones in four parts. Whole pears are let into boiling water for 15–30 minutes, take them out, let the water drain off and put on trays for drying, in order to have dried tasty products, small-fruited varieties are boiled in sugar syrup (100–150 grams of sugar per 1 liter of water) for a few minutes. The large pears cut into parts, are put in cold acidified water (2–4 g citric acid per 1 liter of water) for a few minutes. At the beginning pears are dried at 80–85 °C, and after boiling thoroughly the temperature reduced to 50–60 °C.

Preliminary processing the initial impulse by thermo chemical methods gives vegetables and fruits elasticity, accelerates drying (cabbage and carrots), but slows drying potatoes and beets. It is explained by the partial gelatinization of starch from potatoes and high sugar content in beets [5].

For enzymatic browning (potatoes) sulfitation is used by processing with 0.1–0.5% sodium sulfite (Na_2SO_3), bisulfite ($NaHSO_3$) pyrosulfite ($Na_2S_2O_5$) by immersion the raw materials into them for 2–3 minutes or watering for 20–30 seconds.Cabbage and carrots are usually sulfitated after blanching.

It is advisable to specify that carrots can be purified by alkaline method. It is carried out with 2.5% solution of NaOH for 4 min at 80–85 °C, then washed alkali residues with running water. Then they are cut and blanched for 3–5 min at 95–98 °C.

If the carrot is blanched as a whole by water steam thermic method, then for preserving the color during the process of drying and storing, it is immersed in a 0.25% solution of sodium bisulfite for 3 minutes.

When drying sliced onion it is treated with 02–0,3% sodium bisulfite solution for 3 minutes, and sent for drying.

The cabbage also is chopped with 3–4 mm thickness, is briefly blanched by steam for 2–3 minutes and processed with 0.1% solution of sodium bisulfite. It can then be dried.

When preliminary processing the green-stuffs-fruits they may also be treated with acidic or alkaline solutions. For example, for drying apples are cut into circles of 5–6 mm thick and sulfitated by immersing them in a 0.15% solution of sulfurous acid for 1–2 minutes and sent for drying.

Plum also is blanched with boiling 0.1% alkali solution for 15–20 seconds followed by washing with water. It shortens the drying time to 6 hours.

Apricots are subjected to sulfitation in 0.5–0.6% solution of sulfurous acid for 5–6 minutes before drying. Small fruits are blanched by steam for 2 minutes, and the large ones for 3–4 minutes. Some fruits of grapes are subjected to pre-treatment blanching and sulfuration. Depending on the type of final products of dried grapes blanching is used as the impact of the initial impulse.

For blanching ripe sorted grapes are divided into small bunches, placed in a sieve and immersed in boiling solution (80–100 g per 1 liter of water) for 5–10 seconds depending on the thickness of grape skin. In this kind of blanching much smaller cracks are appeared on the skin, through which water evaporates intensively upon drying.

In order to intensify the drying process, improvement of the quality and preservation of the natural color or restoration of lost color of dried products an operation called turning white or sulfuration (with sulfur gas) is applied before drying; sulfur gas kills microorganisms; sulfurated fruits are not turned black in drying and further storage, form the initial structure of the product. Sulfuration is performed in special chambers, where

sulfur is reduced in the amount of about 2–2.5 kg per 1 ton of raw material.

The fruits of apples, apricots, cherries, peaches, pears, grapes, and others are subjected to sulfuration. In this case sulfitation with sulfur dioxide is occurred, while keeping them in a weak solution of sulfurous acid oxidation enzymes are destroyed and the products are not darkened, the drying process is accelerated.

In sulfuration of grapes (for the production of raisins-Sabza stacking, Sabza golden, raisins — Hermione stacking dried products) lump of sulfur (30–40 g per 1 m^3 of camera) is burnt in a special chamber. Sulfuration is carried out for 0.5–1 hours, then dried at a temperature of 30–35 °C, and completed at 66 °C.

Apricots are cut in half, the bones are removed. Halves are packed in a one layer with hole up. The dried apricots are sulfurated during 2–6 hours (2 g of sulfur per 1 kg of apricots) and then dried at 70 °C for 8–12 hours. The color of ready sulfurated apricots is from light yellow to dark — orange, unsulfurated — light or dark — brown.

Conclusions

Application of the methods of initial impulse (blanching, sulfuration, turning white, processing with alkaline solution, and others.) significantly intensifies the drying process and improves the quality indicators of dried product.

References:

1. Ginzburg A. S. Modern methods of intensification of heat and mass transfer in drying process of capillary-porous materials -In book: Heat and Mass Transfer-VI, VII–Minsk, 1980. P. 139–145.
2. Flaumenbaum B. L., Tanchev S. S., Grishin M. A. Fundamentals of food preservation, – M: Agromizdat, 1986–494 p.
3. Zagibalov A. F., Zvervekova A. S., Titov A. A., Flaumenbaum B. H. Technology of preservation of fruits and vegetables, and control of the product quality. – M.: Agromizdat 1992. – 352 p.
4. Flaumenbaum B. L., Litvinov S. M., Statsenko O. F. Effect of heat treatment on the cell permeability of plant tissues//University Publishing House. Food technology – 1964. – № 5. – P. 66–69.
5. Pento V. B. Technology and technique of drying//Food Industry, Moscow, 2005. – № 9.

Section 5. Technical sciences

Jumanova Miyasar Ortikovna,
Institute of General and Inorganic Chemistry Academy of Sciences of the Republic of Uzbekistan,
junior scientific researcher,
the Laboratory of Phosphate fertilizers
E-mail: jumanova@mail.ru

Namazov Shafoat Sattarovich,
Institute of General and Inorganic Chemistry Academy of Sciences of the Republic of Uzbekistan,
Doctor of Sciences, Professor
E-mail: igic@rambler.ru

Beglov Boris Mihaylovich,
Institute of General and Inorganic Chemistry Academy of Sciences of the Republic of Uzbekistan, Academician
E-mail: begloff@mail.ru

Complex fertilizers based on processing of the nitric-sulfuric acid angren brown coal and phosphorites Central Kyzylkum

Abstract: The results of the study process of producing complex fertilizers by oxidation of the Angren brown coal with a mixture of nitric and sulfuric acids, and subsequent decomposition of oxidation products with dust-like fraction and thermic concentrate phosphate of Central Kyzylkum. The result highly complex fertilizers were obtained. The commodity properties of the resulting product of fertilizers were defined. They are not compressed, even with a high moisture content will remain full their friability.

Keywords: Angren brown coal, the oxidation of a mixture of nitric and sulfuric acids, dust-like fraction, thermic concentrate, complex fertilizers.

Introduction

One of the main problems of agricultural production in Central Asia depended with the soil humus, which is the basis of any soil fertility. Humus is called a compound dynamic complex of organic compounds formed by the decomposition and humification of organic residues in the soil [1, 15–16]. The special role of humus is its comprehensive positive impact on all aspects of soil fertility. Nutrients of fertilizer, whatever their number was applied into the soil, can not replace the humus as a source of nitrogen and other nutrients which are released during mineralization. Enriching the soil by humus reduces the negative impact of chemical fertilizers, pesticides, heavy metals, forms agronomically valuable of soil agro-physical properties [2, 12–20].

The soils of Uzbekistan on the content of this important element related to low income. The meter layer of black soil, for example, on one hectare 350–700 tons of humus contains, while the best cotton soil zone — gray soils contain only 65–85 tons [3, 137–150]. The soils are in the process dehumification. It was found that the decrease of humus content in the soil by 1% leads to lower crop yields by about 5 quintals of grain units per hectare [4, 117–127]. To prevent the loss of humus and even increase its content in the soil can be achieved by improving crop rotation and extensive use of organic fertilizers. Organic fertilizers include manure, poultry manure, peat, green manure, straw, sapropel. In Uzbekistan manure resources is small, there is no peat, bird droppings little. However, there is a lot of coal in Uzbekistan. The explored reserves amount up to 1 billion 900 million ton, including

brown coal in quantity to1 billion 853 million ton, as well as 47 million ton of black coal [5, 20–27; 6, 105–109]. However, no everyone brown coal is suitable for the preparation from it humates. In [7, 15–16] provides a classification of brown coal for fitness for the production of those or other fertilizers. It states that the coal with contain of humic acids above 45% can be used as raw material for the production of humic fertilizers, used in solid form, as well as for the production of plant growth stimulants. Angren brown coal contains only 4.1% of humic acid on the organic matter [8, 55–61].

Therefore, we set ourselves the goal to find the optimal conditions for the oxidation of a mixture of nitric and sulfuric acids to obtain coal with a high content of humic acids, and on the basis of oxidized lignite and Central Kyzylkum (CK) phosphorite create complex fertilizers.

Experimental procedure

In this study, a representative sample of fine coal grade BOMSSH (brown, walnut, small, seed, rubble) has been used, which has, after drying, to air dryness and grinding in a ball mill to a particle size of 0.25 mm, the following composition (wt.%): moisture 14.1, the ash 13.7, organics 72.2, humic acid 4.1% on organic matter; a phosphorite dust-like fraction of the CK, which contains (wt.%): 18.54 $P_2O_{5total.}$; 3.84 $P_2O_{5accep.}$; 44.72 CaO; 0.95 Al_2O_3; 0.80 Fe_2O_3; 0.80 MgO; 2.22 F; 14.80 CO_2; $P_2O_{5accep.}$: P_2O_{5total} = 20.6%, and thermic concentrate of the CK containing (wt.%): 27.26 $P_2O_{5total.}$; 2.54 $P_2O_{5accep.}$; 53.36 CaO; Al_2O_3 1.30; Fe_2O_3 0.51; MgO 0.61; F 2.91; CO_2 2.41; $P_2O_{5accep.}$: $P_2O_{5total.}$ = 9.32%

Oxidation process of coal was carried out by 30% of nitric acid in which sulfuric acid had been entered in an amount to its concentration in the nitric acid solution was 5%. The weight ratio of the organic portion of coal to nitric acid monohydrate was taken 1:1.6 and 1: 2.0. Coal is oxidized then the resulting product oxidation was treated by phosphate raw materials (PRM). The amount of phosphate raw materials was calculated from the amount originally taken on the coal oxidation of a mixture of nitric and sulfuric acids. Norma of these acids on the decomposition of PRM was taken in the range from 40 to 80% of the stoichiometry of calcium oxide in the raw materials. The results are shown in the Tables 1 and 2.

Table 1. – Composition of compound fertilizer, obtained by nitric-sulfuric acid processing Angren coal and dust-like fraction from phosphorite of Central Kyzylkum

The weight ratio of the coal: HNO_3: H_2SO_4: PRM	Norm of the acids on CaO%	Chemical composition,%						
		P_2O_{5total}	P_2O_{5accep}	CaO_{total}	$CaO_{w.s.}$	N	Organic substances	Humic acid
10:20:3.33:60.3	40	12.27	7.14	29.64	10.05	5.41	14.82	8.98
10:20:3.33:48.3	50	11.31	7.47	27.26	10.14	5.96	16.13	9.82
10:20:3.33:40.2	60	10.37	7.79	25.08	10.70	6.45	17.65	10.75
10:20:3.33:34.5	70	9.55	7.82	23.05	10.81	6.71	18.42	11.20
10:20:3.33:30.1	80	8.84	7.61	21.31	10.07	7.63	19.16	11.64
10:16:2.67:48.3	40	11.88	6.67	28.56	8.52	5.16	18.23	10.24
10:16:2.67:38.6	50	10.84	6.95	26.22	9.18	5.89	21.71	12.30
10:16:2.67:32.2	60	9.85	7.09	23.81	9.47	6.22	23.05	13.07
10:16:2.67:27.6	70	9.17	7.26	22.12	9.25	6.54	25.12	14.15
10:16:2.67:24.1	80	8.46	7.05	20.45	8.99	7.37	27.40	15.43

Table 2. – Composition of compound fertilizer, obtained by nitric-sulfuric acid processing Angren coal and thermic concentrate from phosphorite of Central Kyzylkum

The weight ratio of the coal: HNO_3: H_2SO_4: PRM	Norm of the acids on CaO%	Chemical composition,%						
		$P_2O_{5total.}$	P_2O_{5accep}	CaO_{total}	$CaO_{w.s.}$	N	Organic substances	Humic acid
1	*2*	*3*	*4*	*5*	*6*	*7*	*8*	*9*
10:20:3.33:50.5	40	16.72	9.03	33.01	11.38	5.78	15.13	9.26
10:20:3.33:40.5	50	15.30	9.51	29.96	11.64	6.39	16.55	10.12
10:20:3.33:33.7	60	13.98	9.79	27.34	11.73	6.80	18.13	11.15
10:20:3.33:28.9	70	12.93	9.97	25.29	12.32	6.92	18.87	11.67

1	*2*	*3*	*4*	*5*	*6*	*7*	*8*	*9*
10:20:3.33:25.3	80	12.01	9.89	23.34	12.27	7.68	19.34	11.96
10:16:2.67:40.5	40	16.33	8.47	32.02	8.94	5.30	18.73	10.58
10:16:2.67:32.4	50	14.75	8.84	28.90	10.03	6.02	22.28	12.60
10:16:2.67:26.9	60	13.42	9.10	26.36	9.98	6.35	23.61	13.39
10:16:2.67:23.1	70	12.39	9.22	24.25	10.76	6.49	25.67	14.51
10:16:2.67:20.2	80	11.46	9.07	22.43	10.69	7.92	26.52	14.86

The weight ratio among the organic portion of the coal, nitric and sulfuric acids monohydrate and PRM are presented in the first column of the Tables 1 and 2. When obtaining the first of the fifth products, the weight ratio among the organic portion of the coal and nitric acid monohydrate was 1:2, while the concentration of sulfuric acid in the nitric acid solution was 5%, and norm of the acids for decomposition of the PRM ranged from 40 to 80% from the stoichiometry's amount. When preparation of the products the following 6–10 a compare with previous products, the weight ratio among organic portion of the coal and nitric acid monohydrate was 1:1.6, and the norm of the acids for decomposition of the PRM ranged from 40 to 80% from stoichiometry's amount, as well. The optimal condition for obtaining complex fertilizers was found out.

Results and discussion

Experimental results have shown that it is independent on the ratio of the organic portion of the coal: HNO_3: H_2SO_4 increase of the acids' norm for decomposition of PRM from 40 to 80% of stoichiometry leads to decrease in content of the total form of P_2O_5 in the products and increasing the relative content of acceptable P_2O_5, nitrogen, organic substances and humic acids in the fertilizers.

So, when initial weight ratio of the organic portion of the coal to nitric acid monohydrate equal to 1:2, increase of the norm of the acids for decomposition of dust-like fraction from 40 to 80% of the stoichiometry leads to decrease in content of the total form of P_2O_5 from 12.27 to 8.84%, increase the content of acceptable P_2O_5 from 56.14 to 86.09%, nitrogen from 5.41 to 7.63%, organic substances from 14.82 to 19.16%, and humic acids from 8.98 to 11.64% in the products.

In a case of decomposition thermic concentrate with weight ratio of the organic portion of the coal to nitric acid monohydrate equal 1:1.6 from 40 to 80% of the stoichiometry leads to decrease in content of the total form of P_2O_5 from 16.33 to 11.46%, increase the content of acceptable P_2O_5 from 51.87 to 82.35%, nitrogen from 5.30 to 7.92%, organic substances from 18.73 to 26.52%, and humic acids from 10.58 to 14.86% in the products.

For the dust-like fraction weight ratio of the organic part of coal: HNO_3: H_2SO_4: PRM = 10: 16: 2.67: 24.1, acid norm is 80%, the composition of fertilizers (wt.%): 8.46 $P_2O_{5total.}$; 7.05 $P_2O_{5accep.}$; 20.45 $CaO_{total.}$; 8.99 $CaO_{wat.sol.}$; 7.37 N; 27.40 of organic matter; 15.43 of humic acid; $P_2O_{5accep.}$: $P_2O_{5total.}$ = 83.33%.

For the thermic concentrate weight ratio of the organic part of coal: HNO_3: H_2SO_4: PRM = 10: 16: 2.67: 23.1, acid norm of 70%, the composition of fertilizers (wt.%): 12.39 $P_2O_{5total.}$; 9.22 $P_2O_{5accep.}$; 24.25 $CaO_{total.}$; 10.76 $CaO_{wat.sol.}$; 6.49 N; 25.67 of organic matter; 14.51 of humic acid; $P_2O_{5accep.}$: $P_2O_{5total.}$ = 74.41%.

It was defined that product commodity properties of fertilizers. They are compressed, even with a high moisture content will remain full their friability. The strength of the granules exceeds the requirements of GOST. Increased hygroscopicity requires packing of the product in bags.

Based on the results of laboratory experiments and experimental work in the model laboratory plant it was installed that basic technological parameters of the process of obtaining OMF. The basic technological scheme has been proposed, the material balance has been compiled and the economic indexes for production of one ton of OMF have been calculated.

Conclusion

Thus, the resulting complex fertilizers possess considerable advantages. In the first they are concentrated and they can be transported in the long distance and export. The second the economic effect will be not only of benefit when production complex fertilizers, and form application them in the agriculture.

When application humic containing fertilizers unconditionally will increase humic in soil, as well as the structure, physico-chemical properties of soil will improve significantly, using coefficient nutrients of applied fertilizers will increase, the crop of the agriculture plants will raise. Moreover, fixed phosphates in soil will be mobilize partially which are in unacceptable for plant form

Thus, nitric-sulfuric acid processing of brown coal of Angren deposits and phosphorite of Central Kyzylkum allows to obtain highly effective complex fertilizers.

References:

1. Workshop on Soil/Ed. I. S. Kaurichеva. – M.: Agropromizdat, 1986.
2. A. I. Zhukov The balance of humus in the soils of the USSR and the need for organic fertilizer//Proceedings of the All-Union. Research Institute of Agricultural Microbiology. – L., V. 58. 1988.
3. Sattorov D. S., Ergashev A. E., G. I. Kobzev The agrochemical research of soils in Uzbekistan and ways to improve of their fertility//Institute of Soil Science and Agricultural Chemistry, Tashkent, 1990.
4. Derzhavin L. M., Sedova E. V., On the question of humus reproduction//Agrochemistry, 1988, No 9.
5. Klimenko A. I., Rakhimov V. R., Kyaro V. A., The coal industry of Uzbekistan: the stages of formation and development ways//Mining Journal, 2002. Special Edition.
6. Klimenko A. I., Rakhimov V, R., Catherine V., Prospects for comprehensive utilization of resources of coal deposits in Uzbekistan//Mining Journal, 2002, Special Edition.
7. Bobohodzhaev I. Humus and soil fertility//Agriculture of Uzbekistan, 1992. No 8–9.
8. Usanboev N., Namazov Sh. S., Beglov B. M., The oxidation of brown coal from Angren by nitric acid//Chemical Industry, 2006. V. 83, No 2.

Markov Evgenii Albertovitch,
Saint-Petersburg state university of economics,
Saint-Petersburg, Student, The Faculty of Computer science
E-mail: markov.ewgenij@yandex.ru

Jewelry Making with 3D Printing

Abstract: The article describes the stages of jewelry making with the 3D printer. Provides descriptions of the methods of creating jewelry. An analysis was conducted of the use of 3D printers in the jewelry industry on Russian and foreign markets.

Keywords: 3d printer, jewelry, additive manufacturing.

Computer technology is increasingly fused with real life. However, the line between real reality and virtual reality remains. Technologies that allow you to see three-dimensional computer model in real life are not strongly common. Such technology applies 3D printing.

Since the beginning of the new Millennium, the term of "3D" have become part of our everyday life. First of all, we associate it with cinema, photography or animation. But hardly there are people who at least once in my life heard of such a new product, like 3D printing.

A 3D printer is a peripheral device that uses a method of creating a layered physical object on the digital 3D model. 3D printing is construction of the real object from the model of the 3D model created on a computer. Then, a digital three-dimensional model saved in the STL format file, then the 3D printer, which displays the print file, creates an actual product [1].

3D printing is a series of repeating cycles associated with the creation of three-dimensional models, drawing a layer printer consumables on the desktop, wherein the desktop is moving down to the level of the finished layer and removing from the surface of the table waste.

Cycles continuously follow one another: on the first layer of material is applied next, the Elevator is lowered again and so until then while on the desktop will not be a finished product.

The use of three-dimensional printing is a serious alternative to traditional methods of prototyping and small batch production. 3D printer, unlike usual, which displays two-dimensional drawings, photos, etc. on paper, gives the ability to display three-dimensional information or to create a three-dimensional physical objects.

The advantages of such devices over the conventional methods of creating models are high speed, simplicity and low cost. For example, in order to create a model manually, it may take several weeks or even months, depending on the complexity of the product. As a result, significantly increase the costs of development, increases the duration of release of the finished product. 3D printers allow to completely get rid of manual work and to create a model of the future product in just a few hours thus eliminating the possibility of errors inherent in "the human factor".

The term 3D printing has several synonyms, one of which briefly and accurately describes the essence of the process is "additive manufacturing, i. e. manufacturing by adding material. The term was coined not by accident, for this is the main difference between multiple 3D printing technologies from conventional industrial production methods, received the name "subtractive techniques" that is "consuming". When the cutting, sanding and other similar procedures, the excess material is removed from the workpiece, in the case with additive manufacturing, the material is gradually added to obtain a coherent model [2].

To ensure that the technology was classified as "3D printing", it is necessary to build the final product from the raw materials and not from blanks, and the formation of the objects should be random — that is, without the use of moulds. This means that additive manufacturing requires software component. Frankly speaking, additive manufacturing requires the management with the participation of computers, to form final products can be determined by constructing digital models. It is this factor that has delayed wide-spread 3D printing until the time when numerical control and 3D design have become available and high-performance.

Modern 3D printers are not only used in different industries, but in art too. Today jewelers have the unique opportunity to increase the speed of creating products. At that time, as most creative individuals do not even know about the existence of jewelry printer, the happy owners of such devices already own the printed decorations. Of course, the plastic jewelry does not have much value, but with the help of this printer you can create the perfect moulds for casting these products.

First and foremost, it should be noted that 3d printing in jewelry can

be applied in several directions, for example:

- For small batch production of different materials (precious metals, polymers, and others);
- For prototyping decorations;
- For the manufacture of molds;
- For the production of advertising, exhibition products.

For creating jewelry in gold, silver, bronze, copper and brass, we use Lost-Wax printing and casting. This technology builds upon modern 3D printing technology as well as traditional metal casting.

In the modern market of jewelry is impossible to achieve success and firmly hold the leadership without the use of modern technology, which not only dramatically save jeweler's time and money, but also allow you to create true masterpieces of gold and silver jewelry that were previously just out of reach for the vast majority of jewelers.

This is not a rant — it is a fact: the 3D printing technology has made a real revolution in the production of jewelry, allowing you to quickly and inexpensively create original fine jewelry.

But in order to get ready the jewelry, you need to start to make the 3D model. 3D models are created by hand with using computer graphic design or due to 3D scanning. Manual modeling, or preparing geometric data for creating three-dimensional computer graphics, somewhat reminiscent of the sculpture.

3D scanning is the automatic collection and analysis of data of the real object, namely shape, color and other characteristics, is converted to a digital three dimensional model. Manual and automatic creation of 3D-printed models can cause difficulties for the average user. In this regard, in recent years has been the spread of 3D printing marketplaces. Among the popular examples are services such as Shapeways, Thingiverse and Threeding [3].

To download computer models in the software the printer files are used in a common STL format (STereoLithography). This file format is used by the overwhelming majority of CAD programs for storing three-dimensional models of objects and subsequent use in the technology of rapid prototyping. Information about the object when it is stored in text or binary format, as a list of triangular facets that describe the surface and their normals.

The main feature of the device to manufacture jewelry is in high precision printing. This is the most important parameter in this field.

For jewelry making with the 3D printer uses Stereo Lithography Apparatus and Digital Light Processing (DLP and SLA-SLA). These printing methods allow you to create precision products of the photopolymer resin so accurate that no master can not be compared. Some of the SLA plants allow to achieve a thickness of one micron is 100 times thinner than a human hair!

SLA printers allow you to create highly accurate models from photopolymer resins burn with zero residual. Put simply, the decoration can simply draw using three-dimensional graphics editor, print inexpensive photopolymer master model, and then it to use to create the final plaster mold.

Such a photopolymer resin leaves no ash during burning, and therefore the mold will not have to clean. It remains only to pour the molten precious metal. There is, however, one additional step, namely, illumination. A ready model will have to be placed in a chamber with UV light for complete polymerization, i. e., curing.

As for materials, you have to spend on photopolymer resin. One liter of this material is 3–4 more than 1 kg of plastic for printing on FDM printers. Price for 1 liter photopolymer resin — $ 150. But the flow of the material in the work is quite small, a liter will last for a long time.

The main advantages of jewelry 3D printers — the ultra-high print accuracy and excellent quality of the created surface. I emphasize again that due to applied technologies of printed three-dimensional model are extremely smooth and do not require additional treatment or adjustments.

So jewelers can forget about jewelry wax and the variety of related tools. And the most important thing — jeweler can forget about the amount of highly skilled hand work to create master models from wax [4].

Printers for creating jewelry is not yet widely spread in Russian market. However, in foreign countries masters are actively using such devices and jewelry 3D printers many times make your workflow easier. Chinese models of printers have a lower cost, however the quality and accuracy is also low. Russian 3D printers are something in between European and Chinese models. They have lower cost in comparison with European, but with higher quality and precision than the Chinese.

Long gone are the days when to create the form had to wait a lot of days. Due to advanced software and high precision printing, advanced 3D printers are able to create a three-dimensional object in a short period of time [5].

Due to such technologies jewelry industry has reached a new level. While the cost and time to production are significantly decreased.

Thus, use 3d printers in jewelry significantly reduce the complexity in the manufacture of jewelry.

References:

1. Online resource, available at: http://www.somslibrary.org/3d-printer.html.
2. Online resource, available at: https://all3dp.com/what-is-stl-file-format-extension-3d-printing/nnost_ 2011–07–18.html.
3. Isaac Budmen, Anthony Rotolo *The Book on 3D Printing* (2013), 275 p.
4. Online resource, available at: http://explainingthefuture.com/3dprinting.html
5. Online resource, available at: http://usinedesusines.com/rapidprotot.htm

Section 6. Physics

Kaganov William Ilich,
Institute of Radio Engineering
and Telecommunication Systems,
Moscow University MIREA
E-mail: Kaganovwil@yandex.ru

On the transformation of electromagnetic waves in a gravitational: possible experimental verification

Abstract: The idea, expressed more than 50 years ago, on the generation of gravitational waves in the propagation of electromagnetic waves in a constant transverse magnetic field is discussed. Fundamentals of physical experiment for testing this idea with the help of modern radio-electronic means are regarded.

Keywords: electromagnetic waves, gravitational waves, magnetic field/DOT 10.20534.

1. Physical foundations of the method. In [1; 2] in the framework of general relativity, the analysis of excitation of gravitational waves in the propagation of electromagnetic waves in a transverse static magnetic field are discussed.Thanks to the phenomenon of wave resonance arising at propagating oscillations with equal velocities (in this case the speed of light) between the electromagnetic and gravitational waves occurs oscillation process energy exchange. Based on these study, we consider the possibility of experimental verification of the interaction of two types of waves with the use of modern means of electronics. Referring to the formula given in [2], which allows to determine the energy of electromagnetic waves, that are converted into the energy of the gravitational wave. This formula with a different dimension of the parameters is as follows:

$$\alpha = \frac{W_{GV}}{W_{EM}} = K_W \left(\frac{G}{c^4}\right) H_0^2 R^2 = 10^{-32} H_0^2 R^2 \qquad (1)$$

where W_{EM} — total energy of the electromagnetic waves, W_{GV} — energy electromagnetic waves to be converted into energy of gravitational waves, the K_W — constant factor, G — the gravitational constant, c — speed of light, H_0 — magnetic field strength (the dimension MOe), R — region of interaction o waves (dimension m). We will get at R = 100 m and H_0 = 10 MOe according to (1) $\alpha = 10^{-26}$ and therefore, by using a source of electromagnetic waves with a capacity of 1 Mw capacity of gravitational waves is very small value of 10^{-14} μW.

The process of interaction between the two types of waves in a constant magnetic field, according to [1; 2] is oscillating. Therefore, the power of electromagnetic waves, converted from a gravitational waves, it is also equal to 10^{-14} μW. Let us ask ourselves: is it possible to identify such electromagnetic waves, the source of which is the gravitational. For experimental verification of this physical phenomenon is necessary to solve at least four technical problems under pulsed operation.

2. The first problem is related to the a powerful source of electromagnetic waves. The proposed model of the experimental setup is shown in Fig. 1 According to her the signal of microwave synthesizer after the preamplifier 2 is input to the klystron 3 with a pulse power of 1 MW. The signal frequency is 10 GHz, frequency stability of at least 10^{-9}. One of waves propagating through the main channel, is exposed to a transverse magnetic field, the second — no.

The main channel is a rectangular pipe 100 m long and 2 m side, in which the high vacuum is maintained. At the beginning and end of the pipe transmitter (6) and receive (7) parabolic antenna with diameter 1.8 m is installed. What antenna forming at a frequency of 10 GHz radio beam with a solid angle of one degree. Beam diameter is 1.76 m at a distance of 100 m. Thus, as a powerful source of electromagnetic waves is proposed to use a pulsed multiresonator klystron having high efficiency and power gain.

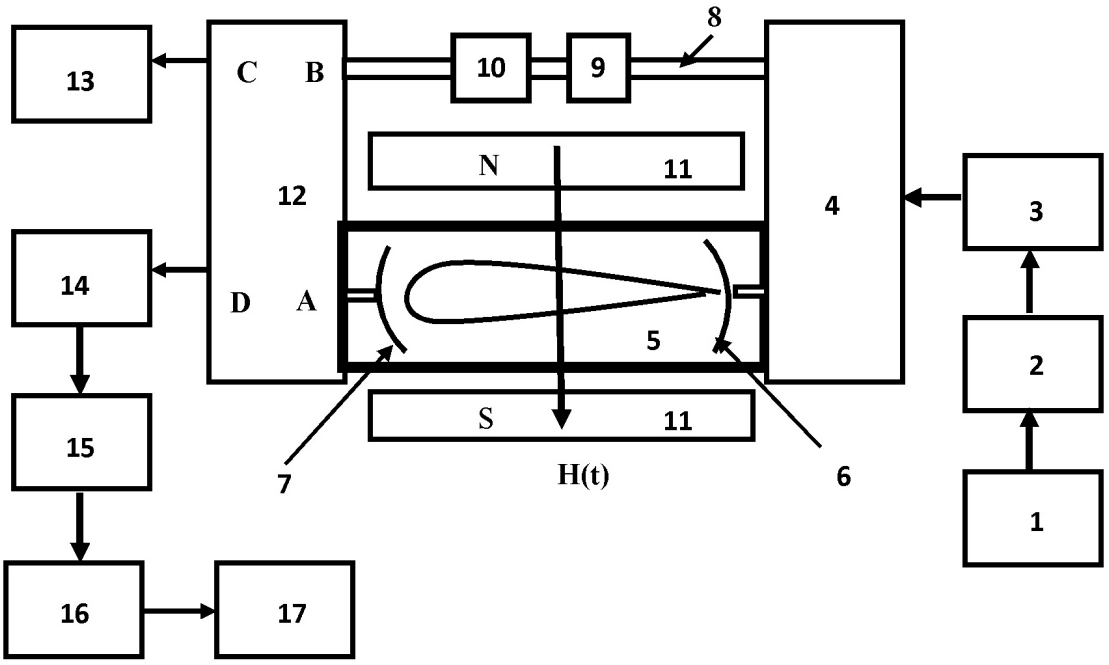

Figure 1. General scheme of a physical experiment

1 – frequency synthesizer; 2 – pre-amplifier of the microwave signal; 3 – pulse klystron; 4 – power divider signal; 5 – tube, along which the electromagnetic wave propagates; 6 – parabolic transmission antenna; 7 – parabolic receiving antenna; 8 – coaxial cable or waveguide supplemental channel; 9 – variable attenuator; 10 – phase shifter; 11 – a group of solenoids; 12 – quadrature bridge device; 13 – load; 14 – low-noise amplifier; 15 – receiver; 16 – signal processing unit; 17 – oscilloscope.

The main channel is a rectangular pipe 100 m long and 2 m side, in which the high vacuum is maintained. At the beginning and end of the pipe transmitter (6) and receive (7) parabolic antenna with diameter 1.8 m is installed. What antenna forming at a frequency of 10 GHz radio beam with a solid angle of one degree. Beam diameter is 1.76 m at a distance of 100 m. Thus, as a powerful source of electromagnetic waves is proposed to use a pulsed multiresonator klystron having high efficiency and power gain.

3. The second problem is related to the creation of a powerful magnetic field. To solve it is proposed to use a large group of solenoids (item 11 in Figure 1), which is located along the main channel and creating a transverse magnetic field with respect to the propagating through the pipe electromagnetic wave.

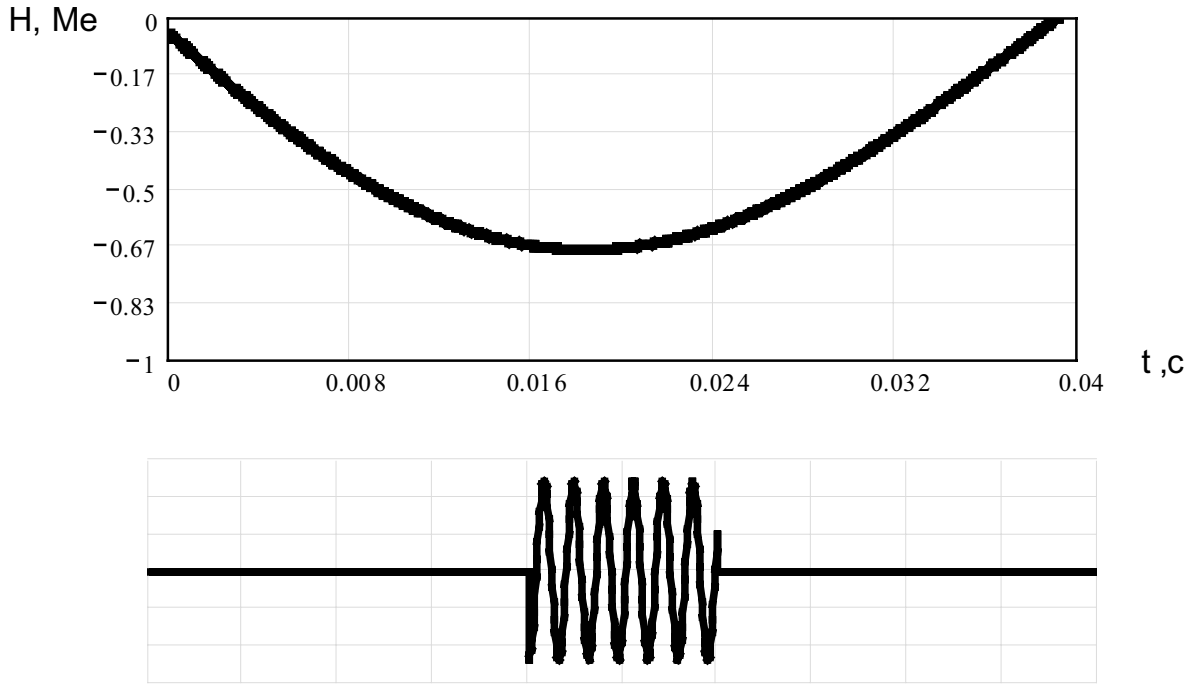

Figure 2. Schedules of change the magnetic field and microwave pulse

Current source for each of the solenoids serves capacitor C = 0.1 F charged to voltage U_0 = 1000 V. When closed L–C circuit where L is the inductance of the solenoid, damped oscillations occur in the circuit. An initial vibration amplitude current I_m=7 kA at a resonance frequency of circuit f = 12,5 Hz, and quality factor Q=8. Coefficient of efficiency converting electrical energy stored capacitor to energy of magnetic field the solenoid in this mode, is 80%. At a electric current 7kA the tension of magnetic field inside the solenoid is 675 kOe, and outside of it — 100 kOe. 100 the solenoids in one plane will create inside the main channel (item 5 in Figure 1) of the field magnetic strength in the 10Me. To maintain this magnetic field along the entire channel length of 100 m will require 10,000 the solenoids. With their help, we can create in a pulse — oscillatory mode magnetic field perpendicular to the propagating through the pipe electromagnetic wave with an amplitude of 10 Mae and duration τ = 10 ms (Figure 2).

The total energy stored all the capacitors to generate the required pulse magnetic field is 500 MJ. Since the capacitor charging time can be many times greater than the time of their discharge, the capacity of the primary power supply does not exceed 100 kW. Processes to incorporate all the solenoids and klystron must be synchronized.

4. The third problem is related to the division useful and interfering signals. According to a calculation at of the magnetic field strength at a 10-MOe are generated gravitational waves and the oscillation process exchange of energy two types of waves. The length and amplitude of the electromagnetic wave as it passes the speed of light along a new geodesic d through the emerged gravitational field in the vacuum of space will change, which corresponds to the amplitude and frequency modulation of the signal.Since according to (1), only a small portion of the electromagnetic wave energy is converted into the gravity, then the output from the primary channel will have two components unexposed and exposed to the action of the gravitational field:

$$u_1(t) = U_1 \sin(\omega_0 t) + U_2\left(1 + m(t)\right)\sin\left(\int_0^{\tau} \omega(t)dt\right) \quad (2)$$

where ω_0 — frequency signal of klystron, amplitude $U_1 \gg U_2$.

The second term in (2) is a useful component, because it contains information about the existence of gravitational waves during the time τ, the first term — a powerful sinusoidal disturbance.

For the separation of wanted and unwanted signals is proposed to use quadrature bridge device (position 12 in Figure 1) by supplying the input of the "A" signal (2), which is exposed to the gravitational field, and the input of the "B" Segal, who was on the supplemental channel 8 — waveguide or coaxial cable (Figure 1). The signal at point B should be shifted in phase relative to the signal at the point A to $\pi/2$:

$$u_2(t) = U_1 sin(\omega_0 t + \pi/2), \quad (3)$$

To obtain two signals of equal amplitude and phase shift equal to $\pi/2$, the second channel are integrated adjustable attenuator (9) and a phase shifter (10). Bridged quadrature device sums two identical fluctuations, offset in phase by $\pi/2$, therefore a signal which is determined by the first term in the expression (2), and the signal (3) is directed to the output "C", which is connected to the load 13 [3]. The useful signal, i. e. second tent of signal (2), will go to the two channel quadrature output device. Thus, reducing the useful signal only 3 dB, it can be separated from the interfering signal.

5. The fourth problem is associated with the identification of the useful signal. Wanted signal separated from the interference signal and is input to the microwave low noise amplifier (item 14 in Figure 1) radio receiver. Define a radio sensitivity required for identification of the useful signal, which contains information about the gravitational wave. Here are the known relation to determine the sensitivity of a radio receiver, referring, for example, [4]:

$$P_r = 10^{-6} kT_0 K_n C_{sn} \Delta f_r \; S \;\; (\mu W), \quad (4)$$

where $kT_0 = 4 \cdot 10^{-21}$ W/Hz — spectral power of the standard at the reference temperature T_0 = 290 °K, K_n — the receiver noise figure, Csn — the required signal to noise ratio at the detector input, Δf_{pb} — receiver bandwidth, *S*- coefficient taking into account the additional loss of signal in the adder

We assume for the parameters in (4): Kn = 1.25 (through the use of low-noise amplifier), the *S* = 2, Δf_r = =10 Hz, C_{sn} = 0.1. Such a small value of the last parameter can be prepared by correlation and other signal processing methods. We get the receiver sensitivity $P_r = 10^{-14}$ μW according to (4) and will be able to identify the useful signal at the output of the signal processing unit 16 (Figure 1).

Generator and receiver must be located in the shielded chambers to avoid direct communication between them.Thus, this physical experiment allows you to test the ideas expressed in [1; 2], and to carry out the generation of gravitational waves in the ground conditions.

References:

1. Герценштейн М. Ь. Волновой резонанс световых и гравитационных волн. ЖЭТФ, т. 41, 1961, вып. 1 (17), С. 113–114.
2. Зельдович Я. Б. Электромагнитные и гравитационные волны в магнитном поле. Препринт № 30 за 1973 г., Институт прикладной математики АН СССР.
3. Altman J. L. Microwave circuits. – INC Princeton, 1964.
4. Каганов В. И. Радиотехнические цепи и сигналы. – М.: ФОРУМ-ИНФРА-М., 2013.

Section 7. Chemistry

Aliyeva Mahira Iosaf,
Azerbaijan State Oil and Industry University
PhD student, the Faculty of Chemical Engineering
E-mail: bvl_ok@rambler.ru
Baghiyev Vagif Lachin,
Azerbaijan State Oil and Industry University, Professor,
Department of chemistry and chemical materials engineering
E-mail: Vagif_bagiev@yahoo.com

Influence of the crystallinity degree of vanadium containing catalysts on their activity in the propylene oxidation reaction

Abstract: The influence of the crystallinity degree of Sn-V-O, Mo-V-O, and W-V-O catalysts on their activity was investigated in the reaction of propylene oxidation. We found that for Sn-V-O, and W-V-O catalysts observed curve with one maximum for yield of acetic acid, while on Mo-V-O catalysts observed curve with two maximum.

Keywords: propylene, oxidation, binary catalysts, vanadium oxide, crystallinity.

One of the possible method for acetic acid production, a valuable chemical for the petrochemical industry, is the direct oxidation of propylene over heterogeneous catalysts. Catalyst systems based on vanadium oxide, molybdenum, tungsten, etc. show high activity in olefin oxidation reaction into acetic acid. [1; 2]. Previous studies provided by us have shown that the synthesized vanadium oxide containing catalysts exhibit high activity in propylene oxidation reaction to acetic acid, [3; 4]. In this paper, we investigated the effect of the degree of crystallinity of vanadium containing catalysts on their activity in the oxidation of propylene into acetic acid.

Experimental

Vanadium-containing catalysts of different compositions were prepared by co-precipitation from aqueous solutions of salts of tin, molybdenum, tungsten and vanadium. The obtained mixture was evaporated and dried under 100–120 °C, decomposed until complete decomposition of the initial salts at 250 °C, and then calcined at temperature 550 °C within10 hours. Thus, the 27 catalysts were synthesized the elements of atomic ratio from Me: V = 1: 9 to Me: V = 9: 1 (where Me is Sn, Mo and W).

X-ray study of the phase composition of the prepared catalysts were carried out by powder diffractometer «D2 Phaser» (CuKα-radiation, Ni-filter). The degree of crystallinity of the synthesized samples are calculated using "Diffrac.eva" program.

Activity of synthesized catalysts were studied in the flow unit at a volume feed rate of 1200 h^{-1} in the temperature range 200–700 °C. The quartz reactor was charged with 5 ml of the catalyst grained 1.0–2.0 mm and its activity was studied in a propylene oxidation reaction. Outputs of carbon dioxide and propylene determined by chromatograph with a column length 3m. packed with polysorb-1 coated by Vaseline oil. Acetaldehyde, acetic acid and acetone yields were determined on chromatograph with a flame ionization detector on a column 2 m in length, filled with sorbent polisorb-1.

Results and discussions

Research of phase structure of binary vanadium containing catalysts have shown that there are three compounds, two modification of WO3 and V2O5 in the catalytic system W-V-O. Analyzing and interpretation of the diffraction patterns of Sn-V-O oxide systems showed that all samples are consist of two phases, namely SnO2 and V2O5. In the catalytic system Mo-V-O phase there are MoO3, V2O5 and various polymolybdates.

On the basis of radiographic data also calculated the degree of crystallinity of the synthesized catalysts. The calculated values of the degree of crystallinity of binary vanadium containing catalysts are given in Table 1.

Table 1. – The crystallinity of the samples in the W-V-O, Sn-P-O and Mo-V-O systems

W-V-O	Crystallinity,%	Sn-V-O	Crystallinity,%	Mo-V-O	Crystallinity,%
1–9	77,7	1–9	79,2	1–9	82,6
2–8	78,9	2–8	74,5	2–8	78,3
3–7	80,0	3–7	76,5	3–7	79,6
4–6	80,2	4–6	74,9	4–6	75,7
5–5	79,8	5–5	73,8	5–5	80,5
6–4	80,5	6–4	72,1	6–4	77,5
7–3	79,2	7–3	70,4	7–3	81,0
8–2	80,9	8–2	63,5	8–2	77,6
9–1	80,6	9–1	62,0	9–1	77,9

As shown in Table 1, and crystallinity of W-V-O and Mo-V-O systems practically does not change with changing of composition, while for an Sn-V-O system crystallinity decreases from 79.2% at the sample Sn-V=1–9 untill-62% on a sample Sn-V=9–1.

The crystallinity of the synthesized catalyst may have any influence on their activity in propylene oxidation reaction. Figure 1 shows the dependence of the activity of Sn-V-O catalysts in the oxidation of propylene on their degree of crystallinity. As seen from figure 1 for the Sn-V-O catalysts with increasing of crystallinity degree of the catalyst the conversion of propylene and acetic acid yield unchanging until degree of crystallinity 70%. Further rising of degree of crystallinity leads to increasing of the conversion of propylene and acetic acid yield. Yield of the carbon dioxide as seen from the figure is slightly reducing with rising of crystallinity degree. This allows us to say that a certain value of the degree of crystallinity of the catalyst plays an important role in the formation reaction of acetic acid.

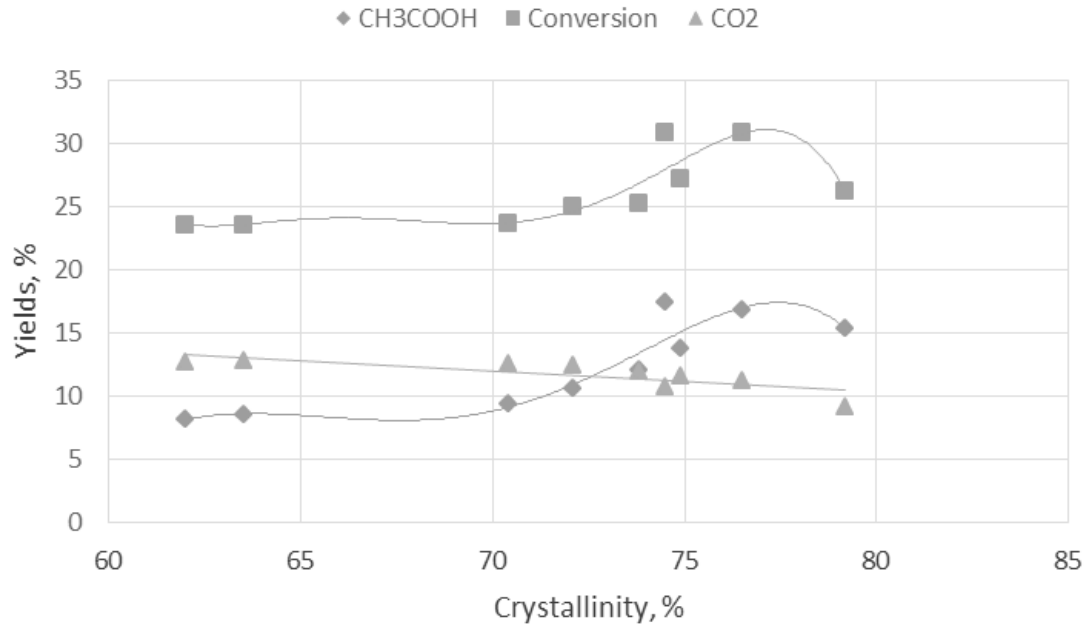

Figure1. Dependencies outputs of acetic acid, carbon dioxide, and conversion of propylene on crystallinity of Sn-V-O catalyst system

Depending outputs of acetic acid, carbon dioxide, and conversion of propylene on the degree of crystallinity of Mo-V-O catalysts are shown in Figure 2. It can be seen that for Mo-V-O catalysts dependences of propylene conversion and yield of acetic acid on the crystallinity degree of the studied samples have the form of curves with two maximum. This is probably due to the fact that the surface of the molybdenum-vanadium catalysts have two types of active centers for propylene oxidation reaction to acetic acid. The figure also shows that carbon dioxide output increases slightly with rising of the crystallinity of the samples.

Figure 3 shows effect of the crystallinity degree of W-V-O catalysts to the conversion of propylene and acetic acid and carbon dioxide outputs. As can be seen, for W-V-O catalysts conversion of propylene and the yield of acetic acid with increasing of crystallinity slowly increasing and peaking after that and falling slowly. Carbon dioxide yield is practically independent of the degree of crystallinity.

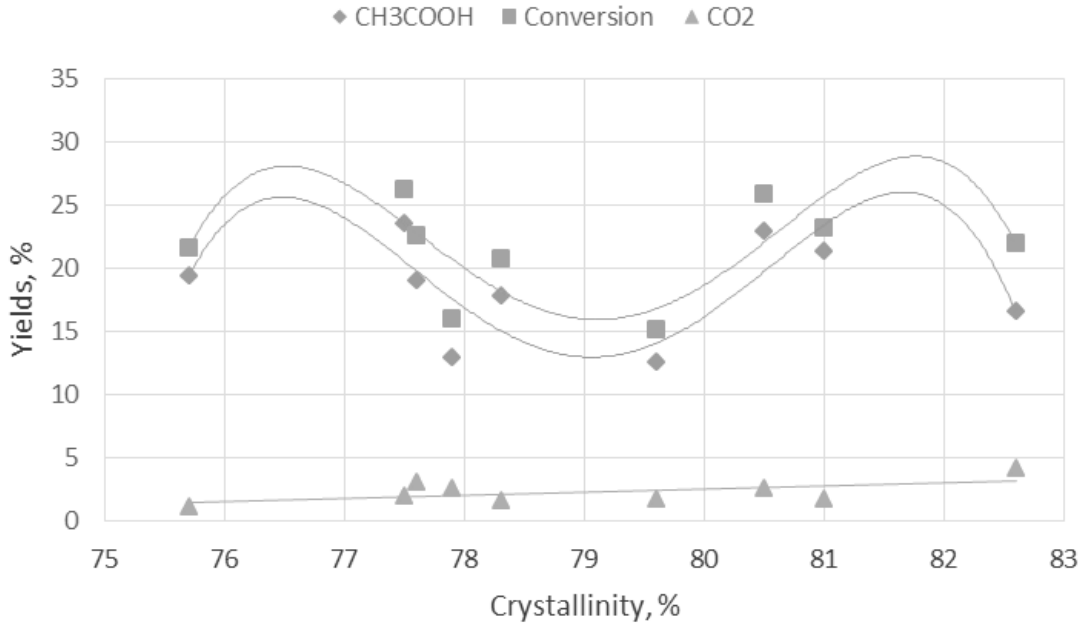

Figure 2. Dependencies outputs of acetic acid, carbon dioxide, and conversion of propylene on crystallinity of Mo-V-O catalyst system

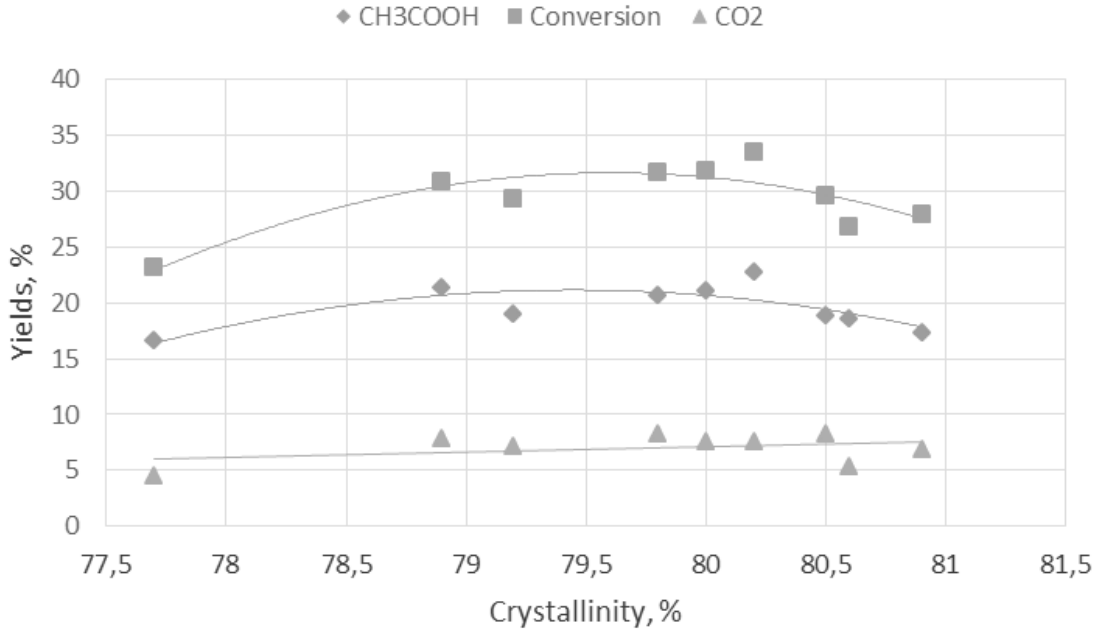

Figure 3. Dependencies outputs of acetic acid, carbon dioxide, and conversion of propylene on crystallinity of W-V-O catalyst system

Thus, it can be say that the crystallinity degree of the vanadium containing catalysts effects on their activity in different way. For Sn-V-O, and W-V-O catalysts curve is observed with a maximum for the yield of acetic acid, while on Mo-V-O catalysts observed curve with two maxima. For the reaction of carbon dioxide formation on all three series of catalysts, influence the degree of crystallinity of the catalysts is weak.

References:

1. Szakács S., Wolf H., Mink G., Bertóti I., Wüstneck N., Lücke B., Seebot H. Catalysis Today, Volume 1, Issues 1–2, 1987. P. 27–36.
2. Abd El-Salaam K. M., Hassan E. A. Surface Technology, Volume 9, Issue 3, September 1979. P. 195–202.
3. Aliyeva M. I., Baghiyev V. L., 15th International Congress on Catalysis, Munich, Germany. 2012. Poster 2.05_8063.
4. Алиева М. И., Багиев В. Л., II Российский конгресс по катализу «РОСКАТАЛИЗ» 2–5 октября 2014 г. Сборник тезисов, Том II, С. 239.

Kurbanova Mohira Abduvahabovna,
Tashkent state technical university,
department "General chemistry",
Faculty Oil and Gas,
person working for doctor degree
Aripdjanova Munira Abdugafurovna,
Tashkent state technical university,
department "General chemistry",
Faculty Oil and Gas, teacher
Mirzaev Usmondjon Mahmudovich,
Tashkent state technical university,
department "General chemistry",
Faculty Oil and Gas, teacher
E-mail: mohira.k@rambler.ru

Spectrally analysis of siloxanes on the basis of meta silicate sodium with borate acid

Abstract: In this article synthesis of boron-containing silicon organical-oligomers is reported. Synthesized oligomers are recommended to use as fire retardants for fire-protective coatings on the base of boron-, nitrogen-, phosphorus and silicon containing compounds in a result of which their thermo stability and fire resistance were increased. It is shown, dependence of yield boron-containing silicon organically oligomers from temperature and ratio of initial reagents. The structure of organically boron-containing silicon has been studied with help of IR- spectra, NMR^{1}H and NMR^{13}C spectroscopy.

Keywords: fire retardants, oligomers, boron-containing silicon, organiacally compounds, nitrogen, phosphorus, silicon, sodium meta silicates, thermo destruction.

It is known that using of polymeric additives containing atoms of boron in their structure has a number of advantages in comparison with low-molecular or inorganic additives: for example formation of deposits and inhomogeneous mass is excluded. Perspective representatives of such compounds are boron-organically polymers.

Earlier it has been shown that using of polyether's and polymethylenethers of phenols and boric acids in epoxide compositions allows to increase their strengths and to lower combustibility [1]. At this possible interaction of boron-polymers and epoxide resins including chemical interactions which haven`t been investigated what complicates of forecasting and using these compounds for obtain compositions with definite complex of properties. On the other hand, there is a problem of improvement and properties of composition materials on the base of rubbers or siloxanes (in particular frictional materials). Also, in last year's connection toughening with ecological requirements, sharply question about replacement of cancer genic asbestos on less toxically components have arised [2].

It is known that owing number of physic-chemical and physic mechanical properties such as substation can be the silicate material which hasn`t possessed by cancer genic properties [3]. It is the other way of regulation properties of compositional materials, introduction in their composition additives of boron-contains and polyorgano-siloxanes changing their properties.

Polyorganosiloxanes have possessed by high thermo stability and low sensitivity to low temperature; their molecules are constructed from silicon atoms connected with atoms and the remained valences of them are saturated by organic radicals (R_1, R_2) or groups. And correspondently their structures can be presented by following schemes:

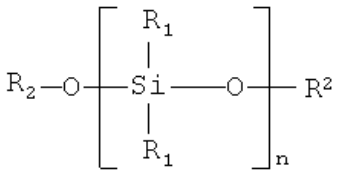

Isolation of link or large site of chain polymeric molecule is connected with necessary rupture of chain in two or three points that is connected with destruction of two or three energetically stable bond Si-O. Therefore, polyorgansiloxanes with spatial bonds irrespective from nature of organic radical, it isn`t observed destruction of chains molecules by bonds Si-O even at 550 °C.

Polyorganosiloxanes differ sharply from organically polymers by structure of their macromolecules and have intermediate state between quartz and organical polymers. The chemical composition and structure of polyorganosiloxanes have defined their properties in technical ratio. All polyorganosiloxanes and organic silicates have possessed by extraordinary high stability to moisture action and thermal destruction.

Synthesis of offered oligomer fire retardant on the base of sodium metasilicate and sodium tetraboron was carried out in glycerin solution. At their molar ratio 1:1. For improvement of thermal stability of formed oligomers the obtained mass was treat by adduct, obtained by interaction of urea with phosphoric acid in molar ratio 1:1.

Scheme reactions of interaction in water solution of sodium metasilicate with sodium tetraborate and adduct area are presented below:

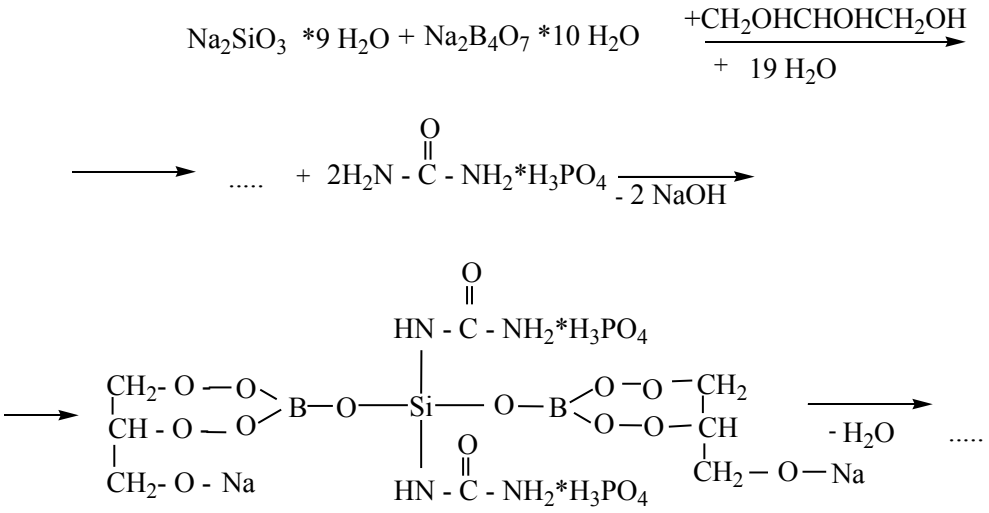

At this dehydration of silicate also was carried out with following addition to silicon atoms of borate and amino- groups and formation three functional silicon-containing oligomers. Synthesis was carried out at temperature 353 °C before obtaining of homogeneous mass. Obtained oligomer has a following characteristics: homogeneous powder of brown color, average molecular mass 2400–2500, nonvolatile, contain of the basic component — 96,66%.

To identify and confirm suspected interactions starting components as well as structures of boron-containing organosiloxanes derived from tetraborate and sodium metasilicate with urea adduct phosphoric acid, we conducted modern analysis methods. Infrared spectra of the samples were recorded on the automatic two-beam infrared spectrophotometer UR-20 in the range of 400–4000 cm^{-1}, thin film at a temperature of 100 °C. Spectra synthesis boron containing organosiloxanes were dropped on the device "Bruker-300" with an operating frequency of 300 MHz and 75. As an internal standard, tetramethylsilane was used.

Considered nuclear magnetic spectral analysis NMR-Unity 400 plus (Varian). Solvent — D_2O, Ref-ce D_2O (4,8 ppm), Expermn; s2pul and C^{13}, NMR Unity 400 plus (Varian), ICPS AS RUz, Solvent; D_2O, Ref-ce; Acetone D6 (30,89 ppm), 20 °C.

Analysis of infrared spectral analysis showed the presence of a boron-containing organosiloxane absorption bands, grafted and block copolymer borate and amine groups and formation of new absorption bands. In the –Si–O–1000–634 sm^{-1}, absorption bands characteristic for the deformation fluctuations siloxane. In the spectrum of characteris bands $–C_2H_5–$ 1160–1180 sm^{-1}, –B–O–1350–1400 sm^{-1} arranged corresponding to vibrations of borate groups, which confirmed the formation of a boron-containing siloxane (Fig. 1).

About occurring, chemical reactions as say ^1H NMR data spectroscopy. In the ^1H NMR spectrum of visible signals in a strong field in the area of 7,6–6,2 ppm (protons of aromatic ring hydrogen), and the signal at 1.14 ppm, characterizing hydrogen protons ethyl — C_2H_5 group, indicates the formation of a graft various functional groups of oligomer synthesized on the basis of borates with sodium metasilicate and the urea adduct of phosphoric acid (Fig. 2).

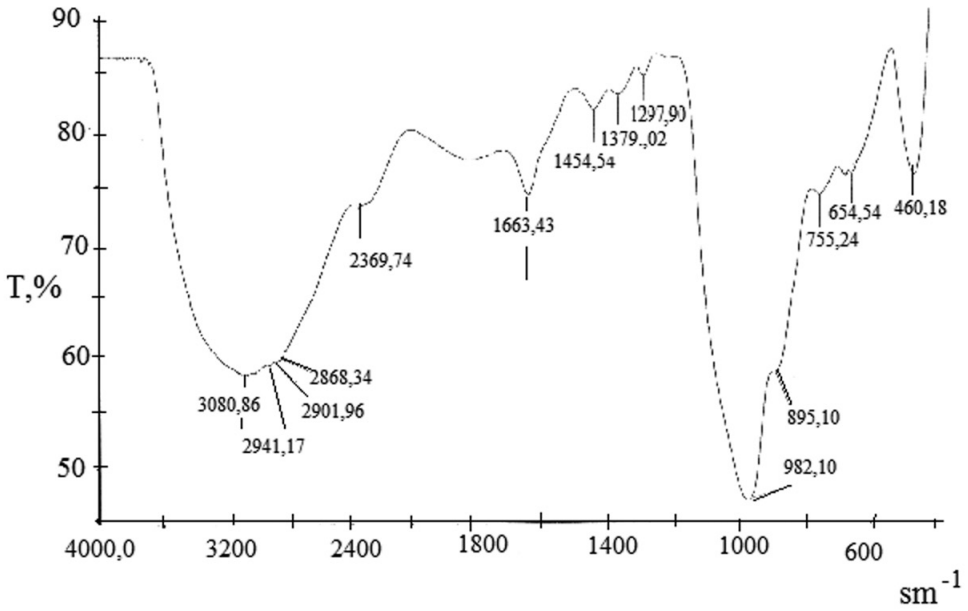

Figure 1. IR- spectral analysis of a boron-containing organosiloxane

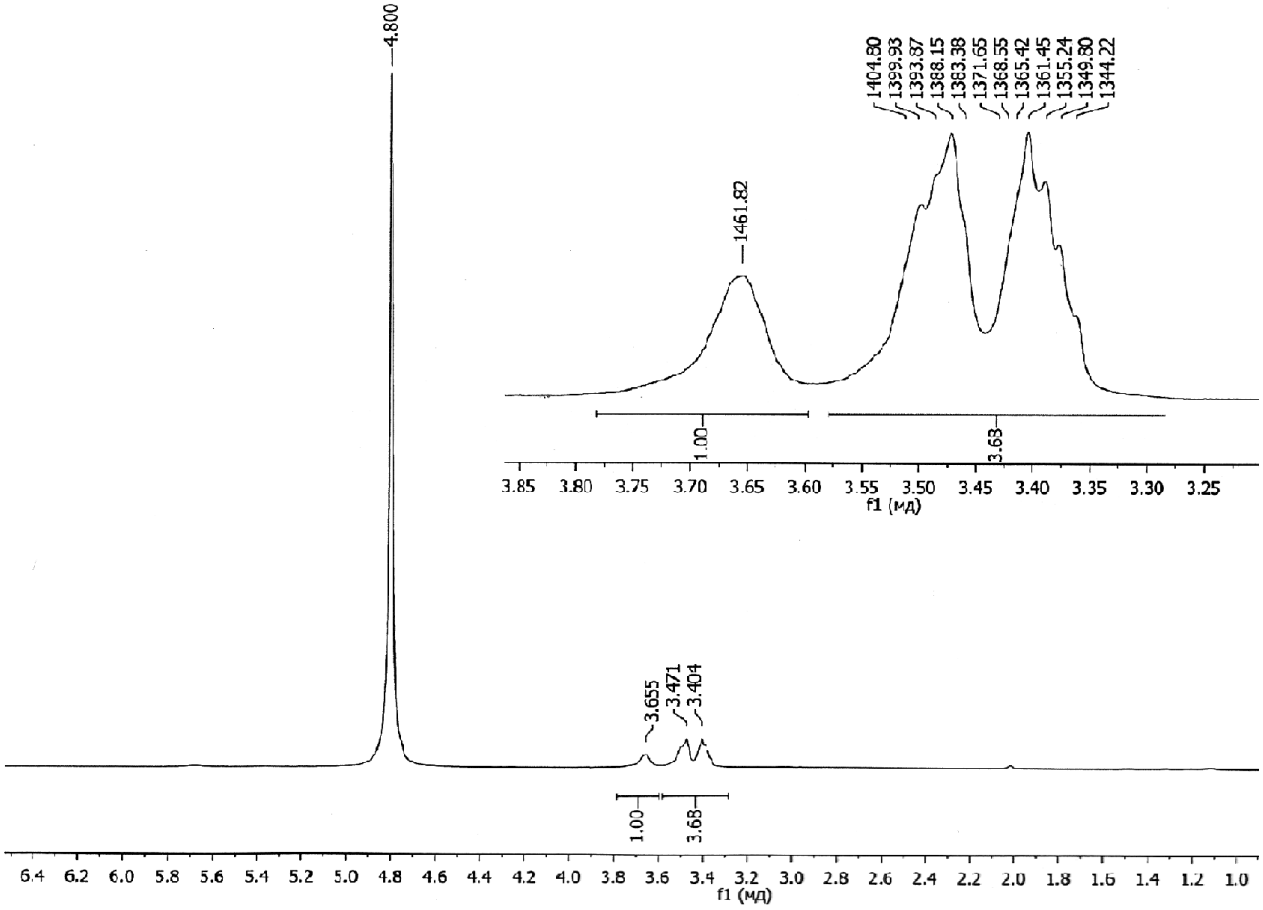

Figure 2. ^{1}H- NMR spectral analysis of the boron-containing organosiloxane

The ^{13}C NMR analysis showed the spectrum (Fig.3), which are signals in strong field (^{13}C <64,141 ppm), i. e. in this compound contains no double bonds. From the ^{13}C NMR spectrum partial suppression of spin-spin interaction implies that there are two polymer macromolecule type -C-O- Si-O- groups (signal at 30,8m. d.), =CH- groups (signal at 46.8 m. d.) bond -CH-CH_2- (signal at 47.6 ppm), type 2 = CH_2-groups (signal at 60.0 ppm and 65.3 ppm) and the quaternary carbon atom (signal at 73.4 ppm). The presence of the quaternary C-atom and a methyl group -CH_2-O- indicates the formation of a graft copolymer proves our proposed mechanism for mechanochemical interactions

with borates organosiloxane. The signal of the protons of the hydroxyl group -OH is located in the region of a weak magnetic field ^{13}C 163 ppm on the chemical shift of signal corresponds to the carbon atom in the substituted aromatic compounds, where possible, and proceeded bormirovanie siloxane groups (p position) [3].

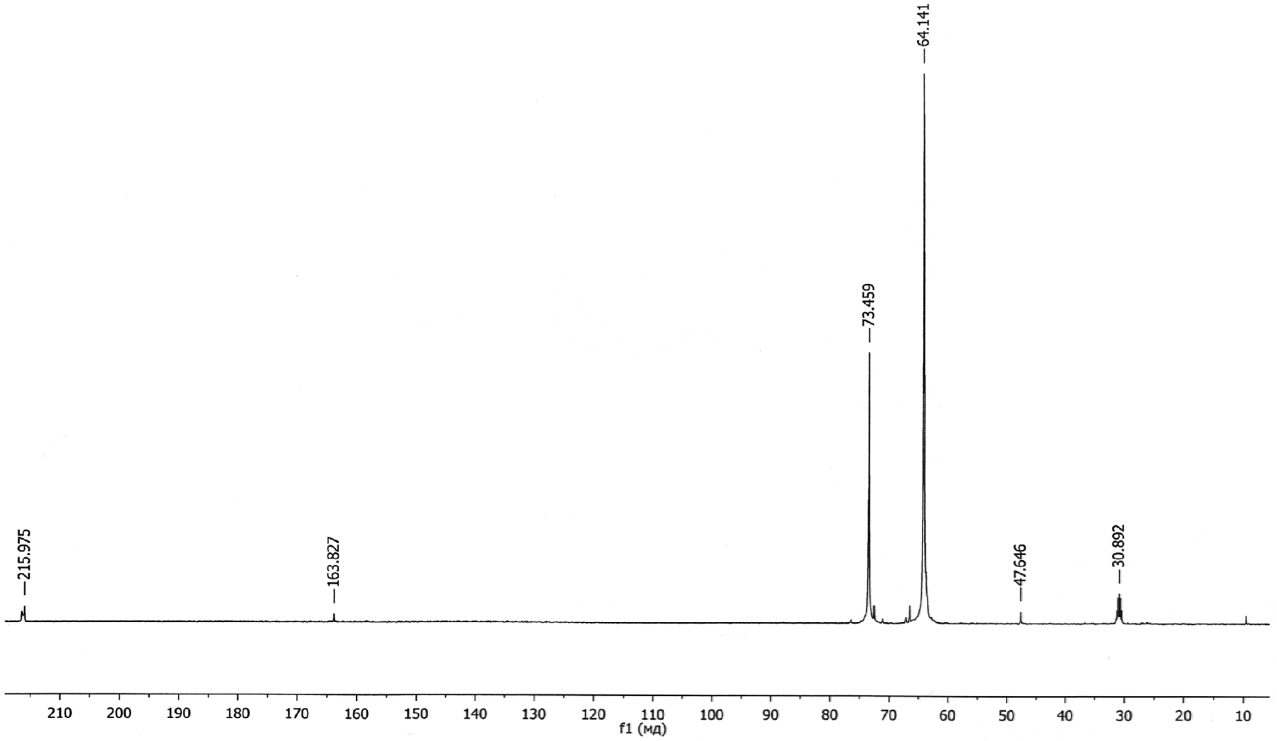

Figure 3. C13-NMR spectral analysis of the boron-containing organosiloxane

Researches in field of formal kinetics, thermal decomposition, polymers are necessary at their process and exploitation and also for some fundamental problems connected with working out of models of carring out reactions in condensed phase [5].

Among methods of investigation kinetics, thermal decomposition of polymers, first of all it is necessary to note as the most informative methods of thermal analysis, as differential scan calorimetric (DSC), the differential thermal analysis (DTA), dynamical and isothermal thermo- gravimetric (TG) [6; 7].

Name of the test material (substance), the composition and physico-chemical properties: Water-dispersion paints fire retardants modified AP-4 based on sodium tetra borate, sodium met silicate and the urea adduct of phosphoric acid.

Thus, organosiloxane resins their excellent qualities have found a various applications [8–13]. Exclusive hydrophobity, thermal stability and other valuable qualities of materials, base have allowed to raise of reliability work machines and equipments, to reduce their masses, to reduce material expenses. Boron and silicon contain compounds are used as fire delays in production of dyers and enamels; for improvement appearance and protection different objects from corrosion and influence of high temperatures, to creation new more perfect electro insulators, sheeting's and so on.

References:

1. Соболевский М. В., Музовская О. А., Попелева Г. С. Свойства и области применения кремнийорганических продуктов./Под.ред. М. В. Соболевского. – М., Химия, 1975. 296 с.
2. Андрианов К.А. Полимеры с неорганическими главными цепями молекул. – М., 1962. – 159 с.
3. Khalanskiy K. N., Lukyanov B. S., Borodkin G. S., Ozhogin I. V., Lukyanova M. B. Study the structures of indolinospiroquinolines by multinuclear and dynamic NMR spectroscopy.//Chemical sciences. Fundamental research. 2013. № 11. P. 456–460.
4. Коптелов И. А., Карьязов С. В. Исследование термодеструкции полимеров методом ДТА и ТГ. //Ж. Пластические массы, 2008. – № 7. P. 24–26.
5. Джалилов А. Т., Тиллаев А., Курбанова М. А., Юсупов И. У. Водно-дисперсионная огнезащитная краска.//Патент РУз. – № IAP 04813.2013.

6. Курбанова М. А., Джалилов А. Т., Тиллаев А. Т., Бекназаров Х., Акбарова С. Р. Огнестойкие кремнийсодержащие соединения.//Аспирант и соискатель. Москва. 2011. – № 5. – С. 163–165.
7. Курбанова М. А., Джалилов А. Т., Тиллаев А. Т. Исследование влияния кремнийорганических соединений на термической деструкции водно-эмульсионных покрытий//Современные проблемы науки полимеров. Тезисы Респуб. научно-прак. конф. Ташкент. 2012. 20–21 Октябрь.
8. Kurbanova M. A., Djalilov A. T., Tillaev A. T., Ismailov I. I., Mirzaev U. M. Updating agnatic-emulsion paints of fluorine contain organosilicon//5th conference "Applied sciences and technologies in the United States and Europe: common challenges and scientific approaches". New York, 2014. P175–178.
9. Курбанова М. А., Исмаилов И. И. Антипирены на основе борсодержащих кремнийорганических соединений//Известия ВУЗов. Серия "Химия и химическая технология". Россия, Иваново, 2015. Т.58. № 12. -С. 10–14.
10. Chi-Long Lee, Gary M. Ronk, both of Midland Mich. Method of preparing fire retardant open cell siloxane foams and foam prepare there from. U. S. Patent. № 4 026 842. 31.05.1977.
11. David J. Romesenko. Midland Mich. Fire retardant resin compositions. U. S. Patent. № 5 412 014. 02.05.1995.
12. Constantions D. Diakomukons. Flame retardant compositions. Midland Mich. U. S. Patent. – № 00566687 A1, 04.03.2010.
13. Smilka O. The complex approach to corrosion protection of steel in coke-plant cool systems. //Chemistry journal, 2015.Vol.1. № 4. p.124-132.

Erkaev Aktam Ulashevich,
Tashkent Institute of Chemical Technology,
Doctor of Technical Sciences, Professor

Kucharov Bakhrom Khayrievich,
Tashkent Institute of Chemical Technology,
Ph. D., Associate Professor

Tairov Zakir Kalandarovich,
Tashkent Institute of Chemical Technology,
Ph. D., Associate Professor

Mursaev Odiljon Alimjonovich,
Tashkent Institute of Chemical Technology,
Master's Degree student

Ulashova Nafisa Aktamovna,
Tashkent Institute of Chemical Technology, Student
E-mail: atabek2004@mail.ru

Crystallization areas of silvine and arcanite involumetric illustration of the system Na^{+}, K^{+}, $1/2Mg^{2+}//1/2SO_4^{2-}$, Cl^{-} -H_2O AT 25 °C

Abstract: There have been constructed projections of silvin and arcanite volumetric imaging offive-component system $2Na^{+},2K^{+},Mg^{2+}//SO_4^{2-},2Cl^{-}-H_2O$ at 25 °C, which allow carrying out technological calculations of their separation from the brine and salt deposits of marine type.

Keywords: arcanite, sylvite, leonite, aphthitalite, halite, picromerite, system, crystallization.

The volume image of the diagrams $Na^{+},K^{+},\frac{1}{2}Mg^{2+}//\frac{1}{2}SO_4^{2-},Cl^{-}-H_2O$ at 25 °C which obviously shows the fields of education of the crystallizing salts and contact of minerals is provided in work [1].

Diagrams of real systems are very complex and difficult to use. In the literature there are known a number of methods of imaging of multicomponent systems [2, 3] — mass centric and the method of translation.

Previously examined method of projecting the isotherm in this case does not result in a significant simplification of its mode. Most often it is more convenient to design a part of the diagram to the area of crystallization

Table 1. – The nodal points of the projection of volume of arcanite and sylvite from the volumetric illustration of the system Mg^{2+}, $2Na^{+}$, $2K^{+}//2Cl^{-}$, SO_4^{2-} -H_2Oat 25°C

Points of structure correspond to points of fig. 1a and 2a	Points of structure correspond to points of fig. 1b and 2b	NaCl	Na_2SO_4	KCl	K_2SO_4	$MgCl_2$	$MgSO_4$	H_2O	Composition of solution,% of the sum of ions			10^{-2} N water number, H_2O mole 100 g Σ salts	Structure of a solid phase
									Na^+	$1/2Mg^{2+}$	Cl^- (SO_4^{2-})		
Projection of volume of a crystallization of an arkanite (SO_4^{2-})													
S_1	E^1_4	–	5,75	–	10,88	–	–	83,37	1	0	0	27,851	Aphthitalite + K_2SO_4
S_3	E^1_5	–	–	25,50	1,05	–	–	73,45	0	0	1	15,369	KCl+ K_2SO_4
E_2	S^3_{12}	–	–	9,00	7,00	11,90	–	72,10	0	0,403	0,597	14,357	KCl+K_2SO_4+ Picromerite
E_3	S^1_3	6,50	1,60	20,55	–	–	–	71,35	0,257	0	0,743	13,836	$NaK_3(SO_4)_2$+KCl+K_2SO_4
E_4	P_{14}	4,09	–	12,37	–	6,62	5,06	71,86	0,104	0,334	0,561	14,187	Aphthitalite+Picromerite+KCl+K_2SO_4
E_5	S^5_3	–	4,38	–	9,53	–	11,83	74,79	0,238	0,762	0	16,142	Aphthitalite+Picromerite+K_2SO_4
	E^3_4	–	–	–	10,80	–	12,60	76,60	0	1	0	18,186	K_2SO_4+ Picromerite
Projection of volume of a crystallization of an silvine (Cl^-)													
S_2	E^1_6	20,42	–	11,14	–	–	–	68,44	1	0	0	12,048	NaCl+KCl
S_3	E^1_5	–	–	25,50	1,10		–	73,45	0	–	1	15,34	KCl+K_2SO_4
E_7	S^4_2	1,8	–	3,55	–	25,85	–	66,00	0,054	0,946	–	11,752	NaCl+KCl+Cryolite
E_4	S^3_{12}	–	–	9,00	7,00	11,90	–	72,10	0	0,757	0,243	14,357	KCl+K_2SO_4+Picromerite
E_6	S^1_4	19,10	2,35	11,20	–	–	–	67,35	0,916	0	0,084	11,46	NaCl+$NaK_3(SO_4)_2$+KCl
E_5	S^1_3	6,50	1,60	20,55	–	–	–	71,35	0,856	0	0,144	13,836	$NaK_3(SO_4)_2$+KCl+K_2SO_4
E_{15}	P_{14}	4,09	–	12,37	–	6,62	5,06	71,86	0,185	0,592	0,223	14,187	Aphthitalite+Picromerite+KCl+K_2SO_4
E_{14}	P_3	10,4	0	8,3	0	7,9	6,45	66,95	0,318	0,49	0,192	11,254	NaCl+Aphthitalite+KCL+Picromerite
E_{12}	P_5	8,6	0	7,9	0	9,3	6,5	67,7	0,263	0,544	0,194	11,644	NaCl+KCl+Leonite+Picromerite
E_{10}	P_7	4,1	0	5,3	0	16,7	6,2	67,7	0,112	0,724	0,164	11,644	NaCl+KCl+Leonite+Kainite
E_8	P_9	1,3	0	3,15	0	25,1	2,05	68,4	0,036	0,909	0,055	12,025	NaCl+KCl+Kainite+Cryolite
S_1	E^3_1	0	0	3,4	0	26,9	0	69,7	0	1	0	12,78	KCl+Cryolite
S_4	S^3_4	0	0	0	7	22,1	1,7	69,2	0	0,819	0,181	12,482	Kainite+KCl+Picromerite
S_3	S^3_6	0	0	3,4	0	24,6	4,2	67,8	0	0,894	0,106	11,698	Kainite+KCl+Cryolite
E_{11}	P_o	3,1	0	4,3	0	13,7	7,55	71,35	0,15	0,675	0,175	12,25	KCl+Leonite+Kainite+Picromerite

of a salt. Here, projection is led by directing the rays from the poles of the salt onto a plane inside the prism. Basing on the volumetric image system $2Na^+, 2K^+, Mg^{2+} // 2Cl^-, SO_4^{2-} - H_2O$ (Figure 1) and the interpolation of literature data projections of volume of potassium chloride and potassium sulfate salts of this system (Figure 1 and Table) are constructed.

Crystallization volume of K_2SO_4 — arcanite is separated by the facets of $K_2SO_4 E_4 's_3^5 E_4^3$, $K_2SO_4 E_4 's_3 'E_5 '$ *and* $K_2SO_4 E_5 's_{12}{}^3 E_4^3$ prism and contacts with the crystallization volume of silvine through the surface $E_5^1 s_3^1 P_5 s_{12}{}^3$ with the volume of salt $K_2SO_4 \cdot MgSO_4 \cdot 6H_2O$ — picromerite (schenite) through the surface $s_{12}{}^3 P_5 s_3^5 E_4^3$ with the salt volume of $3K_2SO_4 \cdot Na_2SO_4$ — aphthitalite (glazerite) through the surfaces $s_3 'P_5 s_3^5 E_4 '$.

The amount of crystallization of KC1 — silvite separated by facets of the KC1 $E_6 's_2 'E_1^3$, KC1 $E_5 's_3 's_4 'E_6 '$ and KC1 $E_5 's_{12}{}^5 s_4{}^3 s_6{}^3 E_1^3$ prism and contacts with the crystallization volume of salt NaCl — halite through the surface of $E_6 's_4 's_2{}^4 P_3 P_5 P_7 P_9$ with the volume of the salt — $K_2SO_4 \cdot MgSO_4 \cdot 6H_2O$ — picromerite through the surface $s_{11}{}^3 P_3 s_4{}^3 P_5 P_9$ with the volume of the salt $3K_2SO_4 \cdot Na_2SO_4$ — aphthitalite through the surface $s_3 's_4 'P_3 P_{14}$, with the volume of the salt K_2SO_4 — arcanite through the surface $s_3 'E_5 's^3{}_{12} P_{14}$ with the volume of the salt $K_2SO_4 \cdot MgSO_4 \cdot 4H_2O$ — leonite through $P_5 P_7$, with the volume of $KCl \cdot MgSO_4 \cdot 3H_2O$ — kainite through $R_7 R_9 s_6{}^3 s_5{}^3 s_4{}^3$ with the salt volume $KCl \cdot MgCl \cdot 6H_2O$ — carnallite through $R_9 s_2{}^4 s_6{}^3 E_1{}^3$ line.

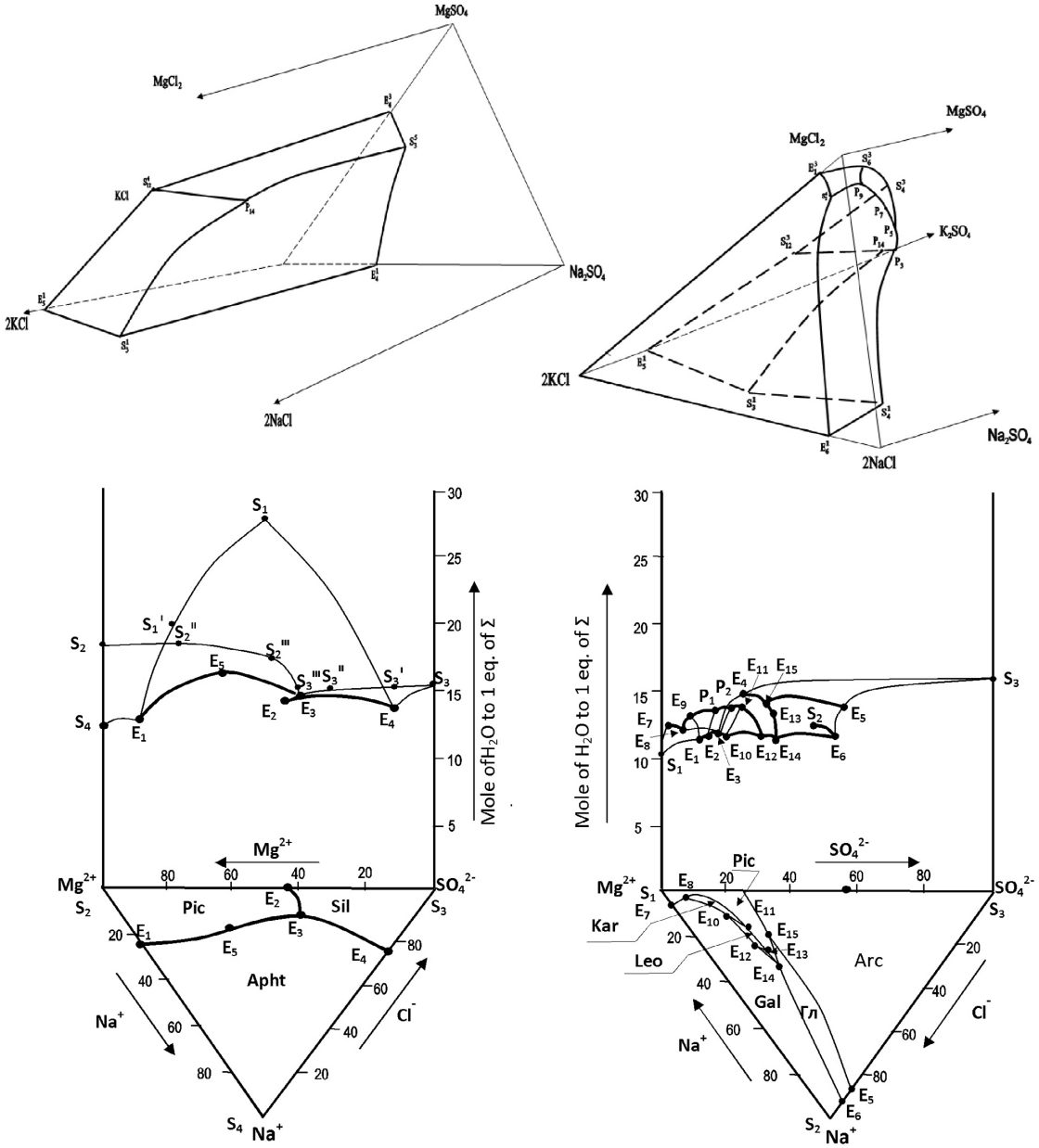

Figure 1. Isotherm volume of (potassium sulfate) arcanite

Figure 2. Isotherm volume of (potassium chloride) sylvite

Figure 1 and 2 illustrates the structure of the projection of the salts field of potassium sulfate and chloride in a plane drawn through the poles of these salts.

The literature shows only the crystallization field of sodium chloride, and we have been first to show the crystallization area of potassium chloride and potassium sulfate in isotherm system; the volumetric projection of other salts can be easy illustrated basing on the proposed volume diagram (Figure 1 and 2).

Thus, there have been constructed projections of silvite and arcanite on volumetric imaging of five-component system $2Na^+, 2K^+, Mg^{2+} // SO_4^{2-}, 2Cl^- - H_2O$ at 25 °C, which allow carrying out technological calculations of their separation from the brine and salt deposits of marine type.

References:

1. Эркаев А. У., Кучаров Б. Х., Каипбергенов А. Т., Тоиров З. К., Мурсаев О. А., Улашова Н. А. Объемное изображение системы $Na^+, K^+, \frac{1}{2} Mg^{2+} // \frac{1}{2} SO_4^{2-}, Cl^- - H_2O$ при 25 °С//Узб. хим. журн. – № 3. – 2016 г. – С. 44–53.
2. Солиев Л., Горошенко Я. Т., Горникова М. А., Патриляк Н. М. – Укр. хим. ж. – 1991. – Т. 57. – № 4. – С. 351.
3. Горошенко Я. Г. Массцентрический метод изображения многокомпонентных систем. – Киев: Наукова думка, 1982. – 264 с.
4. Солиев Л. Прогнозирование фазовых равновесий в многокомпонентной системе морского типа методом трансляции (кн. 2). – Душанбе: Шуҳоиён, 2011. – 147 с.
5. Ксензенко В. И., Кононова Г. Н. Теоретические основы процессов переработки галлургического сырья. – М.: Химия, 1982. – 328 с.
6. Аносов В. Я., Озерова М. И., Фиалков Ю. Я. Основы физико-химического анализа. – М.: Наука, 1976.

Nuhuyeva Shahla Sadraddin,
Master, Azerbaijan Technological University
Environmental Engineering Department
E-mail: ekolog84@gmail.ru

Verdiyeva Farida Bahram,
PhD on agricultural Sciences., assistant
Azerbaijan Technological University
Environmental Engineering Department
E-mail: vfaridayf@mail.ru

Mammadov Elshad Arshad,
Doctor of chemistry., prof.
Azerbaijan Technological University
Environmental Engineering Department
E-mail: elshad1952@mail.ru

Electrocatalytical purification if sewage

Abstract: Physico-chemical methods of decolouration of highly coloured sewage are multivariant and may be applied for preliminary purification. One of this variants is electrocatalytical decolouration. This method is based on the oxidizing properties of anodic current and the active particles formed in catalytic decomposition of hydrogen peroxide.

Keywords: Electrocatalytical, decolouration, anodes, graphite, platinium, decolouration.

Electrocatalytical influences in different combinations on solution, containing various dye-stuff and on natural dye-stuff production sewage decrease the level of colourdensity. According to that, decolouration efficiency

depends greatly on anodes corrosive resistance, potential, current density and catalyst activity in peroxide decomposition reaction. According to experimental data some composite graphite materials may be used in electrocatalytic decolouration of sewage as electrodes-catalyst with high corrosive resistance and activity. The modification of the method based on electrochemical synthesis of hydrogen peroxide in purification plant has been found interesting. Experimental data are used in the task for chemical ecology practice, for the basic course and for various special courses. The big experimental material is obtained and it indicates that the using of eiectrocatalitic methods of sewage treatment from orqanik pollutants, which are methanol, formaldegyde, phenol, different kinds of colorants and biological hard surface active compounds, has some prospects [4, 75–77].

Development and application of highly effective and chemically stable anodes in technology of electrochemical purification of sewage are based on recent achievements of electrochemistry in the field of production of chlorine, soda and chlorates [1, 15–17; 2, 58–60]. Objects of comprehensive researches are diverse graphite material and especially oxides of metals.

The graphite is highly electrochemically active electro conductive anodic material. The combination of these characteristics with low cost stipulates its wide application in organic electro synthesis and represent definite interest for use in technological system of purification. However, graphite anodes owing to significant porosity absorb plenty of solution. Therefore effect of an electrical current is observed not only on the surface of the anode, but also in the electrode, which creates favorable conditions for its destruction. Thus there occurs an oxidation (combustion) of graphite by products of electrolyze, and also loosening of its structure by allocated electrolytic gases.

Essential influence on durability is exerted due to the porosity of graphite. The higher it is, the faster goes the destroying owing to non-uniformity of distributing the current and allocation of oxygen and chlorine inside pore. To increase durability and to decrease porosity of graphite it is impregnated by vegetable oils, by polymers, etc. However that kind of processing allows unsignificant increase in the service life of graphite anodes. Therefore in the recent years the interest for the replacement of graphite with anodes from unwearing out oxides of metals has increased.

Titanium anodes have received their practical development and industrial application in technology of purification [3, 70–72].

For this purpose the sewage was subjected to research, but with attention to durabilities of graphit s to anodi loads. Therefore anodic of a current was reduced down to 10mA/sm^2 and, accordingly, the length of electrolyze was increased. The results of experiments are presented in the table 1.

Table 1. – Elecrocatalytical discolouration of sewage with platinized and not platinized graphite anodes At 1=10 mA/sm^2 (Colour.=20000, OU (oxygen used)=5000mgr/l, CNaCl=5gr/l)

Electrode	Time, h	ph	Colour (beg)	λ,%	OU (final)	α,%
B2L12	3	8,3	12000	40	1940	61
APB	3	8,3	10000	50	1900	61
B2L12	5	8,35	6000	70	520	90
APB*	5	8,3	5500	73	510	90
B2L12	24	8,3	5800	71	180	96
B2L12**	5	8,2	5000	73	500	90
B2L12***	5	86	7500	62	1700	66
Pt/B2L12	3	8,5	6900	65	900	83
Pt/B2L12	5	8,5	3500	82	860	83
Pt/B2L12***	8	8,5	1600	92	640	87

** During 8 hour of anodic loading the anode from graphite APB collapses*

*** Is supplemented with 50ml of 33% H_2O_2*

**** Is supplemented with 2gr of NaCl*

***** after 8 hours 50% of an active phase is supervised from the surface of the anode*

After the analysis of the data indicated on the table 50%, that fact pays attention, that reduction of OU (oxygen used) on net graphites is not correlated with reduction of OU on platinized graphite, which is probably explained with discrepancy of mechanisms proceeding on electrodes. Besides, increasing of the colour during the use of anodes from pure graphites can be explained by destruction of the latter during longlasting anodic loading. By analyzing results of the experiment, it is possible to assert, that optimal time for

operation of graphite anodes is 3..5 hours at density of a current 10mA/sm^2.

On the whole, during the use of graphite anodes the purification is realized unsuffciently effectively, which, with respect to their low stability at high density of a current, makes them nonpractical for industrial application. By the results received earlier the approbation of anodes from titanium, modified by platinum and graphite fibre was of interest. The discolouration was conducted under the above described circuit in various time intervals [5, 308–309]. The results of experiment are presented in the table 2.

As it is visible from the table, during the use of modified titanium anodes the same laws are supervised, as in case of anodes from graphite and platinum. Besides, the advantage of titanium modified by graphite and platinium is obvious enough in comparison with platinized. From this point of view the conduction of the comparative analysis of electrodes in process of electrocatalytical destruction of aniline azodyes was of interest [6, 17–19]. The results are tabulated in the table 3.

With the results of the conducted experiments and given tables 2 and 3, it is possible to reach the conclusion, that the greatest efficiency of electrocatalytical discolouration of sewage is supervised in systems containing Pt/Pt as the Electrode-catalyst and hydrogen peroxide [1, 223–224].

Table 2. – Electrocatalytical discolouration of a real drain with the use of anodes Ti, Ti/Pt, Ti/Pt/C af i. = 20 mA/cm^2 (Colour (beg) = 20000, OU (oxygen used) (beg) = 5000 mg, CNaCl =5 gr/l)

Electrode	time, h	pH	Col (final)	λ,%	OU (final)	*a*,%
Ti	8	8,4	1700	91	2400	52
Ti/Pt	3	8,4	550	97	650	87
Ti/Pt	5	8,4	400	98	540	89
Ti/Pt	5	8,3	350	98	500	90
Ti/Pt	3	8,3	500	98	600	90
Ti/Pt/C*	3	8,4	350	98	600	90
Ti/Pt/C**	5	8,4	200	99	450	96

** Is supplemented with 50 ml of 33% H202*

*** Is supplemented with 2 gr of NaCl*

Table 3. – Electrocatalytical discolouration of real drain of production aniline azodyes (Col (beg) = 20000, OU (oxygen used) (beg)=5000mg/l, pH=10, CNaCl=5gr/l)

Electrode	time, h	i, A/cm^2	Col (final)	λ,%	OU (final)	*a*,%
Pt/C (B2L12)	3	0,0016	550	97	650	87
Pt/C (B2L12)	5	0,0016	320	98	540	90
Pt/Pt	1	0,0016	200	99	290	94
Pt/Pt	3	0,003	50	99,8	80	98
Pt/Pt	5	0,003	20	99,9	45	99
Ti/Pt/C	3	0,0016	550	97	600	88
Ti/Pt/C	3	0,002	450	98	600	90

Hydrogen peroxide as an additional oxidizing agent.

On the basis of all conducted researches the method of purification of sewage with the anode from titanium, modified by platinum and graphite fibre which allows the achievement of practically complete discolouration of a drain was developed. As a result of processing drain can be used in a turnaround cycle of production [4, 75–77].

References:

1. Yakovvlev S. V., Krasnoborodko I. G., Rogov V. M. Electrochemical Clearing of Water. L., 1987,312 p.
2. Krasnoborodko I. G. A textile industry. 1986,4, P 58–60.
3. Bogdanovsky G. A.A Chemical ecology. – M., 1994, 238 p.
4. Мамедов Э. А., Першина Е Д Богдановский Г. А. Электрокаталитические системы и обесцвечивание сточных вод производства азокрасителей. Вестник МАНЭБ, 1997, № 4, С. 75–77.
5. Данилова Е. В., Камкин А. А., Богдановский Г. А. Коррозионная стойкость окисных рутениево-титановых анодов в реакциях электрохимического окисления биологически «жестких» ПАВ. Вести. МГУ, сер.2, т. 32, № 3, 1991, С. 308–309.
6. Wolfson S. K., Yao R. S. I., Geisel A., cash H. R. Reaction og Oxidation on platinium electrodes. Trans. Amer.Soc. Inten Organs, 1970, v. 16. p. s. 193.

Nurkulov Fayzulla Nurmuminovich,
Tashkent Institute of Chemical Technology,
Senior Research Scientist, Uzbekistan, Tashkent
E-mail: nfayzulla@mail.ru
Jalilov Abdulakhat Turapovich,
Tashkent Scientific Research Institute
of Chemical Technology Professor,
Doctor of Chemistry, Director
E-mail: gup_tniixt@mail.ru
Eshkurbonov Furkat Bozorovich,
Termez State University,
Senior Research Scientist, Uzbekistan, Termez
E-mail: furqat-8484@mail.ru

Developing adhesive formulations based on chlorosulfonated polyethylene with phosphorus, boron and amine-containing modifiers

Abctract: The paper designed adhesive formulations based on chlorosulfonated polyethylene with phosphorus, boron and amine-containing modifiers. Studied the resistance of the modified compositions based on chlorosulfonated polyethylene to different chemical environments. From the data obtained it was found that chlorosulfonated polyethylene modified with amine compounds has a good adhesive properties. It is shown that by the interaction of the polymer becomes greater variety of adhesive-reactive functional groups, resistant to various organic solvents, acids, alkalis, oxidizers and high mechanical properties.

Keywords: Chlorosulfonated polyethylene, adhesion, modifier, epichlorohydrin, melamine, urea adduct, vulcanizate modifier.

Chlorosulfonated polyethylene with varying chlorine content sufficiently soluble in some solvents, making it possible to achieve a viscosity of the composition required for use in the paint industry. To use chlorosulfonated polyethylene coatings such as Hypalon 20 and Hypalon 30 [1, 102].

Coatings based on chlorosulfonated polyethylene have been widely applied much earlier than a coating of chlorinated polyolefin. This is due to better compatibility with other film-forming compositions, the possibility of obtaining a more "crosslinked" solidification structures and less duration compared to chlorinated polyethylene [2, 15–17].

Elastic coating based on chlorosulfonated polyethylene are characterized by valuable properties: high strength performance, wear resistance and adhesion, resistance to ozone, acid and alkaline environments and weather conditions, high gas impermeability, fire resistance, superior fire resistance of chloroprene rubber, resistant to oils, fuels and ionizing radiation [3, 122]. Protective coatings based on chlorosulfonated polyethylene have high fracture toughness, elasticity and deformability of the coating film, a high chemical resistance to the gas-vapor medium containing acid gases ($C1_2$, HC1, SO_2, SO_3, NO_2), to form solutions of acids, as well as alkaline solutions and salts. Coatings based on chlorosulfonated polyethylene have high abrasion resistance, a wide range of operating temperatures (from –50 °C to + 120 ° C). They have a relatively low cost with high durability. The service life of protective coatings — up to 20 years, the roof — up to 30 years. Perhaps production and chemical protective roofing using coatings based on chlorosulfonated polyethylene at low temperatures down to minus –15 °C [4, 53–58].

The two-component compositions are mainly used for the production of coatings on concrete, steel, fabrics, fiberglass and rubber, are exposed to liquid or gaseous aggressive environments, high temperatures, mechanical loads, the atmosphere. Typically, the coating is affected simultaneously several of the above factors [5, 195–196]. Successful exploitation of the coatings they must possess chemical and weather resistant, good physic mechanical properties, low gas permeability, the required decorative properties, sufficient adhesion to metal, concrete, rubber.

Composition designed to produce coatings of varying thickness and hardness with a high level of strength,

durability and aggressively, with reduced combustibility on the basis of chlorosulfonated polyethylene, which can be used for obtaining of aggressive, and weather resistant solid different thickness coatings for floors and roofs. The composition includes a filler, a hardener and solvent as a redox curing system consisting of a synthetic or other tertiary amine, and further comprises a phosphorus-, boron and amine containing oligomeric flame retardant.

The most commonly used solvents for these polymers are toluene, xylene, or a mixture thereof. These solvents provide the lowest viscosity and relatively cheap.

It developed a polymer composition based on a chlorosulfonated polyethylene with the Enhance protective coating adhesion and corrosion resistance of coatings on the surface to protect steel structures. It includes chlorosulfonated polyethylene, Epoxy polyurethane resin, and toluene as a modifying additive phosphorus, boron and amine containing oligomeric flame retardant.

For fire protection of building structures and cable products designed composition based on a chlorosulfonated polyethylene, containing as toluene, thermally expandable graphite graphite, zinc oxide, magnesium oxide, stearic acid, diphenyl guanidine and phosphorus, boron-containing oligomeric flame retardant.

The coatings obtained have sufficiently high chemical resistance. After 30 days of storage at 60 °C in a 3%, 10%, 20%, 40%, 50%, 60% of sulfuric acid, 3%, 10%, 20%, 30%, 40%, 50% caustic potash a solution of, 10%, 20% of hydrochloric acid and 20% nitric acid 30% change in mass and physico-mechanical properties were insignificant. When the content is more than 30% nitric acid solution composition obtained begins decompose.

A coating is also designed based on chlorosulfonated polyethylene, modified epoxy containing oligomers. The coatings are characterized by firmness to heat aging at 100 °C having enhanced adhesion strength to a metal substrate, good physical-mechanical properties, high "fracture toughness.". Which can be used for reliable protection of metal and concrete structures in aggressive media. Increasing adhesion properties of the proposed coating takes place is apparently a result of interaction of polymer chains sulfohloridnyh groups chlorosulfonated polyethylene having epoxy group.

As is known, the most reactive group in chlorosulfonated polyethylene is chlorosulfonic group. Modification of the polymer solution was carried out in toluene at normal conditions. Possible schemes of chlorosulfonated polyethylene of macromolecules transformations for the specified group developed modifying additives are listed below.

The paper [1, 102] shows the adhesion the activity phosphorus-containing compounds used in the compositions based on polychloroprene. We investigated phosphorus, boron, nitrogen-containing oligomers as additives for modifying compositions based on chlorosulfonated polyethylene. As used modifiers of epichlorohydrin and reaction products of melamine panels with initial reagents ratio 1:1 (EME-1) and 2:1 (EME-2); reaction products of epichlorohydrin (ECHG) and the urea adduct starting materials at a ratio of 1:1 (EAR-1) and 2:1 (EAR-2).

In addition we synthesized compounds was also studied the the possibility of modifying chlorosulfonated polyethylene molecules with EAR-1, is used in the rubber industry, as an effective and weatherproof. Alleged scheme of interaction EAR-1 and chlorosulfonated polyethylene is presented below. Thus, the modification provides a chlorosulfonated polyethylene polymer having a large number of diverse active groups adhesive.

The scheme of interaction chlorosulfonated polyethylene modifiers based on of epichlorohydrin and melamine production:

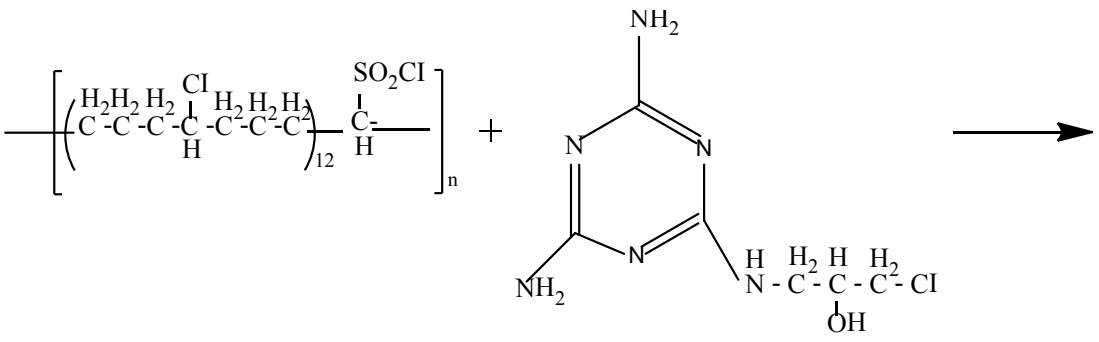

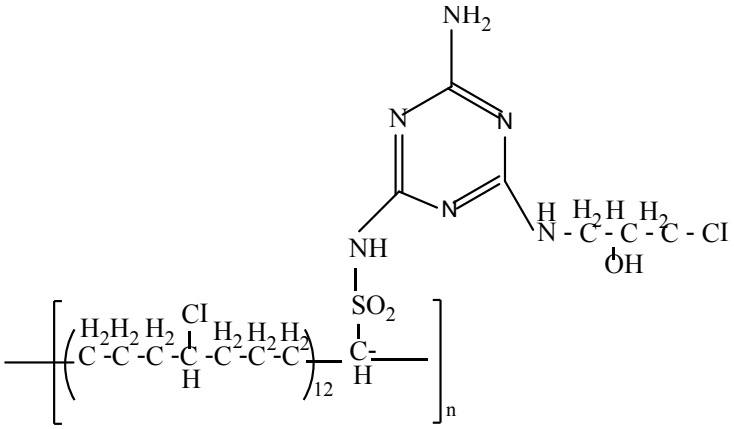

The scheme of interaction chlorosulfonated polyethylene modifiers based on epichlorohydrin adduct of urea:

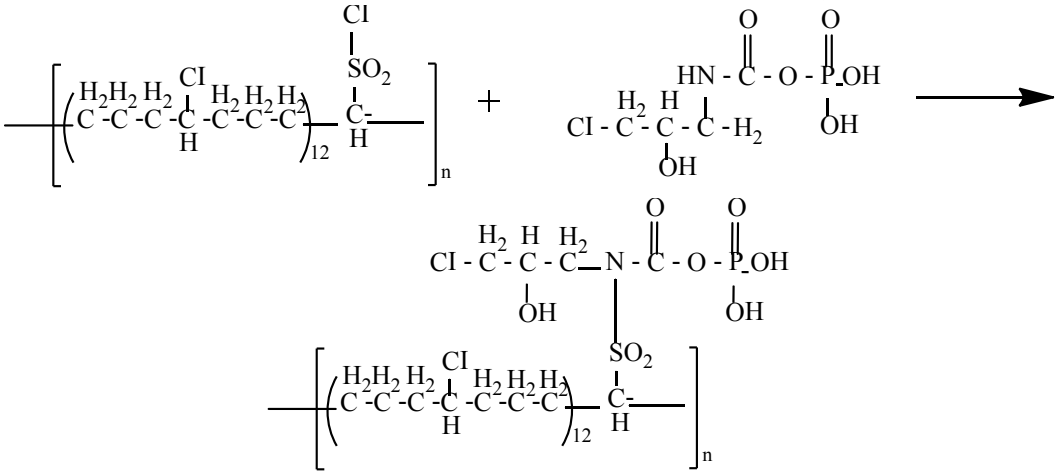

Polymer modification was carried out in toluene solution at normal conditions.

As seen from these schemes, the interaction with the modifier designed chlorosulfonated polyethylene macromolecule according chlorosulfonic group proceeds to form a sulfonamide group and the release of hydrogen chloride, reacts with a second molecule of the modifier.

IR spectra of the starting chlorosulfonated polyethylene and chlorosulfonated polyethylene modified EME-1, represented by new absorption bands in the region 1500–1600 (1505) cm^{-1}, characteristic of the sulfonamide group, indicating that the interaction of the amino groups with chlorine atoms modifier in chlorosulfonated polyethylene.

Study modifiers based polymer composition of chlorosulfonated polyethylene is widely used for coatings, primers, varnishes, enamels and sealants. These materials are characterized by a complex of technical properties: abrasion resistance; thermal and fire resistance; high gas barrier; resistant to oils, ozone and corrosive environments. Comprehensive studies were conducted effect of type, the content and nature of additives for modifying the adhesive strength of polymer compositions based on chlorosulfonated polyethylene when bonding the vulcanizates based on various rubbers, the results of which are presented in Table 1.

Table 1. – The dependence of the adhesive strength of the polymer composition of the content of of modifiers of type EME

Kind modifiers	The content of modifiers, %	Shear strength at bonding vulcanizates MPa		
		SRI-3	SKN-18	SREP-40
Source	0	0,57	0,62	0,37
EME-1	0,5	0,66	0,60	0,88
	1,0	0,78	0,64	1,82
	1,5	0,72	0,55	0,72
EME-2	0,5	0,69	0,54	0,92
	1,0	0,84	0,60	1,84
	1,5	0,70	0,59	0,83

Table 1 shows that the introduction of modifiers based on epichlorohydrin and a melamine resin-based composition chlorosulfonated polyethylene can improve adhesion to SREP-40 based vulcanizate (ethylene propylene rubber) 5 times, compared with the adhesive based on the source chlorosulfonated polyethylene. Since the value of the initial adhesive strength for polymeric compositions based on chlorosulfonated polyethylene is 0.37 MPa, and for a modified, when the content of the modifying additive 1.0% — 1.84 MPa. When gluing the vulcanizates based on SRI-3 (isoprene rubber), the largest increase in adhesive strength is also observed at 1% modifier concentration. The results of studies of the effect contents based on the ECNG modifier and urea adduct are shown in Table 2.

Table 2. – The dependence of adhesion strength of the polymer composition of the content type EAR modifiers

Kind modifiers	The content of modifiers,%	Shear strength at bonding vulcanisates MPa		
		SRI-3	SKN-18	SREP-40
Source	0	0,57	0,62	0,37
EAR-1	0,5	1,42	1,30	0,56
	1,0	1,52	1,34	0,84
	1,5	1,51	1,31	0,82
EAR-2	0,5	1,45	1,34	0,68
	1,0	1,57	1,40	0,92
	1,5	1,54	1,38	0,88

As seen from the table, the type modifiers EAR-1 EAR-2 can improve the adhesion strength of polymeric compositions is 5 times when bonding the vulcanizates based on SREP-40. As in the case of modifiers EAR type, the greatest improvement is achieved when bonding rubber based on SREP-40. For rubbers based SRI-3, SRN-18 (nitrile butadiene rubber, acrylic acid), increased adhesion strength is an average of 2–2.5 times.

Conclusion: Thus, to study the interaction of chlorosulfonated polyethylene with amine compounds. It is shown that by the interaction of the polymer acquires greater variety of adhesive-reactive functional groups. The effect of modifiers on the basis of melamine and epichlorohydrin, epichlorohydrin adduct of urea to the adhesive properties of formulations based on chlorosulfonated polyethylene. It is shown that the use of adhesives when bonding chlorosulfonated polyethylene the vulcanizates based on SRI-3, SRN-18, SREP-40 provides an increase in adhesive strength by 3–4 times.

References:

1. Кейбал Н. А., Бондаренко С. Н., В. Ф. Каблов В. Ф. Разработка аминосодержащих модификаторов для хлоропренового клея//Известия Волгоградского государственного технического университета: межвуз. сб. науч. ст. № 2 Сер. Химия и технология элементоорганических мономеров и полимерных материалов. Вып. 1, Волгоград, 2004 – С. 102.
2. Сафронов, С. А. Разработка динамических термоэластопластов на основе хлорсульфированного полиэтилена/С. А. Сафронов, А. Н. Гайдадин, В. А. Навроцкий, Я. В. Зарудний//Каучук и резина, 2011. – № 6. – С. 15–17.
3. Бондаренко С. Н., Горяйнов И. Ю., Кейбал Н. А. Разработка новых пропиточных составов для модификации синтетических волокон./Сб. матер. Всероссийской конференции: Индустрия наносистем и материалы г. Москва, 2006, – С. 122.
4. Курбатов В. Г. Модифицированные эпоксидные покрытия для противо-коррозионной защиты металла /В. Г. Курбатов, Д. И. Донская, А. А. Ильин, Е. А. Индейкин, И. В. Голиков//НТВП. – 2012. – № 1. – С. 53–58.
5. Каблов В. Ф., Бондаренко С. Н., Кейбал Н. А. Способ повышения адгезии хлоропреновых клеев//11 Всероссийская научно-практической конф. (с международным участием): Резиновая промышленность – продукция, материалы, технология, инвестиции. – М., 2005. – С. 195–196.

Nurkulov Fayzulla Nurmuminovich,
Tashkent Institute of Chemical Technology,
Senior Research Scientist, Uzbekistan, Tashkent
E-mail: nfayzulla@mail.ru
Jalilov Abdulakhat Turapovich,
Professor, Doctor of Chemistry,
Director of the State Unitary Enterprise
of the Tashkent Scientific Research Institute
of Chemical Technology, Uzbekistan, Tashkent
E-mail: gup_tniixt@mail.ru
Tadzhikhodzhaev Zokirkhuja Abdusattorovich,
Professor, Doctor of Chemistry,
Tashkent Scientific Research Institute of Chemical Technology,
Uzbekistan, Tashkent
E-mail: gup_tniixt@mail.ru

New environmentally safe flame retardant phosphorus-based organic compounds

Abstract: Synthesized new multifunctional oligomeric phosphorus-based flame retardants epichlorohydrin adduct with urea and inorganic compounds of silicon, and called the conditional FR-120.

We studied the effect of interaction between the molecules of the oligomeric flame retardant on the fire resistance of paper, cotton fabrics, wood and polymer materials. In this paper we used the methods of impregnation oligomeric flame retardant on the State Standard 16363–98. Accelerated test method used for the control of fire-retardant the effectiveness of fire protection, passed classification test. We determine the dependence of the oxygen index composite sample grades of FR-120 in the polymers in accordance with State Standard 21793–76.

Keywords: phosphorus oligomer, wood, plastics, paper, cotton fabrics, the oxygen index, polyethylene, epoxy compositions.

In modern conditions is essential widely used flame retardants, to be provided by a new generation of environmentally friendly, cost-effective flame retardant compositions with high performance [1]. Useful compositions, after application of fire retardants to the surface of combustible materials increase their fire resistance [2].

New fire safety problems also arise in connection with the accelerated construction of residential, industrial and public buildings. The probability of occurrence of fire can be reduced using in buildings is difficult combustible materials, protecting them special fire compositions [3].

Use of the oligomeric flame retardant fabrics for flammability, cotton paper, wood and polymer is known for a long time and is effectively used today. Explained the mechanisms of action of the individual substances and combinations of the synergistic effect of the action of several substances, such as a combination of borates and phosphates [4]. However, due to a variety of cellulosic and polymeric materials, ingredients and formulations of cellulose or polymer mixtures known direct transfer of data to a particular formulation and the final decision is impossible on the effectiveness of fire retardant group in each case can be taken only after the experiment.

The aim of this study was to investigate the effect of different combinations of fire retardant on the flammability and physical and chemical properties of cellulose and polymer building materials.

Synthesized new multifunctional oligomeric flame retardants based on reaction products of phosphorus-containing compounds, and the flame retardant properties of the FR-120 grades were studied. In this paper we used the methods of impregnation oligomeric flame retardants according to State Standard 16363–98. The essence of the method consists in determining the weight loss of the wood treated with test coating or impregnating composition, when firing tests under

conditions conducive to the accumulation of heat. The classification method is used to determine the group of fire-resistance rating and certification testing. Accelerated test method used for the control of fire-retardant effectiveness of fire protection, passed classification test.

We determine the dependence of the oxygen index composite sample grades of FR-120 in the polymers in accordance with State Standard 21793–76.

For fire protection also use the properties of some substances to decompose when heated to the release of gases that do not support combustion (ammonia, sulfur dioxide gas). Not combustible displace oxygen from the surface of the wood and thus prevent it from burning. Dried pieces of paper and cotton fabric (in which adsorbed flame retardant) were subjected to unexposed flame. After sunbathing samples of paper and cloth had been removed from the flame, and at the same time it was discovered that they just fade. For paper if plain paper is lit with the remainder in the form of fly ash, the prototype look as coke, the same is observed for the tissue sample. Weight of coke reached 70% of the initial value (paper) weight loss of 30% (Table 1).

Table 1. – Tests on the flammability of paper and cotton material with flame retardant additives oligomeric FR-120

paper additives oligomeric flame retardant FR-120						
Sample FR-120	**Weight before the test, g**	**Burning time, seconds**	**Sample, %**	**Weight after testing, g**	**weight loss**	
					g	**%**
1	0,056	10	0	0	0,056	100
2	0,045	10	5	0,017	0,028	62,22
3	0,052	10	10	0,028	0,024	46,15
4	0,101	10	15	0,070	0,031	30,7
5	0,094	10	20	0,070	0,024	25,5
Cotton material with flame retardant additives oligomeric FR-120						
1	0,1150	15	0	0	0,1150	100
2	0,1080	15	5	0,035	0,073	67,6
3	0,1080	15	10	0,038	0,070	64,0
4	0,1500	15	15	0,088	0,062	41,0
5	0,1600	15	20	0,1120	0,048	31,0

Test procedure was performed as follows: Testing of pine wood samples were suspended vertically in a tube of black steel roofing length of 166 mm and a diameter of 50 mm. Under the sample protruding from the tube at 5 mm summed flame gas burner or an alcohol (alcohol burner used in our tests). Distance from the top edge of the burner to the sample was 10 mm. Dwell time in the sample gas flame is 1 min., and the alcohol in the flame of the burner for 1 minute. 30 sec. After removing the burner fixed duration independent of combustion and smolder sample.

Studies conducted on the effectiveness of fire-retardant wood elements. Application of the composition onto the surface was carried out by spraying. The application was made in layers (layer 2). Results of the study compounds FR-120 have shown that the average loss of weight of the sample was 8%, that is flame retardant provides a group I of fire retardant efficiency. (Table 2).

Table 2. – Tests on the flammability of wood material with flame retardant additives oligomer FR-120

№ Sample	**Time, in seconds**		**Weight, g**		**weight loss**	
	self-burning	**Smoldering**	**Before testing**	**After the test**	**gm.**	**%**
1	Absent	Absent	137,41	126,22	11,19	8,14
2			133,89	123,49	10,40	7,77
3			136,97	125,63	11,34	8,28
4			138,85	128,23	10,62	7,65
5			138,33	127,46	10,87	7,86
6			138,58	127,86	10,72	7,74
7			134,19	122,76	11,43	8,52
8			136,72	125,8	10,92	7,99
9			139,04	127,75	11,29	8,11
10			135,66	124,83	10,83	7,99
	On average					8,0

Of these impregnating compositions FR-120, 0.45kg/m^2 consumption can be seen that the oligomeric flame retardants belong to group I of fire retardanteffi-ciency. Solutions of oligomeric compositions penetrate deeper, promachivaya surface layer of wood. After evaporation of the carrier water retardant remains among cellulose fibers, thereby creating a protective layer.

Fire protection effectiveness of compositions FR-120, with weight loss, amounted to 8%. Analysis of ways to improve the fire-retardant impregnating compositions, their use in the construction business for improving fire stability of structures and wood products showed that the priorities are compounds capable of at the lowest cost to provide the required parameters of the vulnerability of the fire, not reducing or impairing the performance properties of the wood. Such a wide range of requirements for modern fire protection requires researchers to constantly expand our scientific research.

Most polymeric materials have a low fire resistance and are flammable. Reduction of flammability of polymeric materials is mainly achieved by the introduction of modifications or combustion retarders into the material (fire retardants).

In operation necessary to determine the flammability characteristics of standard polymers (for example, a polymer oxygen index). The data needed to build the model of polymers of ignition and combustion in conditions close to real. The relevance of this study is defined by the widespread use of polymers in human life and the risk of emergencies when they are burning.

In actual use of polymer products (in the presence of atmospheric oxygen), along with a free-radical processes of degradation of macromolecules inevitable oxidation processes that occur also on the radical chain mechanism. Therefore, to slow down the aging of polymeric materials needed compounds capable of oxidative break off the chain by reaction with peroxide radicals, as well as to destroy the hydroperoxides by the reactions competing with the processes of degenerate chain branching.

Polyolefins — high molecular weight aliphatic hydrocarbons obtained by polymerization of the corresponding olefins. Of this class of compounds have received greatest use polyethylene, polypropylene, and ethylene copolymers and numerous polypropylene. Polyolefins possess a valuable combination of properties: high dielectric characteristics, persisting over a wide temperature range, chemical stability, low gas and moisture permeability, large capacity and in most cases the frost resistance, durability and others.

The construction of the polyolefins used primarily as a waterproofing films, pressure and pressure pipes in water supply and sewerage systems, drainage pipes, molded and sanitary ware, fittings, ventilation ducts, heating formwork.

The main disadvantages of polyolefins and building materials on their basis are low thermal resistance and high fire danger. They relate to flammable materials whose expansion takes place without the formation of coke residue: Oxygen index, the flash point and autoignition are, respectively: 17,4–18,2%; 325–345 °C and 345–390 °C. The oxygen index of the composition of polyethylene grade F-0220 c oligomeric flame retardants in an amount of 10–60% of Oxygen Index – 52%. Results of the study compounds FR-120 to polyethylene are shown in Table 3.

Table 3. – The dependence of the oxygen index of flame retardant content

Name oligomeric flame retardant	**The concentration of oligomeric flame retardant, mass,%**	**Oxygen Index,%**
–	0	18,0
FR –120	10	28
	40	43
	60	52

By oligomers include epoxy compounds having more than one epoxide (ethylene oxide, glycidyl) groups are located at the ends or along the backbone of the molecule or the alicyclic ring. Epoxide groups react with many polyfunctional compounds to form three-dimensional polymers. Despite the variety of epoxy compounds and the constant expansion of their range, most widely used for connecting a variety of reaction products obtained of diols (diphenols, diols) and polyphenols with epichlorohydrin.

Epoxy resins due to high strength parameters, chemical and weather resistance, adhesion to many materials are widely used in construction. However, they have some disadvantages: a relatively low thermal and light stability, increased fire hazard. At a temperature of decomposition begins more than 150–170 ° C at a temperature of 400 ° C, they ignite. The linear polymers and the mass combustion rate equal respectively 3,5–4 mm/min and 7,8 g/(sm^3). The temperature of the combustion of epoxy polymers reaches 500–530 °C, the flame tem-

perature 950–970 °C. Depending on the nature of the starting reactants used in the synthesis of oligomers, and the number and nature of epoxy hardeners oxygen index polymers ranges 19,8–34,7%. They are burning with the formation of black of smoke.

Flame-retardant properties of the oligomeric flame retardant studied by State Standard –12.1.044–84. The oxygen index of the epoxy composition (ED-20) with the addition of 1.0 –.30 mas% of Oxygen Index 63%, it can be used in the polymer industry (Table 4.)

Table 4. – Effect of concentration of oligomeric flame retardants on the oxygen index. The thickness of the ED-20 + PEPA samples oligomeric flame retardant

№	Oligomeric flame retardant	The concentration of the oligomeric flame retardant the masses%	Oxygen Index, %
1	FR-120	1.0	38
2	FR-120	5,0	42
3	FR-120	10,0	46,3
4	FR-120	16,0	57,0
5	FR-120	18,0	60,0
6	FR-120	20,0	62,0
7	FR-120	30,0	63,0

Conclusion. Thus, the analysis carried out work shows that the prospect of the development and use of oligomeric phosphorus flame retardant composite materials as fire and Bioprotective agents for wood and plastics. It is found that as a result of the study revealed that the high fire The security timber and polymeric materials can be achieved by surface treatment of its FR-120 composite structures.

References:

1. Joseph P.; Mcnally S. T. Reactive modifications of some chain- and step-growth polymers with phosphorus containing compounds: Effects on flame retardance: A review. Polym. Adv. Technol. 2011, 22, 395–406.
2. Tang Z.; Li Y.; Zhang Y. J.; Jiang P. Oligomeric siloxane containing triphenylphosphonium phosphate as a novel flame retardant for polycarbonate. Polym. Degrad. Stab. 2012, 97, 638–644.
3. Гоношилов Д. Г., Каблов В. Ф., Кейбал Н. А. Новые пропиточные огнезащитные составы на основе фосфорборсодержащего олигоме и полиакриламида//Фундаментальные исследования – 2011. 8. – С. 627–630.
4. Нуркулов Ф.Н., Джалилов А. Т. Фосфор-борсодержащие олигомерного антипирены для древесины и древесных композиционных материалов. V Международная конференция-школа по химии и физикохимии олигомеров Волгоград, 1–6 июня 2015.

Panjiev Ulugbek Rustamovich, assistant
of a department "Ecology" Karshi institute of a engineering
Saidov Amin Halim-o`g`li, assistant
of a department "Chemie" Bukhara engineering
E-mail: technological institute
E-mail: saidov.amin.15@mail.ru
Mukhamedgaliev Bakhtier Abdukadirovich,
professor of a department "Life protection"
Tashkent state technical university
E-mail: mail: bjd1962@mail.ru.

Synthesis and characterization of new ionits for decision of the problems peelings sewage

Abstract: New phosphor containing ionits were synthesized from quaternary phosphonium salts and divinilbenzole, quaternary phosphonium salts and methylmetacrylate. The copolymers having

an inherent viscosity of 0,34–0,55 dL/g were obtained by the two-phase method using toluene as an organic solvent. The polymers were easily soluble in various organic solvents and had high glass transition temperatures in the range of 220–260°C. An aromatic groups of a copolymers having units was also prepared. However, its inherent viscosity was low because of the occurrence of a side reaction.

Keywords: copolymer, ionit, monomer salt, reaction polymerization, sorbtion, thermal behavior, aromatic groups, solubility.

The industrial sewages oil and gaze to industry contains in its composition toxic ions heavy metal, which at hit in water reservoirs harmful act upon flora, fauna water reservoirs, as well as at hit in organism of the person render the toxicological influence [1]. Clear and repeated use the sewages must not only rescue water reservoirs from the further contamination, but also become the most economical way of the reception additional water resource that particularly it is important and for our republic currently, as well as for Central Asiatic region as a whole [2].

Before ion exchange technology are opened broad prospects. Intensive develops the new application of the ion exchange — in guard surrounding ambiences. They are developed, design and introduced in industry of the scheme peelings sewages with using ionits. The possibility of the use are researched in lieu thereof natural water some type sewages with smaller or alike salt containing on acting water prepare ion exchange installation. The successful decision of this problem will allow broadly introducing the systems of the circulating water-supply, including ion exchange clear recirculation sewages, without additional expansion of the volume of production ionits.

The role of the ion exchange in guard surrounding ambiences and in decision of the ecological problems oil and gaze to industry, it is impossible limit only clear drainage and increasing quality denatured water. Using ion exchange material, for instance, for sanitary peelings ventilation and waste gas surge, forming on some enterprise of the developed countries before 60% and more all gas departure, allows raising reliability a guard air and water pool from contamination and noticeably shortening the amount of the sewages in contrast with traditional absorption gas by water [3]. Clear production solution from bad admixtures noticeably relieves their conversion, promotes increasing a quality produced to product and reduction to dangers of the soiling the ambience in process production and consumptions to product. Clearing the sewages and gas are new and little investigation by application of the ion exchange, which has following five mains of the particularities:

1. Exceedingly rich set ion exchange systems. Since hitherto main application ionits is water prepare, t. e. clear of natural fresh water, that hitherto in the highlight researchers was limited number ion exchange systems, including macro admixture natural water (the ions Sa^{2+}, Mg^{2+}, Na^{+}, K^{+}, Sr^{+}, NSO_3, $HSiO_3$). That concerns the sewages and gas, that they are characterized by broad range of the admixtures (the hundreds and a thousand inorganic and organic join.). Consequently, great and number ion exchange systems, subjecting to study.

2. In view of varied chemical characteristic of the admixtures of the sewages and gas important importance gain the specific chemical interactions changed ion with ionits (forming the complex functional groups, weakly-ionizing forms ionits, complex, weak, hard and gaseous join and t. d.). Ingenious use this interaction allows sharply to raise efficiency of the ion exchange, provide deep clear of water and gas, shorten before stehiometric consumption regenerating agent.

3. The sewages and gases, which the source of the formation are a dynamic industrial production and public facilities, are characterized by inconstancy concentration admixtures, and so processes their peelings hang from conditions of their formation, t. e. from technology and state of working production. Ion exchange installation peelings sewages and gas run on variable load.

4. Increase the specific influences of the cleaned ambience on ionits (raised heat, chemical, radioactive and the other influences).

5. Shaping the composition of the sewages and gas occurs to account of the admixtures usually, typical of given production. Consequently, at right choices regenerating agent extracted admixture can be returned in the main production (for instance, admixture of washing water galvanic and organic production, condensate joist pair, absorption solution, leaving and ventilation gas and etc). This circumstance allows easy to solve a problem salvaging regeneration solution, increases the possibility ion exchange method, and does its economical and ecological. To the main to achievements ion exchange technologies in recent years, in particular our study, having important importance

for successful using ionits in decision environment problems, pertain the development to technologies deep peelings water in a lots of ionits filter with powdery ionits and in trefoil filter mixed action with using grain and fibres ionits (cationit — on base of the phosphoring gossypol resins PUR-1) [4]; technologies of without salting water in two-layer filter of the bulk type and with sailing loading from grain ionits with repugnant-step-like regeneration (strong aside cationit -received on base phosphoring of the copolymers quaternaries phosphonium to salts with divinilbenzole PUR-2) [5]; technologies softening water in large powered and economical ionits filter and device of the unceasing action with using grounds macroporus ionits; introduction repugnant-step-like to regenerations strong aside cationit; the development of the schemes of the desalinization natural and sewages with using thermal regenerated ionits (ionits on base phosphoring of the copolymers quaternaries phosphonium to salts and methylmethacrylate PUR-3) [6]; combining schemes reagent and ion change peelings of water with optimum recirculation and secondary use regeneration solution and washing water; combining membrane, reagent and other methods with ion exchange; all are a more broad use polyamfolits and other complex former ionits for deep peelings of the sewages and gas from toxic and bad admixtures, macrospores ionits for peelings drainage and denatured water from complex and organic join; using for regeneration ionits new chemical agent (nitric, silisiphosphoring aside and phosphoric acid, ammonia, organic solvents and others), forming easy utilized regeneration solutions; the development elektrodializing reconstruction reagent from regeneration solution with using bipolar water destruction membrane; making the efficient methods peelings ventilation and waste gas on fibber ionits and others using ground chemical regenerated organic ionits to series PUR have a significant technical-economic advantage under without salting natural and sewages with source salt containing before 1 g/l, under deep without salting water, hot change and the other capacitor oil referiner enterprise (in filter of the mixed action), at deactivation of the radioactive sewages, under concentration water microamins (tabl.1). As the table shows the value of the equilibrium constant of adsorption is much higher than unity, indicating a strong binding of arsenazo (III) sorbent PUR-2. It should be noted that with increasing temperature increases and decreases the value of the equilibrium constant. Such constant values change with temperature indicates that the binding occurs not only through ion exchange but also other weak binding forces which are attenuated with an increase in temperature and lead to a decrease in the value of the equilibrium constant. Is it possible to use this binding polymer reagent for the analytical determination of various metal ions.

Interesting results were obtained in a comparative study of the adsorption of halogens from aqueous solutions of potassium salts of the above sorbents. Use as solvents potash dissolves these halogens allows them molecular form to form ion. At the same time revealed that most of the absorbing capacity sorbent has PUR-2 having a higher SEC among the studied sorbents. If regeneration solutions are processed in useful product (for instance, in mineral fertilizer), as well as at elektrodializ reconstruction reagent from regeneration solution and in row of the other events ion exchange successfully can be used for without salting water with source salt containing before 2 g/l. Using ground and fibres thermal regenerated ionits (ionits PUR-2 and PUR-3) allow to raise the upper optimum limit salt containing without salting water before 3 g/l. Ion change process successfully concurrent with elektrodializ and more perspective for reduction of salt containing water with 3 before 0,3–0,5 g/l. The further deep without salting can be realized with using usual chemical regenerated ionits.

Table 1. – The characteristic to ionits to series PUR, got phosphoring gossypol resins (PUR-1) and phosphoring of the copolymers quaternaries phosphonium to salts with divinilbenzole (PUR-2) and phosphoring of the copolymers quaternaries phosphonium to salts and methylmethacrylate (PUR-3)

ionit	Functioning group	$K_{to\ distend.}$	τ, sek	SOR by UO^{2+}, mg ekv/g	F Degree filling the sorbent by ion, D	D, $см^2$/sek
PUR-1	P^+, CH_3, NH $PO(OH)_2$	1,8	1000	1,17	0,48	$6{,}8.10^{-8}$
PUR-2	P^+, $PO(OH)_2$	2,4	1200	2,55	0,64	$7{,}1.10^{-8}$
PUR-3	CO, OCH_3, P^+, $PO(OH)_2$	2,7	1600	2,80	0,82	$7{,}4.10^{-8}$

For without salting fresh and salting water with salt containing 1–10 g/l perspective multifunction schemes, including reagent softening (with coagulation), deep ioning softening with using ground cationits, elektrodializ with using ion change membrane and ion change without salting. If take into account that main amount of the sewages to industry and public facilities has salt containing below 2 g/l (the to blow through, surface, town sewages, washing water, condensates and others), that becomes comprehensible that ionit and ion change membrane belongs to the main role in without salting, clear from radioactive material, selective to clear from dissolved admixtures and repeated use the sewages for necessities of industry. Creation powdery, fibres ionits and filter has allowed with high efficiency to clean the condensates on hot change from macrocuality dissolved not only, but also rough weighted and colloidal admixtures. Creation macrospores osmotic stable organic ionits with extended possibility has allowed to in sphere of the using ionits clear drainage and denatured water from pesticides, detergent and other organic join. Thereby, ion change material except demineralization, deactivation and selective of the separation of the dissolved admixtures of the inorganic join turned out to be capable to execute the functions to filtering disperse material and reversible sorption of the organic join. Graund and fibres ionits series PUR successfully execute the role of the restorers and catalyst of the chemical processes; fluid — a role coagulant and exreagent; the monopolar ion changes membrane — a role of the efficient carrier ion, bipolar — a role of the carrier ion and generator of the products of the fission of water — an ion H^+ and OH^-; fibres ionits — a role of the efficient sorbent of the gaseous products from leaving, ventilation and wastes gas. Using designed sorbent to series PUR in oil and gaze of industry for peelings of the sewages and gas surge will provide newly to solve actual and global problems to not only branches, but also region as a whole.

Ionits and ion change membrane, as means of protection surrounding ambiences from chemical and radioactive contamination, belongs to future.

References:

1. Ergojin E. Ionits and ion change by smoly. – Alma-ata: Nauka. 1998. – S. 240.
2. Gafurova D. A. Physic-chemical particularities of the formation and characteristic ionits. The Abstract dissert. Doctor of chemical sci. – Tashkent. NUUz, 2015 y. – P. 75.
3. Gafurova D. A., Shohidova D. N. New complexity on base polyacrylonitryl. Uzb. Chemical journal. – Tashkent, 2013. № 2. – P. 25–28.
4. Panjiev U. R., Ziyaeva M. A. Develope new ionits for peelings of the sewages oil and gaze to industry. Journal Oil and gas Uzbekistan. № 4, 2015. – P. 58–62.
5. Panjiev U.R, Kasimova F. B., Mukhamedgaliev B. A.A new ionits on base departure. Journal Composition materials. № 4, 2015. – P. 17–19.
6. Panjiev U.R, Kasimova F. B. Ionits for peelings of the sewages. Journal Ecological herald of a Uzbekistan. № 11, 2015 y. – P. 45–48.

Ergashev Dilmurod Adiljonovich,
research assistant of the Institute
of General and Inorganic Chemistry
the Academy of Sciences of Uzbekistan
E- mail: dilmurod-ergashev@rambler.ru

Askarova Mamura Komilovna,
candidate of chemical sciences
(Ph. D. in Chemistry),
senior staff scientist of the Institute
of General and Inorganic Chemistry
the Academy of Sciences of Uzbekistan.
E-mail: ionxanruz@mail.ru

Saiydiaxral Tukhtaev,
the head of Defoliant laboratory,
doctor of technical sciences, professor, academician,
honored inventor and innovator of Uzbekistan,
the Institute of General and Inorganic Chemistry
the Academy of Sciences of Uzbekistan
E-mail: ionxanruz@mail.ru.

Physico-chemical studies of novel chlorate containing defoliant

Abstract: The dependence of solution physico-chemical properties changing from components compositions in aqua system including calcium, magnesium chlorates, chlorides and mono ethanolamine acetate has been studied. It has been drawn that diagram "composition-property" of the system. The composition of the novel chlorate containing defoliant possessing growth of ripening and opening cotton bolls has been recommended based on obtained results.

Keywords: defoliant, physiologically active substance, calcium, magnesium chlorate and chlorides, calcium-magnesium chlorate defoliant, acetic acid, mono-ethanol amine, mono- ethanolamine acetate, thermogravimetric and radiograph analysis.

Introduction

In the Republic of Uzbekistan, where cotton is one of the important branches of agriculture in the cultivation of cotton with one of the most important activities is to collect the accumulated harvest. For high-quality and timely harvest — raw cotton there is necessary artificial leaf abscission through effective, low-toxicity defoliants.

It is known that leaf abscission and ripening harvest begins when the plants are in the body decreases the content of auxin and ethylene levels and other of antiauxin compounds increases. That is, in order to defoliant to act effectively on the plant and helped accelerate the ripening necessary to increase the content of ethylene and other antiauxin compounds in plant tissues [1–5].

Currently, the creation of high-performance, soft acting on plants domestic defoliants, on the basis of local raw materials, is an important problem of cotton of the country.

One solution to this problem is the preparation and use for defoliating cotton defoliants chlorate containing defoliants jointly with compounds containing ($-CH_2-CH_2-$) ethylene group, in particular mono-ethanolamine acetate, which is a stimulator of physiological processes.

Employees of the Institute of General and Inorganic Chemistry AS RUz developed technology for producing calcium-magnesium chlorate defoliant [6].

This technology is based on the use as a raw material instead of import — "Bischofite", hydrochloric acidic decomposition products of the local "dolomite", to obtain a calcium, magnesium chloride, and processing them with sodium chlorate by conversion method in calcium-magnesium chlorate defoliant.

There is currently no comprehensive action drugs that are both effective defoliants, stimulants of physiological processes, accelerators full maturation and opening cotton bolls.

Therefore, in order to increase defoliant-like activity new chlorate, calcium-magnesium defoliant and the acceleration full maturation and opening cotton bolls physicochemical study mutual influence of components are held in a complex aqueous system consisting of chlorates and chlorides of calcium, magnesium and physiologically active compounds — mono-ethanolamine acetate.

Experimental procedure

The objects of study are the calcium and magnesium chlorate defoliant and acetate of mono-ethanolamine. Calcium and magnesium chlorate defoliant prepared by hydrochloric acidic decomposition of dolomite and subsequent conversion of the decomposition products with sodium chlorate [6]. Mono-ethanolamine acetate is synthesized by reacting acetic acid with mono-ethanolamine, taken at a molar ratio of 1:1 and vigorous stirring [7].

Quantitative chemical analysis used the well-known techniques of analytical chemistry, in particular: chlorate ion is determined by volumetric permanganatometry [8]; calcium and magnesium were determined by complexmetric technique [9]; content of chloride ion by the method of Moore [10]. The content of elemental carbon, hydrogen was carried out according to [11].

Solid phase methods have been identified by a variety of physico-chemical analysis. Thermal analysis study

of new phases was carried out on the system derivatograph Paulik — Paulik — Erdei.

X-ray diffraction analysis was performed on diffractometer Dron — 3.0. Values-spacings found under the directory [12, 13], according to the angle of reflection, and the intensity of the diffraction lines was evaluated by hundred scales.

Results and Discussion

In order to physico-chemical study of the process of obtaining a new more effective preparation of local raw materials having a high defoliant-like activity and a "soft" effect on cotton is based on chlorate, calcium-magnesium defoliant and mono-ethanol ammonium acetate studied dependence of physico-chemical properties of the solutions of the composition of the components of the system [22.52%Ca $(ClO_3)_2$+17.51%Mg $(ClO_3)_2$+4.33%$CaCl_2$+3.12%$MgCl_2$+52.52%H_2O] — $CH_3COOH{\cdot}NH_2C_2H_4OH$.

To determine the influence of components on the physicochemical properties of the above defined system solutions change crystallization temperature, pH, refractive index, density and viscosity of the composition solution. Based on these results the diagram of "composition-property" of the system has been drawn (Table, Figure 1). According to the data chart "composition-temperature crystallization" of the system is characterized by the presence of two branches of crystallization, with a clear break in the curve solubility (Fig. 1, curve 1). The first branch corresponds to crystallization [47.3%Ca$(ClO_3)_2$+36.88%Mg $(ClO_3)_2$+9.12%$CaCl_2$+6.57%$MgCl_2$] and continues until 2% content of mono-ethanolamine acetate at 3.8 °C.

With increasing concentrations of mono-ethanolamine acetate more than 2% in the system crystallized compound composition $CaOHClO_3{\cdot}NH_2C_2H_4OH{\cdot}2H_2O$. Analysis of the diagram "composition-pH" (Fig. 1, curve 2) shows that as adding mono-ethanolamine acetate the value of pH solutions gradually increases. In the double point of pH value is 4.30. Further, with an increase in concentration of mono-ethanol ammonium acetate more than 2% i. e. compounds in crystallization field, the pH formed solution increases from 4.30 to 4.47.

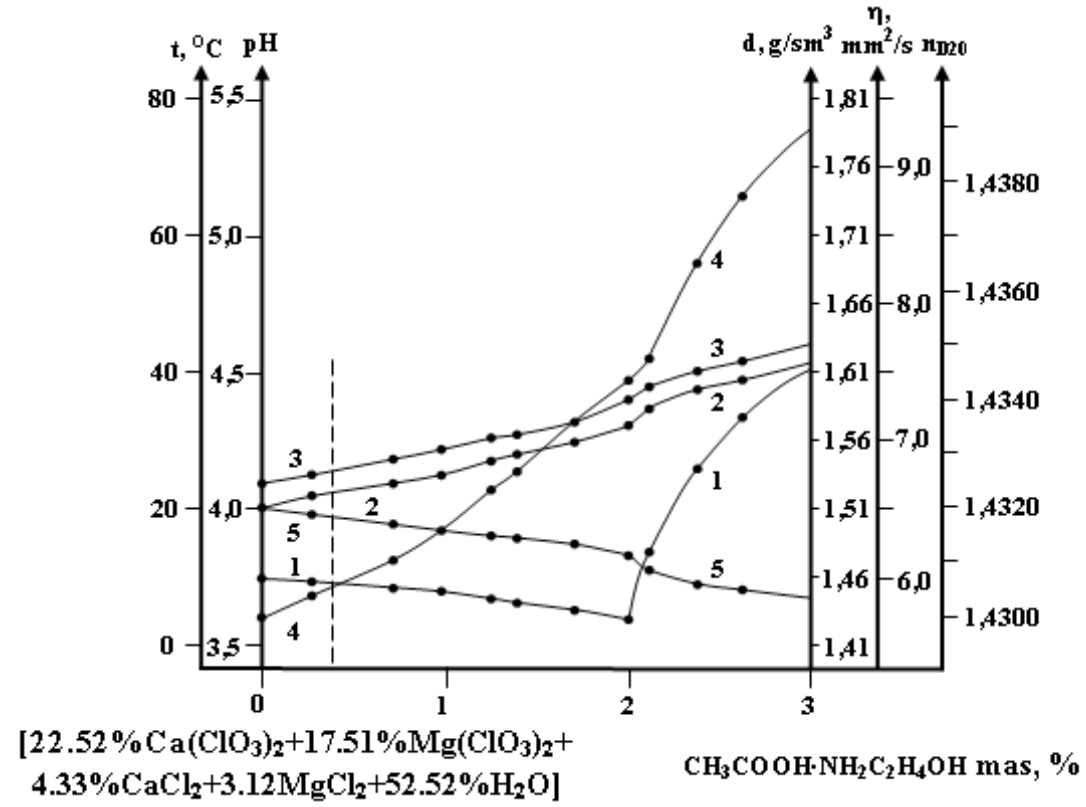

Figure 1. The Diagram "composition-property" of [22.52%Ca $(ClO_3)_2$+17.51%Mg $(ClO_3)_2$+ +4.33%$CaCl_2$+3.12%$MgCl_2$+52.52%H_2O]-$CH_3COOH{\cdot}NH_2C_2H_4OH$ systems.
1 – crystallization temperature, 2 – pH, 3 – viscosity, 4 – refraction index, 5 – density

The diagram "part of the refractive index" is also characterized by the presence of the two branches of the crystallization with a break in the curve (Fig. 1, curve 3). Viscosity solutions studied system is gradually increased from 6.69 mm^2/s and reaches 7.28 mm^2/s at a double point, i. e. with 2% of mono-ethanolamine acetate (Fig. 1, curve 4).

With increasing concentrations of mono-ethanolamine acetate viscosity newly formed solution increases and reaches 7.59 mm^2/s, which is explained the change in the area of the crystallization system.

Analysis of the diagram "composition-density" system (Fig. 1, curve 5) shows that increasing concentrations of mono-ethanolamine acetate density of the newly formed solution decreases. Curve 5 diagrams "composition-property", there is also a break. Branches of crystallization amounts of calcium, magnesium chlorates and calcium and magnesium chloride correspond to solutions density 1.511÷1.475 g/sm^3 (Table.).

The density values of the solution were 1.475÷1.451 g/sm^3 match crystallization branch connection $CaOHClO_3 \cdot NH_2C_2H_4OH \cdot 2H_2O$.

Table 1. – Dependence of change of the crystallization temperature, refractive index, pH, viscosity, density, solution composition of components in the system [22.52%Ca $(ClO_3)_2$+17.51%Mg $(ClO_3)_2$+4.33%$CaCl_2$+3.12$MgCl_2$+52.52%H_2O] — $CH_3COOH \cdot NH_2C_2H_4OH$

№	Components content,%		Tcr., °C	η, mm^2/s	d, g/sm^3	pH	n_{D20}
	[22.52%Ca $(ClO_3)_2$+ 17.51%Mg $(ClO_3)_2$+ 4.33%$CaCl_2$+3.12$MgCl_2$+52.52%H_2O]	$CH_3COOH \cdot NH_2C_2H_4OH$					
1	100	-	10	6.69	1.511	4.01	1.4300
2	99.72	0.28	9.5	6.75	1.505	4.05	1.4304
3	99.28	0.72	8.6	6.87	1.500	4.09	1.4311
4	99.02	0.98	7.9	6.94	1.495	4.12	1.4317
5	98.75	1.25	6.8	7.02	1.492	4.17	1.4324
6	98.61	1.39	6.3	7.05	1.488	4.20	1.4327
7	98.3	1.70	5.2	7.13	1.484	4.24	1.4336
8	98.0	2.00	3.8	7.28	1.475	4.30	1.4343
9	97.88	2.12	14.0	7.39	1.465	4.37	1.4347
10	97.63	2.37	25.9	7.51	1.456	4.44	1.4365
11	97.37	2.63	33.2	7.59	1.451	4.47	1.4378

Compounds formed in the studied system, isolated in crystalline form and identified by chemical, X-ray and thermal methods of analysis.

According to chemical analysis for $CaOHClO_3 \cdot NH_2C_2H_4OH \cdot 2H_2O$:

It has been found (mas.%): C = 10.2; H = 5.10; N = =5.92; Ca = 16.95; ClO_3 = 35.41; H_2O = 15.11.

It has been calculated (mas.%): C = 10.105; H = =5.053; N = 5.89; Ca = 16.84; ClO_3 = 35.158; H_2O = =15.158.

Compound formation $CaOHClO_3 \cdot NH_2C_2H_4OH \cdot \cdot 2H_2O$ was confirmed by X-ray diffraction. Compare diffraction lines and the corresponding values of the interplanar distances compound and its components showed that the compound is individual, with its crystalline lattice structure (Figure 2.).

For sample heating curve $CaOHClO_3 \cdot \cdot NH_2C_2H_4OH \cdot 2H_2O$ found three endothermic effect at 170, 225, 282 and three exothermic effect at 310, 545, and 690 °C. Nature endothermic effects determined by removal of water and the beginning of the decomposition of the complex. Intensive exothermic effect at 310 °C flows with a strong product explosion. This process proceeds in the range of temperatures 300–320 °C. The nature of the two following exothermic effects is specified by completion of the decomposition product thermolysis. On the composition of the final product of decomposition is calcium oxide (Figure 3.).

Based on the results of study of "composition-properties" of the above mentioned systems and carried out agrochemical testing defoliant compositions implies that for an effective "soft" effect of the preparation, which has defoliant –like and physiological activity to be dissolved in a solution of chlorate of calcium-magnesium defoliant acetate mono-ethanol ammonium at a weight ratio of 1.0:0.0035.

There has been formed that solution defoliant with good physico-chemical properties, having a crystallization temperature of 9.4 °C, viscosity of 6.79 mm^2/s, density of 1.502 g/sm^3 and pH of 4.07.

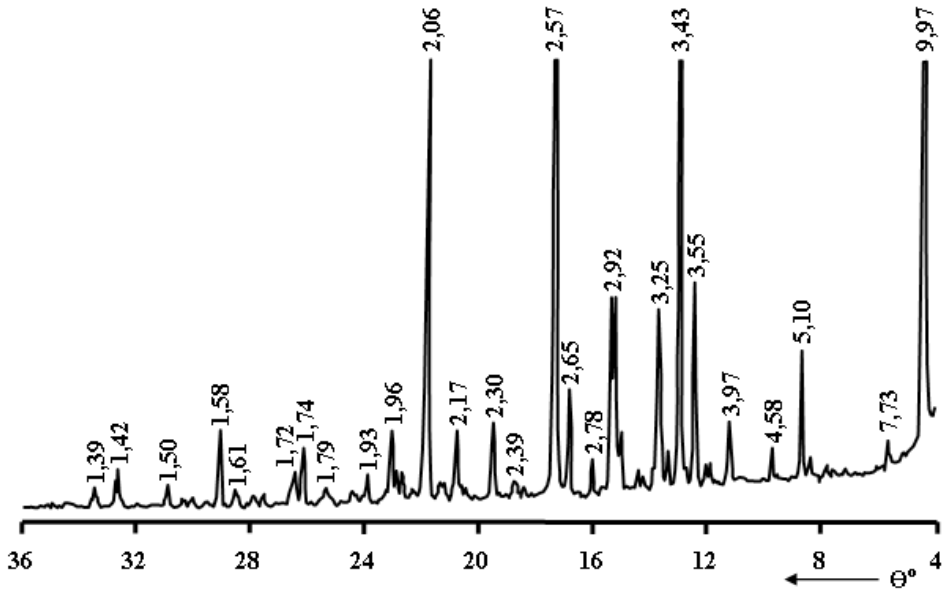

Figure 2. Radiograph of $CaOHClO_3 \cdot NH_2C_2H_4OH \cdot 2H_2O$

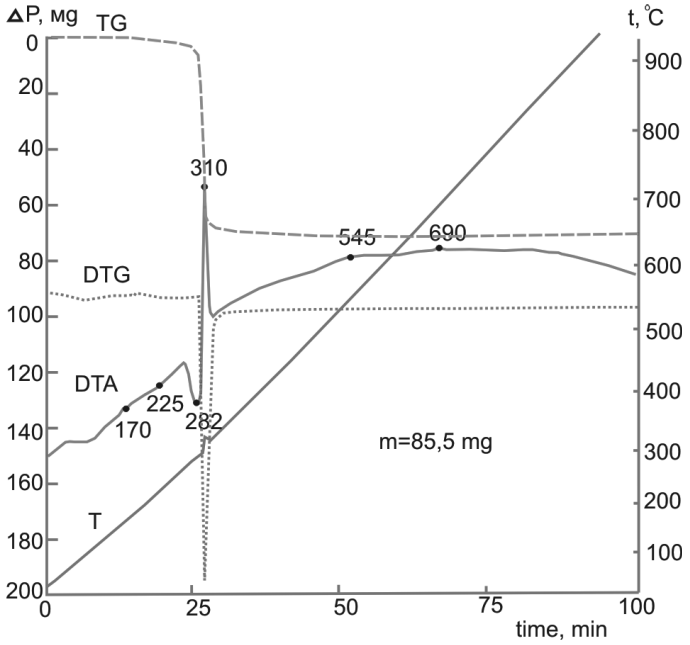

Figure 3. Thermogravimetric of $CaOHClO_3 \cdot NH_2C_2H_4OH \cdot 2H_2O$

Conclusion

Thus, according to the study changes in physicochemical properties of the solutions of the composition of the system [22.52%Ca $(ClO_3)_2$+17.51%Mg $(ClO_3)_2$+ 4.33%$CaCl_2$+3.12%$MgCl_2$+52.52%H_2O] — $CH_3COOH \cdot NH_2C_2H_4OH$ showed that on its diagram "composition-properties" identified branch crystallization connection of $CaOHClO_3 \cdot NH_2C_2H_4OH \cdot 2H_2O$. The results of the studied system are the basis for recommendations to the composition of the new liquid chlorate containing defoliant, accelerating the maturation of cotton bolls and disclosure.

References:

1. Rakitin Yu. V. Nature of action 2-chloroethylphosphonic acid and other ethanol leaching growth regulators and plant development.//Agrochemistry. 1979. – № 5. P. 126–146.
2. Nurijanyan KA, Gudkov AG, Zubkov NF, Georgian N. A. Chemistry and application of defoliants and desiccants. M.: NIITEKHIM. 1989. P. 78.
3. Kefeli V. I. Physiological basis of defoliation and production process. Tashkent: Fan. 1991. P. 183.
4. Rakitin Yu. V. Chemical regulators of plant life. M.: Nauka. 1983. P. 260.

5. Curci B. A., Koidan G. N. Mechanisms of action of growth regulators//Chemistry and life. 1985. – № 10. P. 68–69.
6. Hamrakulov Z. A., Askarov M. K. Tukhtaev S. Conversion of calcium chloride and magnesium with sodium chlorate. Reports of the Academy of Sciences of the Republic of Uzbekistan. Tashkent. 2014. – № 6. P. 52–57.
7. Shukurov J. S. Obtaining complex action of new defoliants based on sodium chlorate having a physiologically active and insecticidal properties: Dis. PhD in technique sciences. -Tashkent, 2012. P. 168.
8. The liquid magnesium chlorate defoliant. Specifications. Tsh 00203855–34: 2015. P. 14.
9. Schwarzenbach G., Flaschka G. Complexometric titration. – M.: Chemistry, 1970. P. 360.
10. Dorokhova E. N., Prokhorova G. V. Analytical chemistry (physical-chemical methods of analysis). M.: Higher School, 1991. P. 250.
11. Klimov V. A. Basic micromethods analysis of organic compounds. M.: Chemistry, 1975. P. 224.
12. Giller J. L. Table-spacings. V.2. – M.: Nedra, 1966. Vol. 1. P. 362.
13. Ned I. Explanation X-ray powder. – M.: Metallurgy, 1975. P. 423.

Erkaev Aktam Ulashevich,
Tashkent Institute of Chemical Technology,
Doctor of Technical Sciences, Professor
Reymov Karjaubay Dauletbaevich,
Tashkent Institute of Chemical Technology, Researcher
Kaipbergenov Atabek Tulepbergenovich,
Tashkent Institute of Chemical Technology, Researcher
Ulashova Nafisa Aktamovna,
Tashkent Institute of Chemical Technology,
Students
E-mail: atabek2004@mail.ru

Mineral composition of precipitation coast western large Aral Sea

Abstract: The work is devoted to the study of the mineral composition of the water-soluble salts of bottom sediments formed after the drying of the Aral Sea. Based on the studies the regularities of distribution of clay materials and soluble salts in three soil layers of the west coast of the Big Aral Sea.

Keywords: minerals, mirabilite, thenardite, halite, blodite, konyite, loweite, vanthoffite, pentahydrate, starkeyite, sanderite, kieserite.

The UN has recognized that the disappearance of the Aral Sea — one of the biggest environmental disasters of recent times. Confirmed the planetary nature of the Aral Sea crisis and the need to mobilize the international community's efforts to address it. At the end of his visit to the region, UN Secretary-General has called the death of the Aral Sea, "one of the most serious environmental disasters in the world" and said that the struggle with its consequences is a "collective responsibility of the whole world, not just the countries of Central Asia." At the initiative of President Islam Karimov in the city of Urgench on 28–29 October 2014 the international conference "Development of the Aral Sea region cooperation to mitigate the environmental disaster." It was attended by representatives of 24 authoritative international and regional organizations, financial institutions such as the UN, SCO, the Regional Centre for Preventive Diplomacy for Central Asia, the International Centre for assessment of groundwater resources, ADB, IDB, World Bank, Organization for Economic Cooperation and Development OPEC, scientists and ecology experts, climate change and water resources management from 26 countries, including Austria, Hungary, Germany, Spain, China, Latvia, Malaysia, the USA, France, Switzerland, South Korea, Japan and other. To identify further ways to solve the problems of the Aral Sea, we are well aware that the recovery of the

sea in its former borders is not possible. This process has gone so far that it can not be reversed. The very process of solving related problems is very difficult. It is necessary, first of all, to save the people who live around the dying sea, and stabilize the ecosystem of the Aral Sea region.

a

Wells 1, 2

b

Wells 7, 8

c

Wells 9, 10

g

Wells 11–14

Figure 1. Place soil samples from the western and eastern coasts of the western part of the deep-water (3–10) and the feed zone on degree salt of a volatility (1, 2, 11–14) of the Big Aral Sea. Non wells corresponds to the wells Table 1

All the more exacerbated the negative situation in the basin of the Aral Sea region and the surrounding area is strongly calls for urgent additional measures to overcome the disastrous consequences of the Aral Sea dries, create the necessary socio-ecological and humanitarian conditions for living here and in the vicinity of more than 60 million. Man. The scale of the challenges to be dictated by the need for more effective coordination, pooling of resources at the national, regional and international levels in order to prevent even greater disaster in this area [1–5]. From the literature data [1, 3, 6] and the results expedition 15–25 June 2014, has to be that the rate of formation of the dried surface decreases from 1 to thous.km^2 0.15–0.20 year at 32.85 m depth, water surface area — 3.34 km^2, the volume of water mass — 95.95 km^3 with an average content of 12595.38 million tons of salt. In the period from 2002 to 2014 there was indented shores with the formation of 1.92 km^2 of water surface in 2015 on March 17 in the western part of the sampled and measured the indentation from the coast than from 1 May 2012, which on average amounted to 50–55 m/year [7].

The study of modern bottom sediments of water bodies to a certain extent characterizes the depositional environment, which is essential for the establishment of the geological origin of these reservoirs. The literature has accumulated a large amount of factual material on the chemical composition of the sludge water of the oceans, sea and large lakes. According to the 1973–1984 bienniums in the bottom sediments of the Aral Sea are common and terrigen beds of rock-forming and accessory minerals. They present 37 of the 63 minerals found in the studied bottom, coastal and deltaic sediments. Beds of minerals are mainly calcium and magnesium carbonates, calcium sulfate and sodium [1, 2]. The bottom of the Aral Sea sediments in the modern period after drying have not been studied. In 2012–2015, we have been selected and studied sediments from the 30 columns of soil to a depth of 600 cm. Total 160 analyzed samples, most of which are determined by the content of Ca^{2+}, Mg^{2+}, Na^{+}, K^{+}, HCO^{3-}, $SO_4^{2-}$and Cl^{-} — ions.

We have previously [3] it was shown that the dried bottom of the Aral Sea has three in the degree salt volatility zone defined phase-salt formations.

In the first zone of the salt composition of groundwater varied from sulfate-chloride to chloride-sulfate with a predominance of sulfate and chloride salts, respectively. The amount of volatile salts thus proved practically balanced. Total salt content was not more than 60 g/l, the water level from the bottom — less 1–2.5m. The second zone — this is the most terrible greatly excited salt alopecia area as the remaining (3119.548–62.39·20=1871.75 mln. t.) salt is enough for more than 100 years for the annual average in the ash dust storm 18.71 mln. t. salts the eastern basin of the Big Aral.

The third zone — a free from volatility salts. Despite the great volatility of 1.4 times a weight of about three times less than in the second zone. This is due to the fact that one part of the salt is in the form of crystals with a continuous layer thickness 2–48 cm, and the second part is covered with the liquid brine depth of 1–20 cm.

Soil samples for analysis were selected on an expedition in the period 15–25 June 2014 from the western basin of the Aral Sea Big cuts from 45°30' to 44°30' N western coast at a depth of 20–340 cm (Figure 1). The soil surface is covered with clay marsh prominent large cracks 15–30 cm width of 5–10 m and a depth of 1.0–2.0 m (Figure 1a). On the eastern shore of the western deep-water part of the Big Aral Sea meet mirabilite salt deposits are formed is formed in the winter, and in spring and summer are dissolved atmospheric precipitation. In the deep part of the Big Aral Sea salt-water mirror retreats from the shore at an average speed of 40–60 m/year, forming the bottom of the drained (Figure 1c).

On the dry bottom of the south side of the eastern part of the Big Aral Sea, which was formed in the 90 of the twentieth century, increased salt tolerance to salt tubercles (Figure 1g) appeared around the roots by alluvium volatile salts.

The soil samples were determined by humidity, moisture retention, the composition of the insoluble and soluble salts. Water retention samples were directly proportional to the content of clay materials. To determine water retention 20 g sample was dissolved in 1000 liters of distilled water, the resulting suspension was filtered through a filter «blue tape» and washed with water. After washing the precipitate till disappearance of chloride ions wet cake left on the filter funnel until no drops. Then the humidity was determined the precipitate that is insoluble water retention portion samples. Table 1 shows the chemical composition of clayey sand and salt deposits of samples taken from the north side of the eastern part of the wells 1, 2 (2–3 km from the Barsakelmes reserve); with the western and eastern shores of the deep part (wells 3, 9, 10, 4–8); with the eastern part of the Big Aral Sea south side (wells 11–14).

From the obtained data it is visible that water retention of samples in wells 1–5, 8, 9 and 10 fluctuates within 54.08–72.96%, and humidity and the maintenance

of water insoluble part in them makes 0.9–35.20% and 69.05–99.70% respectively. Humidities of wells 6, 7 make 0.05–0.25%, and the maintenance of water insoluble part does not exceed 0,2%.

Table 1. – The chemical composition of the soil samples obtained from the western shore of the deep-western part of the Large Aral

№ well	Date of sampling	Coordinates		Depth selection samples sm	Humidity,%	Water retention,%	Insoluble residue,%	Ion content, wt.%						The ratio of ions	
		Northern latitude	Eastern longitude					Na	K	Ca	Mg	Cl	SO_4	SO_4|Cl	Mg| Na
3	20.06.14	45.3001	58.3648	0–0,2	14.9	72,2	94,88	0,43	0,039	0,087	0,05	0,55	0,58	1,05	0,12
				2	33,02	69,13	97,2	0,8	0,046	0,6	0,159	1,1	2,1	1,91	0,2
				0,2–20	26.35	68,68	98,35	1,67	0,1	0,67	0,325	2,54	3,22	1,27	0,19
				20–36	32,9	68,12	86,86	0,516	0,045	0,099	0,098	0,55	0,88	1,6	0,19
				40	31,7	70,2	99,7	0,4	0,03	0,149	0,098	0,49	0,91	1,86	0,25
				40–60	25,67	67,9	69,6	0,53	0,039	0,137	0,083	0,71	0,77	1,08	0,16
				100–120	29.87	59,97	92,8	0,53	0,059	0,125	0,076	0,77	0,69	0,9	0,14
				120–140	28,9	66,58	96,1	0,66	0,055	0,219	0,09	0,77	1,24	1,61	0,14
				140–180	32,15	61,08	91,7	0,426	0,0449	0,062	0,076	0,55	0,59	1,07	0,18
				310–360	21,17	54,08	73,9	0,38	0,039	0,099	0,068	0,44	0,72	1,64	0,18
5		45.2487	58.3951	0–2	7,47	56,07	80,16	0,79	0,034	0,58	0,18	1,1	2,3	2,09	0,23
				2–15	16.4	74,8	91,69	1,25	0,04	0,3	0,15	1,05	2,8	2,67	0,12
6		45.2486	58.3529	0–6	24,4			31,24	0,007	0,9	0,04	0,25	65,9	263,6	0
				6–15	19,6	40,26	69,05	1,45	0,06	0,52	0,3	1,8	2,57	1,43	0,21

The content of water insoluble part in samples of wells 11–14 up to the depth of 5 cm makes 90.40–96.28% with humidity of 0.5–1.0% and manifestations by the increased water-retaining power (wells 11–14–77.3–77.5%). As a part of soluble salts contain in the basic sodium, chlorine and sulfate ions which contents increases in process of transition from the first to the third samples.

The chemical analysis of the contents of sodium and calcium ions was determined by flame photometry [8], and magnesium — complex metric [9, 10]. Sulphate is determined by the gravimetric method, which consists in the precipitation of $BaSO_4$. The content of Cl^- ions were determined by mercurimetry, HCO_3^- and CO_3^{2-} — acid titration [9].

In samples of wells 1, 2 up to the depth of 30 cm water content in insoluble salts was in limits of 3–6% at a ratio SO^{2-}_4: Cl^-=3:5. In samples of depths more than 30 cm this ratio of ions decreased to values less than 0,81.

Depth of a section of the third well reached 360 cm from where also the homogeneous exemplars through each 20 cm were selected. Water retention of insoluble part of exemplars of the soil from the Earth's surface in a depth changes in zigzag fashion (Table 1). Thickness of the third well was divided into three layers: the first — 20 cm, from 0 to 20 cm; the second — 100 cm, from 20 to 120 cm; the third — 240 cm, from 120 to 360 cm. In the first coat of regularity of change of observed indexes it was not observed. Indexes of the second and third

layer changed on particular regularities. For example, with increase of depth from 20 to 120 cm water retention of insoluble part decreases from 72.96 to 59.97%, and in the third layer — from 66.58 to 54.08%. It follows from this that water retention in the third layer is 5.80–6.38% less than in the second layer. Therefore, in the second layer with increase of depth the maintenance of clay components of soils decreases, and at the beginning of the third layer increases again, but it is less than at the beginning of the second layer.

From results of analyses of exemplars of the fourth well it is visible that with increase of depth of a section from 0.2 to 60 cm water retention of tests decreases from 72.00 to 63.90%, and it means decrease in content of clay substances as a part of insoluble part of exemplars. Humidity of exemplars made 11.65–15.35%, and quantity of insoluble part — 93.03 and 88.06%. Here too as well as in other cuts of wells in soluble salts contain in the basic sodium, chlorine and sulfate ions. Content of soluble salts on a surface 0–0.2 cm thick makes 11.96%. The ratio of ions of SO^{2-}_4/Cl^- is 1.18 times more than in salts of the high layer of the third well and up to the depth of 60 cm practically remains to constants within 1.38–1.40.

Samples of wells 5–8 received of east coast of the deep-water western part of Big Aral having salt deposits (fig. 1) consist only of salt cake (a well 5, depth of 0–2 cm and a well 7, depth of 0–15 cm).

In samples of wells the 9 and 10 nature of distribution of moisture in soluble salts on depth is almost identical in comparison with exemplars of wells 3 and 4, but the ratio of ions of SO^{2-}_4/Cl^- is 1.5–3.0 times less at a depth more than 20 cm. At a depth more than 20 cm on east coast of deep-water western part of Big Aral the ratio of ions of SO^{2-}_4/Cl^- decreases from the North to the southeast. At a depth from 0 to 20 cm the specified ratio of ions of SO^{2-}_4/Cl^- changes spasmodically and does not exceed 0,1 that is bound to a wind soleunos, shown especially in samples of wells 11–14. Thus, compositions of water-soluble salts in exemplars of soils from the North to big Aral's southeast changes from sulphatic to chloride and sulfate and chloride.

With increasing content of clay materials in their retention of salt samples increases. For example, down the second layer contents sodium, magnesium, chlorine and sulfate ions decreases from 1.47, 0.18, 1.93 and 1.56 to 0.53, 0.076, 0.77 and 0.69% respectively, and in the third layer — from 0.66, 0.09, 0.77 and 1.24 to 0.38, 0.068, 0.44 and 0.72%.

Layered comparison ratio SO^{2-}_4/Cl^- ions indicates that the third to the second layer is decreased from 1.61 to 0.88, and from the second to the first, on the contrary, increased to 2.44. This is due to high speed mobility capillary SO^{2-}_4 — ions than Cl^- — ions. This pattern is also observed in other sections of the wells.

Samples 6 and 8 wells were selected from a salt precipitation of white eastern shore of the salt deposits to 15 cm thick and the soil, respectively. Sample 6 wells contained sodium and sulfate ions, and at a depth of 0–6 cm is practically insoluble portion were absent, and at a depth of 6–15 cm, it is contained in an amount of 69.05%. The chemical composition of the soil sample 8 wells varies differently. From the soil surface to a depth of water retention, and increased salinity. For example, when increasing the depth of 60 cm 2 to the content of sodium ions, chlorine and sulphate increases from 0.58, 0.07 and 0.84 to 0.65, 1.07 and 1.49%, respectively. This is justified when the content of clay minerals in the soil, their content with increasing depth becomes greater.

For physico-chemical studies of the composition of salt deposits deep part of the west coast of the Big Aral Sea used samples listed in Table 1 correspond to the numbers which the curves of physical and chemical analysis are shown in Table 2.

Table 2. – Non-curves corresponding to sample numbers of Table 1

Numbers of curves	Numbers of wells correspond to numbers of wells of Table 1	Depth of samples, cm
1	3	140–180
2	3	310–360
3	5	0–2
4	5	2–15
5	6	0–6
6	6	6–15
7	9	200–240
8	15	0–2

The results of the physico-chemical analyzes are presented in Tables 3–4, and Figures 2, 3.

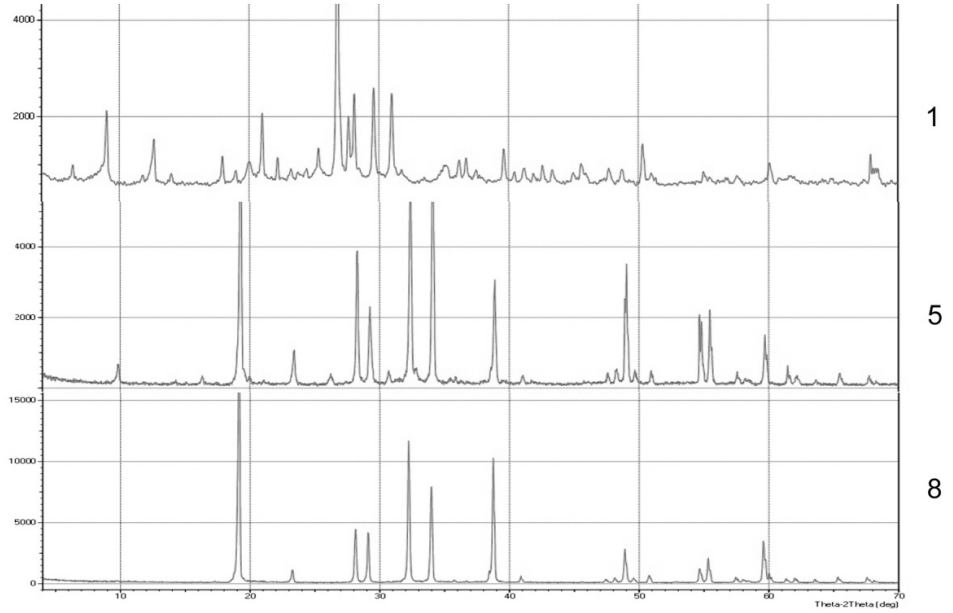

Figure 2. XRD patterns of samples. Numbers of samples correspond to numbers of Table 2

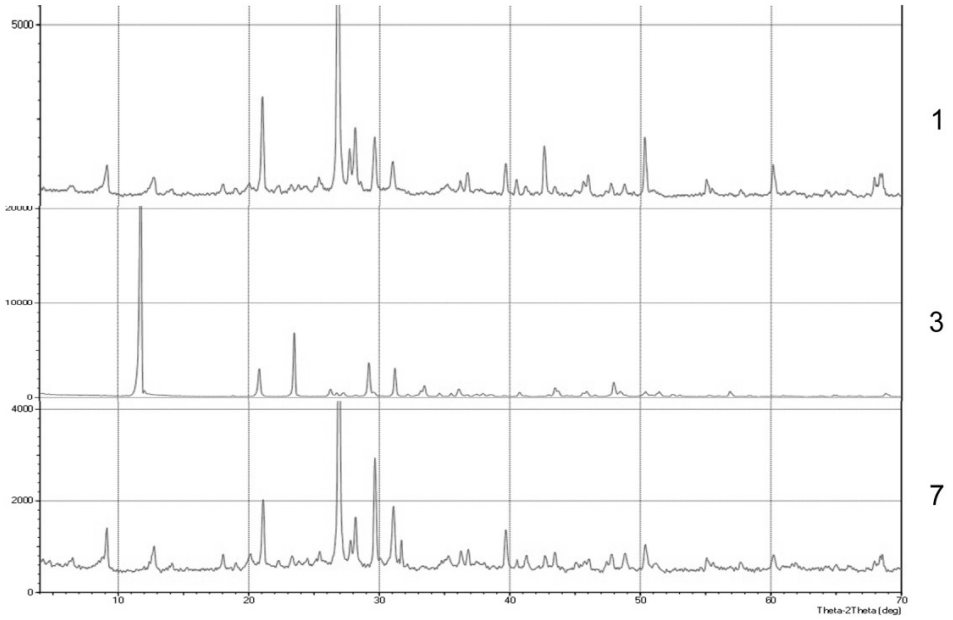

Figure 3. XRD patterns of the samples after washing. Numbers of samples correspond to numbers of Table 2

Identification of the samples was carried out on the basis of diffraction patterns, which were recorded on a XRD-6100 machine (Shimadzu, Japan), computer controlled. We used CUK α-radiation (β-filter, Ni, 1.54178 current mode and the tube voltage of 30 mA, 30 kV) and a constant rotation speed detector 4 °C/min in increments of 0.02° (ω/2θ-clutch), and and the angle of scanning changed from 4 to 50°.

Thermal stability of crystalline samples studied were determined on the instrument Netzsch Simultaneous Analyzer STA 409 the PG, thermocouple K-type (Low RG Silver) and aluminum crucible. All measurements were carried out under an inert nitrogen atmosphere with 25–600°C flow rate, heating rate — 5 K/min. Number of sample per measurement of 5–6 mg. The measuring system was calibrated standard set material KNO_3, In, Bi, Sn, Zn, CsCl.

XRD analysis of samples without rinsing and after washing of the soluble salts showed that the solid phase samples 1 and 2 comprises an insoluble portion and the soluble sulfate and chloride salts are characterized by the presence of X-ray diffraction peaks at different intensities. At sample 1 radiograph revealed strong intensity diffraction peaks belonging to the insoluble portion. For identification of selected soluble salts of at least two characteristic diffraction having intensity not less than 10% [11–13]. The characteristic peaks of the insoluble part of the samples are shown in Figure 3 and Table 3.

Table 3. – The characteristic peaks in the samples of minerals

Name minerals	Sample numbers correspond to Table 2							
	1	2	3	4	5	6	7	8
Thenardite	+	–	+	–	+	+	+	+
Mirabilite	–	–	–	+	+	+	–	–
Halite	–	+	–	+	–	–	–	–
Blodite	+	+	+	+	+	+	+	+
Konyite	+	+	–	+	+	–	+	+
Loweite	+	+	+	+	+	+	+	+
Vanthoffite	+	+	+	+	+	+	+	+
Epsomite	+	+	+	+	–	+	+	–
Hexahydrite	–	–	–	–	–	–	–	–
Pentahydrate	+	+	+	+	+	+	–	+
Starkeyite	+	+	–	+	–	–	+	+
Sanderite	+	+	+	+	+	+	–	+
Kieserite	+	–	+	+	–	+	+	–

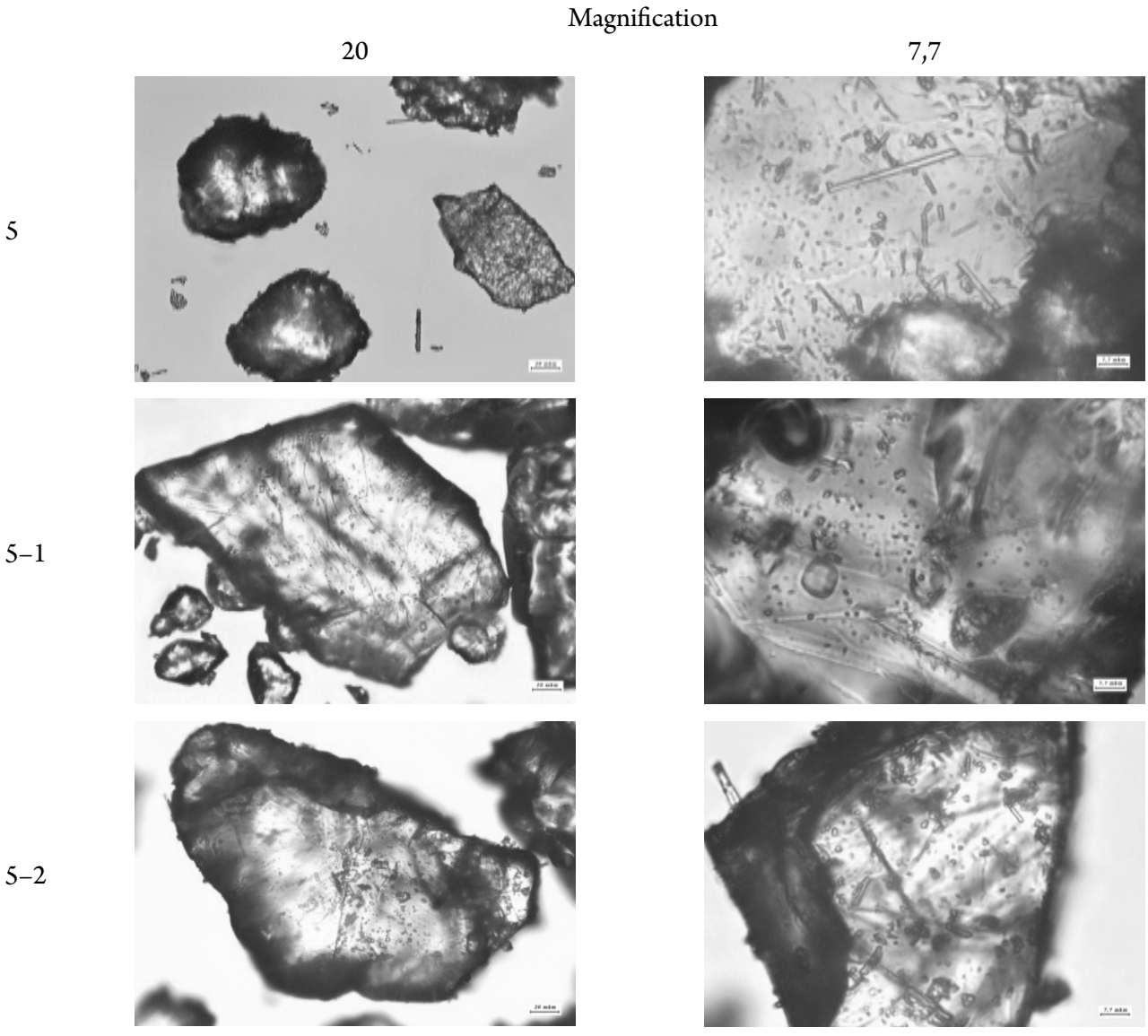

Figure 4. A micrograph of the morphology of the samples.
Number samples correspond to the numbers in Table 2

Based on X-ray, microscopic and chemical studies of water soluble and insoluble parts found that rock samples contain the following water-soluble minerals mirabilite, thenardite, halite, blodite, konyite, loweite, vanthoffite, pentahydrate, starkeyite, sanderite and kieserite. It is characteristic that in the salt rocks are virtually no carbonates as HCO_3 and CO_2 content in the samples did not exceed 0.02–0.078 and 0.002–0.009%, respectively (Table why 2 is omitted). This is probably due to the fact that in conditions of high hydrochloric carbonates precipitated in the early stages of salinization of water [1].

The relatively high content of magnesium Mg|Na 17–21% indicates the presence of magnesium in the mineral samples: blodite, konyite, loweite and vanthoffite. Loweite and blodite longer occurs in wells Samples 3, 5, 6 and 9, which are formed incorrect crystalline form aggregates of up to 854 microns (transparent glassy minerals, clay coated crystals ranging in size from 1 to 5 microns).

According to microscopic analysis, samples 5 and 15 are crystals thenardite length of 7.2 to 854 microns and a width of 1.2 to 545 microns.

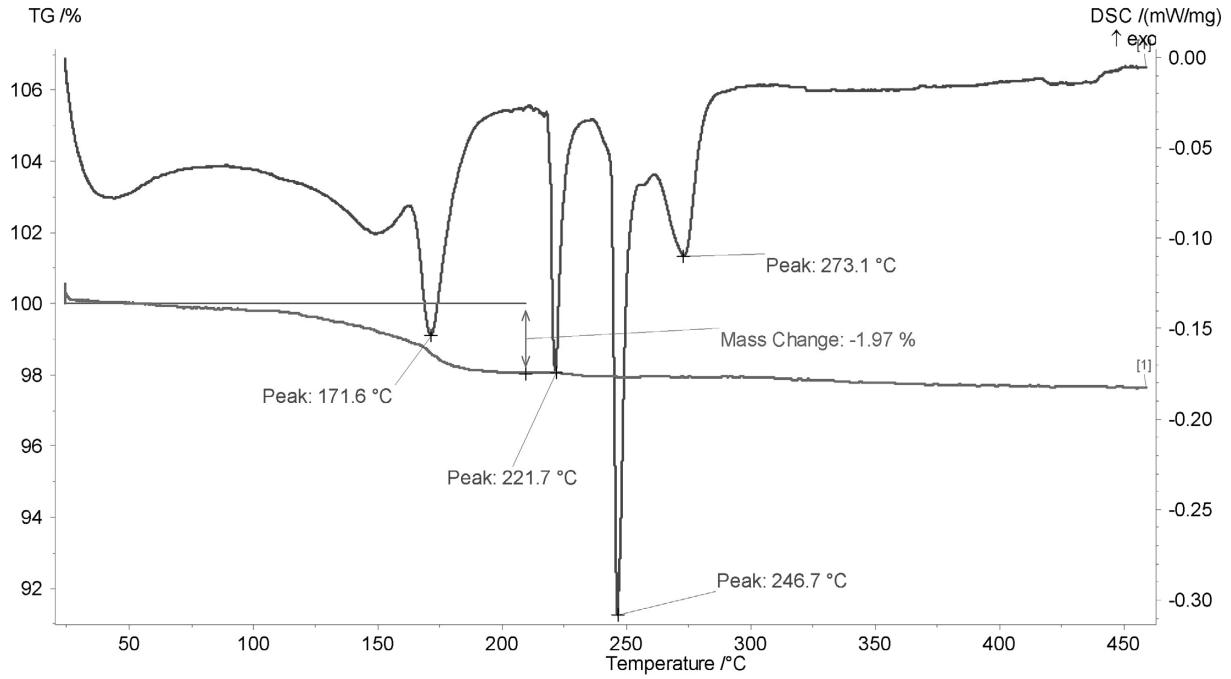

5

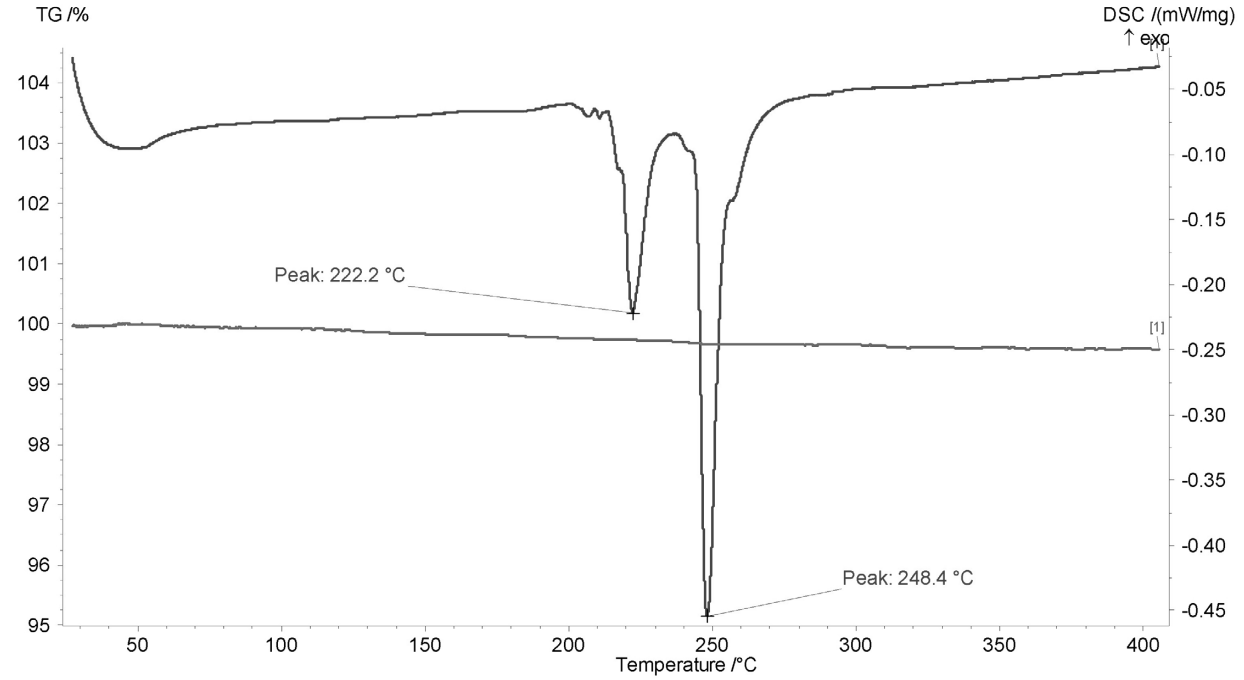

15

Figure 5. Derivation of the sample 5. The sample number corresponds to the number Table 2

Samples 1 and 2 are also formed crystals of Na_2SO_4 * $MgSO_4$ * $4H_2O$ — blodite (Astrakhanite), as well as konyite and loweite structure is short-length from 11.2 to 854 mkm and a width of 5.6 to 400 microns. There Na_2SO_4 — thenardite friends and granular aggregates. Found crystals typical of fibrous $MgSO_4 \cdot 7H_2O$ and $MgSO_4 \cdot 5H_2O$, and $MgSO_4 \cdot 4H_2O$, $MgSO_4 \cdot 3H_2O$ and $MgSO_4 \cdot 2H_2O$ dense granular tablet and prismatic structure.

On Derivation (Figure 5 Sample 5) there are four deep endothermy effect at 171.6, 221.7, 246.7 and 273.1 °C with a weight loss of 1.97%, which can be attributed to the dehydration of salts and blodite.

On Derivation other samples are also observed these endothermy effect with different depths depending on the content of hydrated minerals. In the absence of hydrated minerals, some of the characteristic effects are not observed. For example, in the sample 8 are shown two uncharacteristic endothermy effect at 222.2 and 248.4°C virtually no loss of weight, which is associated with polymorphic transformation thenardite.

Thus, the present work is devoted to the study of physical — chemical properties and mineralogical composition of bottom sediments of the Aral Sea after it dries.

On the basis of the conducted researches with establishment of regularities of distribution of clay materials and soluble salts of soils is thicker than the west bank of the Big Aral Sea it was divided into three layers: the first — 20 cm from 0 to 20 cm; second-100 cm from 20 to 120 cm; the third — 240 cm from 120 to 360 cm. In the first coat there is no regularity of change of observed indexes. The second and third layers separately and have certain patterns of interconnection. It was established that in the second layer to increase the depth of the soil content of clay components is reduced, and at the beginning of the third layer increases again but less than at the beginning of the second layer. These phenomena influence the allocation of soluble salts; Chemical and physicochemical methods of investigation of water-soluble salts and insoluble in water, soil residue found that the samples contain the following water-soluble minerals mirabilite, thenardite, halite, blodite, konyite, loweite, vanthoffite, pentahydrate, starkeyite, sanderite and kieserite.

References:

1. Рубанов И. В., Ишниязов Д. П., Баскакова М. А., Чистяков П. А. Геология Аральского моря.Ташкент: Фан,1987. – 246 с.
2. Курбанбаев Е., Артыков О., Курбанбаев С. Аральское море и водохозяйственная политика в республиках Центральной Азии.Издательство "Каракалпакстан", 2011. – 128 с.
3. Большое Аральское море в начале XXI века: физика, биология, химия/П. О. Завьялов, Е. Г. Арашкевич, И. Бастида и др.; Институт океанологии им. П. П. Ширшова РАН. М.: Наука, 2012. – 229 с.
4. http://www.oceanology.ru/aral-sea-shallow
5. www.uza.uz «Развитие сотрудничества в регионе бассейна Аральского моря по смягчению последствий экологической катастрофы». международная конференция. г. Ургенче 28–29 октября 2014 г
6. http://www.Cawater.info/index.htm. База данных по Аральскому морю: Г. Н. Трофимов: Палеоклиматическая ситуация, сток древних рек и водный баланс Арала в позднем плейстоцене и голоцене.
7. Реймов К. Д., Тоиров З. К., Каипбергенов А. Т., Туремуратова А. Ш. Современное экологическое состояние и солевые отложения Аральского моря. Узбекский химический журнал. № 5. 2014. С. 4–20.
8. Полуэктов Н. С. Методы анализа по фотометрии пламени. – Л.: Химия. – 1967. – С. 307.
9. Позин М. Е. Практикум по технологии неорганических веществ. М.: Высшая школа. – 1987. – 172 с.
10. Шварценбах Г., Флашка Г. Комплексонометрическое титрование. – М.: Химия. – 1970. – С. 360.
11. Недома И. Расшифровка рентгенограмм порошков. – М.: Металлургия. – 1975. – С. 423.
12. Американская картотека ASTM. Diffraction Data cards and Alphabetikal and Group Numerical Index of X-Ray Diffraction Data/Изд-во Американского общества по испытанию материалов. Нью-Йорк. 1973.
13. Миркин Л. И. Справочник по рентгеноструктурному анализу поликристаллов. М.1991. – С. 863.

Khamdamova Shokhida Sherzodovna,
Candidate of Science (PhD) in Technics
Tukhtaev Saiydiaxral,
Doctor of Science, academician,
Institute of General and Inorganic Chemistry
of the Academy of Sciences of the Republic of Uzbekistan,
E-mail: hamdamova79@mail.ru

Solubility polytherm of the system of sodium chlorate — calcium chloride — water

Abstract: The mutual behavior of internal section component of the quadruple system Ca^{+2}, 2Na//2ClO_3^-, 2Cl $^-$ H_2O, sodium chlorate — calcium chloride — water has been explored by visual — polythermic method. The polythermic diagram of solubility of the system has been built. The compositions of equilibrium solution of the system and the corresponding crystallization temperatures have been determined.

Keywords: mutual system, diagram of solubility, chlorides, chlorates of calcium and sodium, the crystallization temperature.

Introduction. For qualitative and well-timed realization of the collection of the harvest of the raw cotton it is extremely necessary to undertake perharvest removing cotton leaves by means of chemical preparations, defoliants. Since defoliation is an important land treatment action, without which it is impossible to reach the desired success in cotton growing [1].

In our republic, fluid magnesium chlorate produced on JC "Ferganaazot" is basically used for defoliation of the cotton plants [2]. Bischofite (the magnesium chloride), bought from the other countries for foreign currency, is used as raw material for production of the given preparation. So, there is undoubted interest in organization of import substitution as such as production of the cheapest chemical preparation, defoliants, in particular, based on local raw materials, for agriculture of the republic.

It is well known that distiller suspension, forming in amount 8–10 m^3 per 1 ton of soda containing 15–16% solutions of calcium and sodium chlorides, hydroxide and sulphate calcium is the worst and high-volume production of ammonium Solvay process. That is predestined by the existing technology itself on, which does not allow reaching full utilization of raw materials. Also, 27–30% solutions of calcium chloride are formed as waste during decontamination of hydrogen chloride in production of caustic soda by electrolysis of the sodium chloride at ***JC*** "Navoiazot". It may be concluded on the base of the above-stated that the most perspective solution of the ecological problems of chemical industry and utilization of such wastes is their use as raw materials for production of concentrated calcium chlorate defoliant which is used to defoliate cotton plants.

The Objects and methods of the studies. The objects of the study are sodium chlorate and calcium chloride. Common methods of analytical chemistry had been used at quantitative chemical analysis, including: chlorate-ion was by spatial permanganatometry method [3]; calcium was defined by spatial chelatometry method [4]; the contents of chlorine-ion — by Mohr method [5].

The Results and their discussion. For physicochemical substantiation and delivering recommendations on technologies of producing defoliants on the base of sodium chlorate and chloride calcium, as well as determination of crystallization field of source components and resulting components, it is necessary to know the solubility and components interactions in broad range of the temperature and concentration. The study of these problems allows to determine the nature of the chemical interaction between components, physicochemical characteristics of solution and to ascertain the optimum technological parameters of the process of producing efficient defoliants on the base of above-mentioned components.

The internal section of the quadruple mutual system Ca^{+2}, 2Na//2ClO_3^-, 2 Cl^- — H_2O, sodium chlorate — chloride calcium — water is studied in the range of from the temperature of system's full freezing –52.0 to 80 degrees Centigrade by visual-polythermic method [6].

The lines of liquidus of ice and calcium chloride of different hydrates are revealed on the solubility curve of calcium chloride in water. The separation of ice on solubility curve of the system of chloride calcium — water lasts until reaching 30.6 percentage of chloride calcium

at –49.7 (eutectic). Six-hydrated chloride calcium crystallizes at this point and forth that remains stable until 29.7 degrees Centigrade. The temperature range of 29.7–45.4 degrees Centigrade corresponds to the area of crystallizations of four-aqueous chloride calcium. Crystallization of two-water calcium chlorate starts at 56.6 percentage of calcium chloride from 45.4 degrees Centigrade.

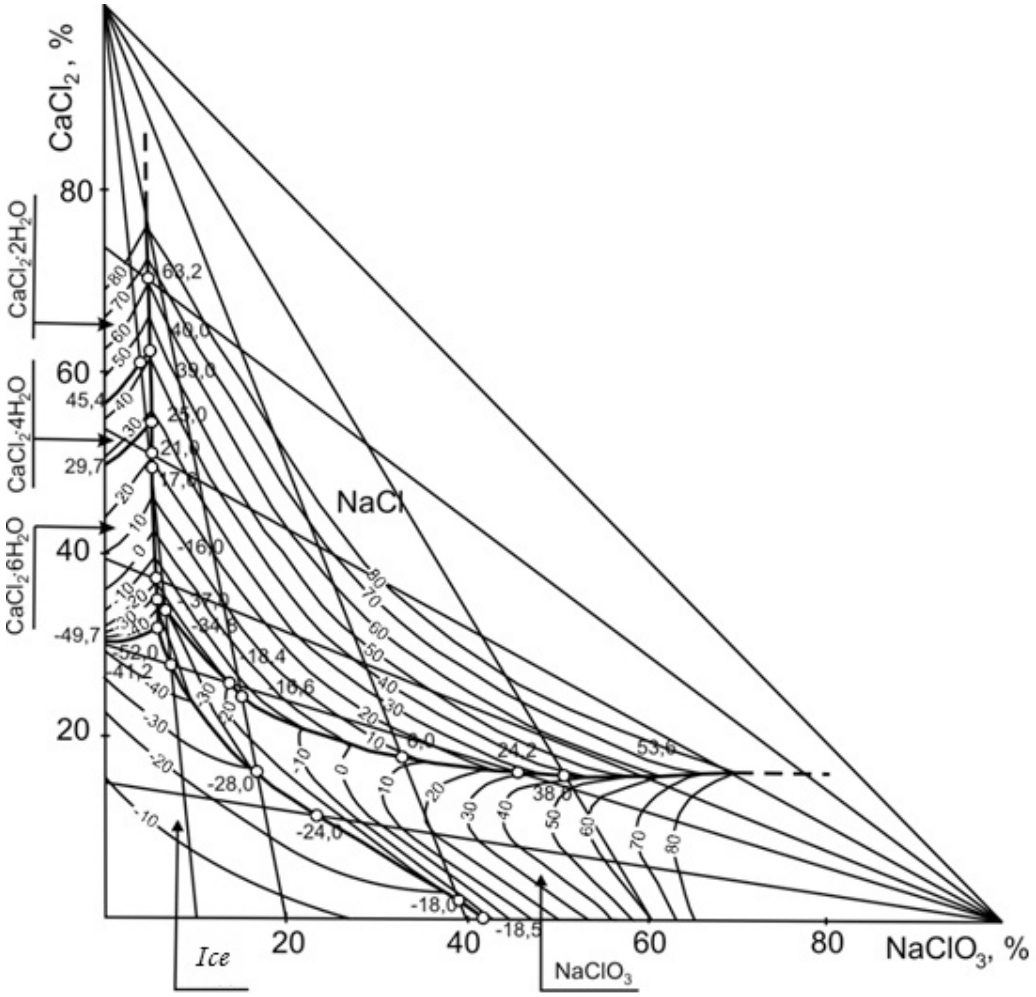

Figure 1. Polythermyc diagramme of solubility of the system $NaClO_3$ — $CaCl_2$ — H_2O

The liquidus of the binary system of sodium chlorate — water is composed of two branches of crystallizations of hard phases: ice and two-water of sodium chlorate, which eutectic at 41.9 percentage is 18.5 degrees Centigrade.

Binary systems of sodium chlorate — water and calcium chloride — water, included in the considering system, have been subject of study of several authors [7,8]. The results we obtained well-correspond with those in the literary.

Six internal sections had been studied for study of the triple system of sodium chlorate — calcium chloride — water: of them I–III were done from the side of chloride calcium — water to the top of sodium chlorate, and VI–IX from the sideof sodium chlorate — water to the top of calcium chloride. On the base of polytherms of the lateral binary systems and internal sections, polythermal diagram of solubility of the system of sodium chlorate- chloride calcium — water, had been built on which field of crystallization fields of ice, sodium chlorate, six-, four-, and two-hydrated chloride calcium and chloride sodium were delimited (figure 1.).

The specified fields converge in five triple points of joint existence of ice, sodium chlorate and chloride, and two-, four- and six hydrated calcium chloride. The compositions of equilibrium solutions and the corresponding crystallization temperatures are determined for these points (table 1).

On the polythermal equilibrium diagram, isothermal solubility curves are inflicted after every 10 degrees within the temperature range of –40 to +80 degrees Centigrade. The projections of polythermal solubility curve on the lateral side of the system of sodium chlorate — calcium chloride — water have been built.

The studies of the internal section of the quadruple mutual system had revealed that because of interaction

reactions within the system, chloride sodium is produced in hard phase as well as calcium chlorate in fluid, the field of crystallizations of the latter, due to better solubility, comparatively to other components of the system, is absent on the diagram. The analysis of the diagram of solubility of the studied system shows that the field of crystallizations of sodium chloride expands along with increasing of the temperature and concentrations of source components. The mutual system is of simple evtonic type and evident salting-out effect of sodium chlorate on sodium chloride, which increases with temperature rise, is observed within it.

Table 1. – Double and triple points of the system of $NaClO_3$ — $CaCl_2$ — H_2O

Composition of liquid phase,%			T_{cr}	Solid phase
$Na(ClO_3)_2$	$CaCl_2$	H_2O		
41.9	–	58.1	–18.5	Ice+ $NaClO_3$
39.4	1.8	58.8	–18.0	The same
24.0	13.6	62.4	–24.0	The same
17.0	16.0	67.0	–28.0	The same
7.6	27.9	64.5	–41.2	The same
	30.6	69.4	–49.7	Ice+$CaCl_2 \cdot 6H_2O$
6.0	32.0	62.0	–52.0	Ice+ $CaCI_2 \cdot 6H_2O$+ $NaClO_3$
5.6	35.0	59.4	–37.0	$Ca(ClO_3)_2 \cdot 6H_20$+ NaCl+ $NaClO_3$
5.6	37.4	57.0	–16.0	$Ca(C1O_3)_2 \cdot 6H_2O$ + NaCl
5.4	44.5	50.1	17.6	The same
–	49.8	50.2	29.8	$CaCl_2 \cdot 4H_2O$ +$CaCl_2$–$6H_2O$
6.2	54.4	39.4	25.0	$CaCl_2 \cdot 4H_2O$+ $CaCl_2 \cdot 2H_2O$+ NaCl
–	56.3	43.7	45.0	$CaCl_2 \cdot 2H_2O$+$CaCl_2 \cdot 4H_2O$
4.2	60.9	34.9	39.0	The same
5.0	62.0	33.0	40.0	$CaCl_2 \cdot 2H_2O$+ NaCl
6.9	33.6	59.5	–34.8	$NaClO_3$ + NaCl
13.4	26.0	60.6	–18.4	The same
15.3	24.7	60.0	–16.6	The same
30.8	17.5	51.7	6.0	The same
46.0	16.4	37.6	24.0	The same

This condition implies that, with temperature rise, conversion of calcium chloride with sodium chlorate in water environment flows easily and in greater depth. The results obtained show practicability of undertaking the process of conversions at temperatures above 40 degrees Centigrade. At these temperatures, minimum concentration of sodium chlorate in fluid phase, causing conversion of the calcium chloride with formation of sodium chloride and calcium chlorate makes 4.2 percent.

References

1. Umarov A. A. Kutyanin L. I. New defoliants: search, properties, use. – Moscow, Chemistry Publishers, 2000.142 p.
2. Fluid chlorate-magnesium defoliant. Specifications. Tsh.88. 16–47–2010. 12 p.
3. Schwarzenbach G., Flashka G. Complexometric titration. M. Chemistry Publishers, 1970. 360 p.
4. Kreshkov A. P. The Basics of Analytical Chemistry. M. Chemistry Publishers, 1965. Second Book. 376 p.
5. Klimova V. A. Main micro methods of the analysis of organic compositions. M. Chemistry Publishers, 1975. 224 p.
6. Trunin A. S., Petrova D. G. Visual-polythermal method/Kuybyshev Polytechnic Institute/Kuybyshev. 1977. 94 pages./AUISTI (All-Union Institute of Scientific and Technical Information) No. 584–78 Dep.
7. Manual of solubility./The responsible editor V. V. Kafarov, Moscow-Leningrad, Academy of Sciences of the USSR, 1961. V.1. Book 1, 960 p.
8. Kirgintsev A. N., Trushnikova L. N., Lavrentiyeva V. G. Solubility of inorganic substances in water. Leningrad. Chemistry Publishers. 1972. 248 p.

Pulatov Khayrulla,
Tashkent institute of chemical technology (Uzbekistan),
Chairman, Department of Industrial ecology,
E-mail: sherzod_mamatov@mail.ru

Turabjanov Sadritdin,
Tashkent institute of chemical technology (Uzbekistan),
Rector, Doctor of technical sciences, professor

Tursunov Tulkun,
Tashkent institute of chemical technology (Uzbekistan),
Professor, Department of Industrial ecology

Nazirova Rano,
Tashkent institute of chemical technology (Uzbekistan),
Professor, Department of Analytical,
physical and colloidal chemistry

Furfural based policondensation type sulfonic acid cation-exchange resin

Abstract: By polycondensation of styrene with furfural obtained new polymer which can be used as a polymeric matrix for introduction ionogenic groups. Methods of the chemical analysis, IR- and mass-spectroscopy confirm structure of obtained polymer. By sulfonation of styrene-furfural polymer obtained and researched the sulfonic acid cation-exchange resin with high chemical and thermal, and mechanical durability.

Keywords: cation-exchange resins, sorption, furfural, styrene, polycondensation, sulfonation.

Introduction

Obtaining of ion-exchange resins and areas of their application extends now fast rates. From the ecological point of view, it is defined by the practical and theoretical importance of ion-exchange polymers in various areas of a science and technics. Application of ion-exchange polymers leads to simplification of processes of division of mixes of ions, dimineralization and softening of waters, clearing and concentration of solutions of ions of colour and rare metals which contain in industrial and waste waters of hydrometallurgical manufactures.

Despite considerable number of the researches devoted to ion-exchange method of extraction and division of metals from various solutions, softening of waters, the decision of these problems continues to remain a paramount problem for a hydroiron and steel industry and water preparation. [1]. For manufacture creation ion-exchange polymers in our Republic there is a raw-material base — a waste and secondary raw materials petrochemical, chemical, agricultural, cotton scrape and the hydrolytic industry. The enterprises agricultural, cotton scrape and the hydrolytic industry of our Republic are the richest sources of cheap, accessible and large-tonnage by-products being the basic and perspective raw materials for obtaining of various polymers including ion-exchange resins with the improved indicators of the basic properties [2]. Perspectivity and validity of a choice of this product as initial raw materials for creation of ion-exchange resins it is caused by presence in its structure heterocyclic furan nucleus which allows to obtain polymers with universal thermal-chemical stability and mechanical durability. Noted also has defined statement of the given work having for an object receptions new earlier not described in the literature sulfonic acid cation-exchange resins with in advance set properties, by sulfonation of new styrene-furfural polymer. The task in view decision has allowed, to obtain sulfonic acid cation-exchange resins, possessing enough in high exchange capacity to ions of heavy metals at high thermal-chemical stability and mechanical durability [3].

On obtaining of sulfonic acid cation-exchange reins as a polymeric matrix for introduction sulphonic-acid groups we had been used polymer obtained by polycondensation of furfural with styrene. Use instead of divinyl benzene furfural is caused on the one hand by availability of the last in the conditions of our Republic, and the raised thermal-chemical stability of some cation-exchange resins, owing to presence in structure of a polymeric matrix of aromatic ring and furan cycles. For elimination of internal pressure and improvement

of kinetic properties of cation-exchange resins, polymer preliminary subjected to swelling in ethanol, dichlorethane, dimethylformamide, and the concentrated sulfuric acid. The greatest degree of swelling to 180% at T=25 °C was observed on using of sulfuric acid. It has been studied the nature influence sulphonating agent on degree of sulfonation. We had been used the concentrated sulfuric acid and 5% solution of oleum. On using of the last in the course of reaction of sulfonation of polymer is strongly crushed, i. e. becomes fragile.

On the basis of the spent researches of influence of various factors on process sulfonation of styrene-furfural polymer following conditions of reaction are established: mole parity of styrene to furfural is 1:1, duration of reaction of 6–7 hours, temperature of sulfonation 70 °C, sulfonating agent — the concentrated sulfuric acid, used preliminary bulked up polymer in concentrated sulfuric acid.

Results and Discussion

Good results of size of exchange capacity on 0.1 N solution of NaOH — 3 mg-ekv/g and on 0,1 N solution of NaCl — 3 mg-ekv/g have been received at usimg in quality of sulfonating agent the concentrated sulphuric acid. Influence of duration and temperature of reaction to degree of transformation of polymer, i. e. degree of sulfonation has been investigated. Properties of sulfonic acid cation-exchange resin obtained in optimum conditions are resulted in table 1.

The obtained data of the chemical analysis have shown, that values of bromic numbers correspond for: initial furfural — 161.0, oligomer — 178.5, outcast polymer — 175.8, i. e. values of bromic numbers of the last differs from value of bromic number initial furfural a little. According to the received data, it is possible to assert, that double connections -CH=CH- furan cycle don't participate in polycondensation reaction.

Table 1. – Physicochemical parameters of cation-exchange resin KU-FS

Indicators		Unit of measure	Mole ratio of styrene to furfural		
			2:1	1.5:1	1:1
Bulk weight		g/ml	0.68	0.6	0.5
Specific volume		ml/g	2.5	2.8	3.4
Static exchange capacity (SEC):					
on 0.1 N solution of NaOH		mg-ecv/g	3.2	3.4	3.6
on 0.1 N solution of NaCl		mg-ecv/g	2.6	2.8	3.4
on 0.1 N solution of $CaCl_2$	H-form	mg-ecv/g	2.6	3.3	4.4
	Na-form		3.8	4.4	5.2
on 0.1 N solution of $MgCl_2$	H-form	mg-ecv/g	1.6	2.0	3.6
	Na-form		2.0	2.4	4.8
on 0.1 N solution of $CuSO_4$	H-form	mg-ecv/g	0.9	1.5	3.8
	Na-form		1.0	2.0	4.2
Mechanical durability		%	99	98.5	99

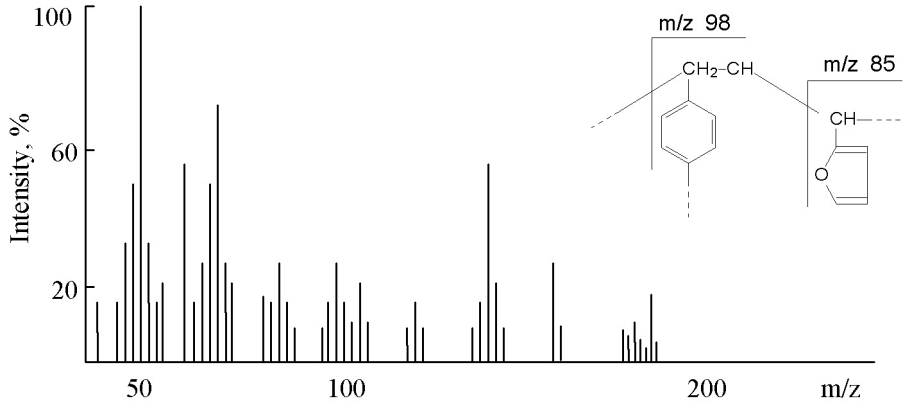

Figure 1. A mass spectrum outcast styrene-furfural polymer

Data received by the chemical analysis will be coordinated with results mass and IR-spectroscopic researches. So mass spectroscopic researches of structure of polymer show, that the available peak of an ion with mass unit equal 183 corresponds to molecular weight of an elementary link of styrene-furfural polymer. Peaks of ions with weight unit equal 85 and 98 it is described by the formula of a following structure (fig. 1).

Peaks of ions of small intensity obviously specify in presence of insignificant quantities of not reacted initial components of reaction of styrene and furfural. IR-spectra of initial furfural and the obtained outcast polymer have shown characteristic strips in the field of 1030–1050 sm^{-1} corresponding to fluctuations of interfaced double communications of a heterocycle of furfural. Strips of absorption in the field of 1690–1670 sm^{-1} corresponding aldehydic group of furfural, in a spectrum of outcast polymer are absent. The received researches allow to draw a conclusion that reaction of polycondensation of styrene with furfural proceeds under the following scheme:

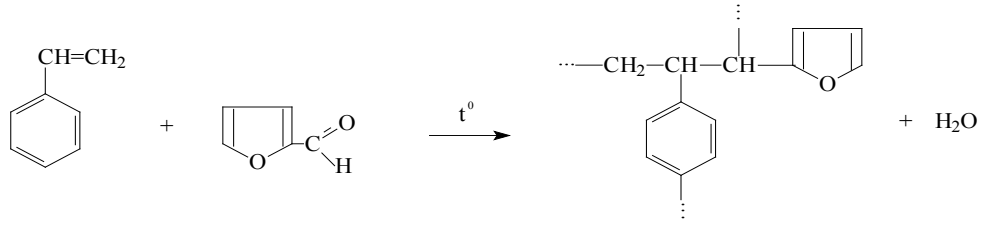

On the IR-spectrum of sulfonated polymer of a strip of absorption in the field of 1260–1150 sm^{-1}, 1060–1010 sm^{-1}, according to literary data, correspond to SO_3H-groups. Obtained sulfonic acid cation-exchange resin is monofunctional. In the IR-spectrum of sulfonic acid cation-exchange resin is absent strips of absorption in the field of 2600–3200 sm^{-1}, 3400 sm^{-1} corresponding fluctuations hydroxyl and carboxylic groups. Strips deformation fluctuation -C-H- in the field of 900–860 sm^{-1} correspond 1,3 replaced benzene ring of styrene and in 800–860 sm^{-1}–1,3,4 replaced benzene ring of styrene [4].

Proceeding from it sulfonic acid cation-exchange resin and the reaction scheme of sulfonation of styrene-furfural polymer it is possible to present structure as follows:

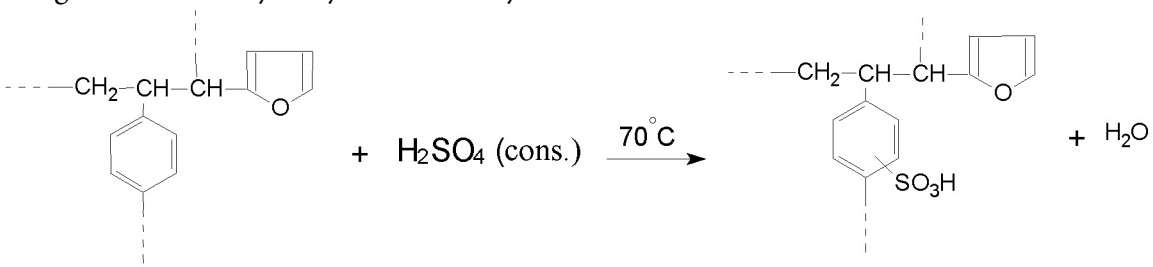

From the basic chemical properties of ion-exchange resin the great value has ion-exchange ability which characterises ion-exchange resins for the purpose of an estimation of their operational properties. Its size, basically, depends on quantity ionigenic groups of ion-exchange resin, their degrees of dissociation, and also the nature and concentration of exchanging ions.

As is known, at strong acid resins value of pH environments is practically does not influence of size of exchange capacity. Static exchange capacity of obtained sulfonic acid cation-exchange resin defined on absorption of ions of sodium as in neutral, and the alkaline environment.

Besides defined exchange capacity of cation-exchange resin in the Na-form on calcium and magnesium ions. In table 2 values of size of exchange capacity and size of a seeming constant dissociation of active groups of cation-exchange resin (pK_H) are resulted.

For an establishment of functionality and their degree of dissociation there has been made the curve potentiometric titration. The seeming constant of dissociation (pK) of ionogenic groups cation-exchange resin, found of a titration curve on Grissbakh is equal pK_H=1.8–2.2. Value of pK — a seeming constant of dissociation also testifies, that obtained cation-exchange resin concerns group of strong acid ion-exchange resins.

Table 2. – Exchange capacities of sulfonic acid cation-exchange resin

Ioniogenic group of cation-exchange resin	Exchange capacity, mg-ecv/g:					pK
	The theoretical	Under the content of % of sulphur	On titration curves	Static exchange capacity		
				on 0.1 N solution of NaOH	on 0.1 N solution of NaCl	
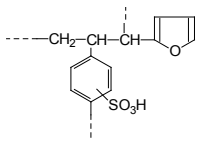	3.8	3.53	3.4–3.5	3.4–3.6	3.2–3.4	1.8–2.2

Presence of SO_3H-groups at structure of obtained cation-exchange resin is confirmed with absorption IR-spectra of sulfonated polymer. So SO_3H-groups in a spectrum of sulfonated polymer are characterised by a strip of absorption in the field of 1200 sm^{-1} that will be co-ordinated with literary data. From given tab. 2 it is visible, that size of exchange capacity of cation-exchange resin received of a curve potentiometric titration, calculated under the content of sulphur and practically differ from values of static exchange capacity a little.

As is known, in many regions of our Republic used in a life and on manufacture water has high rigidity which sometimes reaches to 12 mg-ekv/l instead of according to standards — 2 mg-ekv/l. For the purpose of use possibility cation-exchange resins KU-FS in water preparation processes, investigated its sorption ability to ions of calcium, magnesium, sodium from the waters brought by us for research from some areas of the Surkhandarya area and Karakalpakstan [5]. Cation-exchange resin is tested in H- and Na-forms. Results of researches are resulted in table 3.

Table 3. – Application of cation-exchange resin in processes of demineralization of waters

Cation exchange resin KU-FS	**Shurchi district of Surkhandarya**		**Muynak district of Karakalpakistan**		**Tahiatash district of Karakalpakistan**	
	Hardness of water, mg-ecv/l:					
	before	**after**	**before**	**after**	**before**	**after**
at H-form	12.2	4.05	10.7	3.2	11.0	3.8
at Na-form		2.2		2.5		2.4

From table 3 data it is visible, that at use of the examinee cation-exchange resina KU-FS in processes of softening waters, hardness of water after contact with cation-exchange resin corresponds to requirements of standards.

Conclusion.

By polycondensation of styrene with furfural obtained new polymer which can be used as a polymeric matrix for introduction of ionogenic groups. Methods of the chemical analysis, IR- and mass spectroscopy confirm structure of the obtained polymer. By sulfonation of styrene-furfural polymer obtained and investigated sulfonic acid cation-exchange resin, differing high thermal-chemical stability and mechanical durability. On the basis of the spent researches of optimum conditions of obtaining cation-exchange resin are defined. The structure and properties of obtained cation-exchange resin is investigated with application of chemical methods of the analysis in a combination with IR-spectroscopy, potentiometry, photocolorimetry, etc. It is established, that obtained cation-exchange resin is monofunctional, contains only sulphonic-acid group, that allows to use it in processes of an ionic exchange in neutral and alkaline environments.

References:

1. Korshak V. V., Vinogradova E. N., Nonequilibrium polycondensation, Chemistry, – Moscow, 1970. – 360 p.
2. Tadzhihodzhaev Z. A., Djalilov A. T., Synthesis and research of properties sulphonic acid cation-exchange resins on the basis of by-products of chemical enterprises, J. Applied Chem. (St.Petesburg), 9, 1998. – P. 1578–1580.
3. Turobjonov S. M., Pulatov Kh. L., Tursunov T. T., Nazirova R. A., Mutalov Sh. A.. Patent of RUz. IAP 03486. Method of preparation of cation-exchange resins.
4. Pulatov Kh. L., Tursunov T. T., Nazirova R. A., Ismailov K., Sulphonic acid cation-exchange resin on a basis of styrene-furfural polymer, J. Chemistry and chemical technology (Tashkent), Special Release, 2005. – P. 87–90.
5. Pulatov Kh. L., Tursunov T. T., Nazirova R. A., in II Republican scientifically-practical conference devoted to the 75-anniversary of acad. A. Ganiev, Termez, 2005. – P. 47–48.

Yuldasheva Mukhabbat Razzoqberdievna,
National university of Uzbekistan,
the Faculty of Chemistry
E-mail: ymuxabbat@bk.ru

Amidoalkylation of aromatic hydrocarbons by meathylol and ethylol derivatives of imides

Abstract: In the result investigation of amidoalcylation of isomeric xylenes, mesitylene and psevdocumol with N-methylolsukcinimide, β-hydroxyethylmaleinimide and β-hydroxyethyl phtalimide the amidoalkyl derivatives have been obtained and also influence of different factors on their yields and direction of investigated reactions was determined. Synthesis of amidoalkyl derivatives of aromatic hydrocarbons. The structure of the obtained compounds was determined by means of IR and NMR spectroscopy.

Keywords: aromatic hydrocarbons, xylenes, mesitylene, psevdocumol, amidoalkilation, N-hydroxyalkylimide, phtalimide.

The most part of compounds using in different branches of national economy and medicine are organic substances of aromatical number. At present time intensive and expedient investigations by search of new biologically active compounds between derivatives of aromatical substances are carried out what can be explain by their high activity and selectivity of the action. Amidoalkyl derivatives of aromatical hydrocarbons and their functional derivatives are the potential biologically active compounds. By this reason elaboration of effective methods of their synthesis and determination of the optimal conditions of caring out of corresponding reactions is one of the important tasks of the synthetical organic chemistry.

In this aspect reaction of Chernyak-Ainhorn has a large possibilities. Amidoalkyl derivatives of aromatic hydrocarbons and their functional derivatives are initial compounds for synthesis of almost inaccessible antibiotic, amines, medical preparates [1; 2]. Early possibility of amidoalkylation of benzodioxane-1,4 and isomeric xylens by N-methylol- and N-ethylol alcohols of phtalimide has been shown with aim of obtain of biologically active compounds [3; 4]. As continuation of investigation of reaction of isomeric xylenes with N-methylphtalimido and β-hydroxyethyl phtalimide in the presence of proton catalysts the interaction of tolyol, mesitylene, psevdocumol with different methylol- and ethylol derivatives of acid's imides acids has been investigated. For carrying out of amidoalkylation of aromatical hydrocarbons the initial amidoalkylating reagent- β-hydroxyethylmaleinimide (β-HEM) was synthesized from malein anhydride and monoethanolamine according to following reaction:

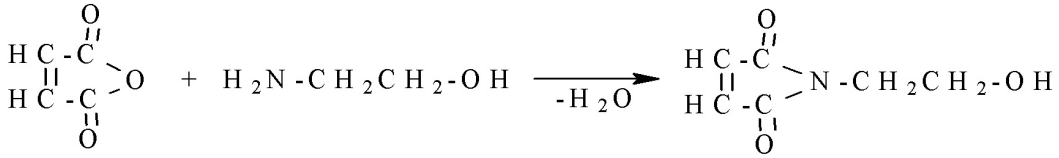

Exothermical reaction has been carried out in acetone with yield 73% at following conditions: moles ratio of initial reagents 1:1, temperature 10 °C. Reaction of o-xylene with N-ethylolmaleinimide in the presence of H_2SO_4 has carried out at heating of mixture of initial reagent and catalyst at their molar ratio 3:1:1 and at this the optimal duration of reaction was 6h. In these conditions the yield of N- (3,4-dimethylphenylethyl) maleinimide was equaled 35%; increasing of temperature of reaction has carried out to decreasing of product yield. N- (3,4-dimethylphenylethyl)maleinimide was crystal compound with T_m=172–174 °C. In it's IR-spectrum the following characterical bands (ν, sm^{-1}) were observed: 820 (1, 2, 4-threesubstituted benzol), 1645, 1614 (C–C в ArH), 3030 (=C-H в ArH), 2921 ($\nu_s CH_2$), 2857 ($\nu_s CH_3$). In NMR spectrum of this compound there are following typical signals ($CHCl_3$, DMSO, δ., м. д.) 2–2,2 с (6 H, CH_3), 2,4 с (2 H, CH_2), 6,38 с (2 H, CH_2-N), 6,6–6,8 (2 H, CH=CH), 7 м (4 H ArR_3H_3).

It was supposed that if in aromatic ring both methyl groups are in cordon in positions-1,3 them reaction of electrophilic substitution must be carried out easily and by this reason amidoalkylation of m-xylene by β-HEM in presence of H_2SO_4 was investigated and at this yield of obtained product N- (2,4-dimethylphenylethyl)maleinimide was equaled 51%. Thus in cordon interaction of methyl

groups in aromatic ring has carried out to increasing of product yield. The optimal conditions of carring out reaction are following: molar ratio of m-xylene, β-HEM and H_2SO_4 3:1:1, temperature 120 °C, duration — 2h.:

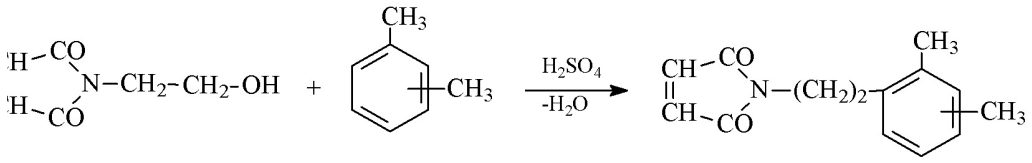

N- (2,4-dimethylphenylethyl) maleinimide was an crystalical compound with T_m = 192–194 °C (CH_3COOH) R_f= 0,7 (silyfol, system benzol: aceton = 3:2). In NMR spectrum of this compound there are following typical signals ($CHCl_3$, DMSO, б., м.д.) 0,6–0,9 с (6 H, CH_3), 4,1 с (2 H, CH_2-N), 6,2 (2 H, CH=CH), 7,2–7,7 м (4 H ArR_3H_3). Also amidoalkylation of p-xylene by β-HEM in the presence of H_2SO_4 and PFA as catalysts was carried out and at this influence on the yield of product such parameter as molar ratio of reagents and temperature was investigated; but in these conditions investigated reaction did it carried out.

Also amidoalkylation of m-xylene with other reagent –N-methylolsukcinimide was carried out. This reagent was synthesized from sukcinimide and formalin. Reaction of m-xylene with this reagent in presence of H_2SO_4 (catalyst) was carried out at 95–100 °C, molar ratio of reagents and catalyst 3:1:1 and duration 3h. Reaction was carried out with formation of 4- (N-sukcinimidometil)-m-xylene with yield 61%. Obtained compound is crystallical substance with T_m = 175–178 °C (CCl_4) In it's IR-spectrum there are following typical bands of absorption (ν, sm^{-1}): 880, 800 (1, 2, 4-threesubstituted benzol), 1580 (C–C в ArH), 3040 (=C-H в ArH), 1690 ($\nu_{C=O}$), 2750 ($\nu_S CH_2$), 2800 ($\nu_{as} CH_2$), 1400 (δCH_2). В ПМР спектре (CCl_4, C_6D_6, б., м.д.) 2,04–2,07 (CH_2CO), 3,4–3,6 т (2 H, CH_2-N), 6,5–7,4 м (3 H, $C_6H_3R_3$). Sulfur acid is the most distributed and active catalyst of alkylation of aromatic compounds. At caring out of amidoalkylation of mesitylene by β-hydroxyethylphthalimide (β-HEP) in the presence of H_2SO_4 (catalyst) at their molar ratio 3:1:3 at heating at 96–100 °C and duration of reaction 3h it was obtained entirely other product then has been expected. In result of this reaction owing to high reaction ability of mesitylene the product of it's sulfuration was obtained. Reaction of β-HEP and mesitylene in the presence KU-2 was carried out at 140–150 °C at it's duration 3h at molar ratio of compounds 3:1 and at quantity of catalyst (KU-2) 30% from mass of reaction mixture. However this reaction didn't carried out. Reaction of mesitylene with β-HEPin the presence of H_3PO_4 as catalyst also didn't carried out. Further p-tolyensulforacid was used as catalyst. Reaction was carried out at molar ratio: β-HEP, mesitylene and p-tolyensulforacid 0,01:0,1:0,015. The reaction mixture of all components in benzene was heated on water bath at 80 °C at duration 30 min.; then from dropping funnel mesitylene was added at duration 10 min. Product — (2,4,6-threemethylphenylethyl)phtalimide was obtained with yield 78%, which has T_m=125 °C (C_2H_5OH). It's spectral data are presented in table 3.

At using of 1,2,4-threemethylbenzen as substrate in the presence of tolyensulfoacid 2,4,5-threemethylphenylethylphtalimide was obtained with yield 58%. Amidoalkylation of psevdocumol was carried out at 80 °C at duration 30 min. Psevdocumol, β-HEP and p-tolyensulfocaacid were used at molar ratio 2:1:1:

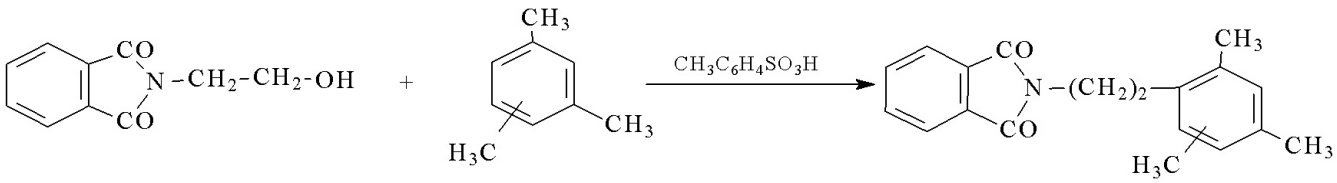

In tables 1,2 conditions of amidoalkylation are present and in table 3-some spectral data of obtained compounds.

At caring out amidoalkylation of ethylbenzen by β-HEP in the presence of H_2SO_4 (catalyst) at their molar ratio 3:1:3 at heating at temperature 96–100 °C and duration 3h 2-phtalimidoethyltolyol (8%) and 4-phtalimidoethyltolyol (45%) were obtained. In these conditions reaction of tolyol with β-HEP didn't carried out. At amidometilation of tolyol by methylolphtalimide only p-substited derivative 4- (N-phtalimidomethyl) tolyol with yield 68% was obtained.

Table 1. – Amidoalkylation of mesitylene by β-HEP in the presence 0f acid catalysts

№	Catalyst	Molar ratio of reagents: mesitylene: b	Temperature, °C	Duration of reaction, h	yield, %	T_m., °C
1	H_2SO_4	1:1:3	95–100	3	Sulfuration of mesitylene	
2	H_2SO_4	1:1:1	95–100	1		
3	H_2SO_4	1:1:0,1	50–60	0,25		
4	p-tolyolsulfoacid	1:0,2:1	75–80	3	56	124–128
5	p-tolyolsulfoacid	1:0,2:2	75–80	0,5	78	124–125
6	p-tolyolsulfoacid	1:0.2:2	95–100	1,5	47	125–128
7	p-tolyolsulfoacid	1:0,2:2	95–100	3	35	125–128

Table 2. – Amidoalkylation of psevdocymol by β-HEP in the presence acid catalysts

№	Catalyst	Molar ratio of reagents: psevdocymol: b	Temperature, °C	Duration of reaction, h	yield,%	T_m., °C
1	H_2SO_4	1:1:3	95–100	3	Sulfuration of psevdocymol	
2	H_2SO_4	1:1:1	95–100	1		
3	H_2SO_4	1:1:0,1	50–60	0,25		
4	p-tolyolsulfoacid	1:0,2:1	75–80	2	47	118–119
5.	p-tolyolsulfoacid	2:1:1	75–80	0,5	58	118–119
6.	p-tolyolsulfoacid	1:0.2:2	95–100	1,5	32	118–119

Table 3. – Data of IR-spectrums of obtained compounds

№	Name of compound	Oscillations of CH_3 groups	Oscillations of CH_2 groups		Oscillations of $N\text{-}CH_2$ groups	Oscillations of N-CO groups	Oscillations of C=C bad of aromatic ring	Deformation oscillations of CH groups of aromatic ring
			s	as				
1	2,4,5-threemethylphenyl-ethyl- phtalimide	1362 1448	2886	2952	1428	1696, 1767	1608	770–650 1,2,4,6-ternary-substituted
2	2,4,6-threemethylphenyl-ethyl- phtalimide	1371 1462	2848	2946	1430	1710, 1768	1614	883–862 1,2,3,6-ternary-substituted

References:

1. Zaugg H. E. α-Amidoalkylation of Carbon: Part I//Synthesis. – New York, 1984. – № 2. P. 85–110.
2. Zaugg H. E. α-Amidoalkylation of Carbon: Part II//Synthesis. – New York, 1984. – № 4. P. 181–212.
3. Ахмедов К.Н, Юлдашева М.Р, Фаёзова Д. Изучение взаимодействия N-метилолфталимида с бензодиоксаном-1,4//ДАН РУз. – Ташкент, 2003. – № 6. – С. 24–27.
4. Ахмедов К. Н., Юлдашева М. Р. Амидоалкилирование ксилолов//Вестник НУУз. – Ташкент, 2005. – № 4. – С. 59–62.
5. Ахмедов К. Н., Азимова Г. З., Тожибоева М. З., Юлдашева М. Р. Реакции β -гидроксиэтилфталимида с *о-*, *м-* и *п*-ксилолами в присутствии протонных кислот//Вестник НУУз. – Ташкент, 2005. – № 4. – С. 67–70.

Yakubov Yuldosh,
Junior researcher,
Laboratory of Elemental Analysis
of Institute of General and Inorganic Chemistry
of Uzbekistan Academy of Sciences
E-mail: yuldoshyakubov@mail.ru

Rakhmatkariev Gairat,
Dr in chemistry, Prof.,
Head of Laboratory of Elemental Analysis
of Institute of General and Inorganic Chemistry
of Uzbekistan Academy of Sciences;

Rakhmatkarieva Feruza,
PhD, Researcher of Institute of General
and Inorganic Chemistry
of Uzbekistan Academy of Sciences

Adsorption energetics of gases in $H_{3,25}$ZSM-5 zeolite

Abstract: Differential heats and isotherms of carbon dioxide and n-heptane adsorption in a zeolite $H_{3.25}$ZSM-5 have been measured by Tian-Calvet-type microcalorimeter and volumetric system at 303 K. Based on the data obtained, the mechanism of n-heptane adsorption and $(CO_2)_n/H^+$ complexes formation in the zeolitic matrix of $H_{3.25}$ZSM-5 is revealed. The adsorption isotherms are quantitatively reproduced by VOM theory equations.

Keywords: zeolite ZSM-5, isotherm of adsorption, carbon dioxide, n-heptane, differential heats of adsorption.

Introduction. Most of industrial processes are accompanied by the release of carbon dioxide. Being a product of combustion and greenhouse gas it has set a global society issue of a need to its capture and reuse. One way of its regeneration is the use of the adsorption process. Potential material for the selective adsorption and separation of carbon dioxide is a well-organized system of microporous zeolites. In addition, a well-defined structure of zeolites is the cause of ever-increasing use of them as a model to study the interaction of adsorbed molecules with a solid surface. Their adsorptive properties can be modified by ion exchange and Si/Al ratio change.

Earlier studies were performed mainly with zeolites containing alkaline cations [1–4]. However, zeolite $H_{3.25}$ZSM-5 is much more effective catalyst of a number of practically important processes of oil refining and petrochemical industry than in compare with its predecessors.

There are data on the adsorption of carbon dioxide in the zeolites of ZSM-5 type, which have been prepared by various physical and chemical methods [5–7]. However, hitherto there is no data reliably reflecting energy and the mechanism of adsorption of carbon dioxide in the zeolite ZSM-5 in its hydrogen form.

Less attention is paid to energetics of non-specific adsorption of interacting molecules such as hydrocarbons. Adsorptive N-alkanes are those agents that do adsorb with high energy and fill the entire sorption space of zeolites ZSM-5 in contrast, for example, with benzene, which fills only ~ 70% of the pore space of ZSM-5 [8]. Consequently, n-alkanes can be used to characterize the zeolite's channels for assessment of the sorption volume, which ultimately is the quality indicator of the adsorbent.

Objective: to study isotherms and main thermodynamic characteristics of adsorption and the mechanism of adsorption of carbon dioxide and n-heptane in zeolite of ZSM-5 type with exchangeable H^+ cations.

Subjects and Methods. Adsorption studies were carried out with zeolite $H_{3.25}$ZSM-5. As adsorptives the quadrupole molecule of CO_2 and non-polar n-heptane molecule were selected. Adsorption-calorimetric method used in this paper provides a high-precision molar thermodynamic characteristics of adsorption systems and through them to reveal the mechanism of

adsorption processes occurring in the adsorbent. As a calorimeter the microcalorimeter Tian-Calvet-type, with high accuracy and stability was used [8, 9].

Results and discussion. The curve of the differential heats of adsorption (Q_d) of CO_2 in the zeolite $H_{3.25}$ZSM-5 at 303 K is shown in Figure 1. There is a heat wave-like fall with filling increase. In adsorption (a) of 0.56 mmol/g the curve of CO_2 condensation heat (ΔHv) reaches a level equal to 27 kJ/mol. Further else ~ 0.56 mmol/g of the adsorbate still adsorbs with a heat close to the heat of condensation. The length of the first section (0.56 mmol/g) exactly corresponds to the number of protons contained in the unit of the zeolite cell. This region corresponds to the ion-quadrupole interaction of CO_2 with protons to form a monomeric complexes of CO_2/H^+ in the zeolite matrix. Considering the fact that the zeolite's matrix itself does not appreciably adsorbs carbon dioxide at a temperature of 303 K [10], a second section (following 0.56 mmol/g) can be attributed to the formation of the dimer complexes $(CO_2)_2/H^+$ in the zeolite ZSM-5 matrix. Acidic centers in $H_{3.25}$ZSM-5 are heterogeneous and differ greatly in their adsorption energy. The first section can be divided into five sub-sections in accordance with the wavelike curve Q_d. The first 0.06 mmol/g of protons possess the most strong acidic properties, the heat in this region is reduced from 60 down to 42 kJ/mol. Next 0.10 mmol/g of protons are adsorbed with energy increasing up to 43 kJ/mol, and then falling down to 35 kJ/mol. The third subsection (0.13 mmol/g) Q_d increases up to 36 kJ/mol, and falls down to 30.7 kJ/mol. In a fourth subsection (0.14 mmol/g), the heat of adsorption increases up to 33.9 kJ/mol, and falls down to 27.9 kJ/mol, and finally, a fifth subsection (0.15 mmol/g) Q_d increases up to 30.7 kJ/mol, and falls down to the heat of condensation of CO_2 equal to 27 kJ/mol. Considering the propensity of carbon dioxide to the association, the wavelike nature of the heat of adsorption change can be attributed to the imposition of the heat of adsorption of the adsorbate — adsorbate interactions on the general background of the adsorbate — adsorbent interaction.

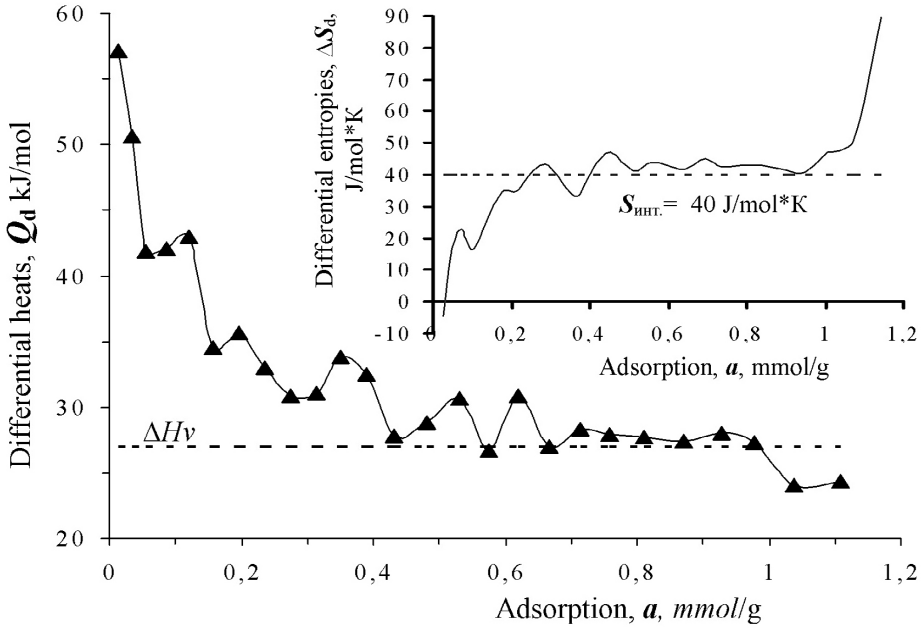

Figure 1. Differential heats of adsorption, Qd, of carbon dioxide molecules, (a), in $H_{3,25}$ZSM-5 zeolite at 303 K. The horizontal dashed line is the heat of condensation of bulk carbon dioxide. Top: corresponding differential molar entropy of adsorption. The entropy of liquid carbon dioxide is taken as zero. Dashed line is integral mean molar entropy

Equilibrium pressure for small fillings at the adsorption isotherm reaches $P/P°=4\times10^{-5}$. Before adsorption equal to ~ 0.56 mmol/g, corresponding to the total number of protons, isotherm looks like concave, with further increase in adsorption it is almost rectilinear. CO_2 adsorption isotherm for zeolite $H_{3.25}$ZSM-5 is described by two-term equation of the theory of volumetric micropore occupancy (VMOT) [11]:

$a = 1.808 \exp[-(A/12.07)^2] + 0.863 \exp[-(A/13.07)^5]$,

where a — is adsorption, mmol/g, A = RTln (P°/P) — is a transfer work of 1 mmol of gas from the surface (pressure P°) into the equilibrium gas phase (pressure P).

Differential molar entropy of adsorption of n-heptane in the zeolite $H_{3,25}$ZSM-5 is calculated for the Gibbs-Helmholtz equation and is presented in Fig. 1, top. Entropy as a whole is located above the entropy of

liquid carbon dioxide. In accordance with the curve of differential heats of adsorption the curve of ΔS_d wavelike rises to fill ~ 0.56 mmol/g, then it is constant, and closer to saturation it continues to grow. Reacting of carbon dioxide with protons in a ratio 1:1 passes at lower entropy. Integral average mole entropy (S_{int}) at 40 J/mol·K is above the entropy of liquid carbon dioxide, which indicates a significantly higher mobility of carbon dioxide molecules in the zeolitic matrix.

CO_2 adsorption time of establishment of equilibrium in the low carbon dioxide sorption filling space (up to 0.16 mmol/g) is slowed and reaches 1 hour, while the remaining space is filled within 12–18 minutes, sometimes rising up to 1 hour at a = 0.73 mmol/g and 36 min for a = 1 mmol/g.

Adsorption heats of n-heptane in $H_{3,25}$ZSM-5 zeolite at low fillings (up to 0.09 mmol/g) are reduced from 100 kJ/mol down to 90 kJ/mol (Figure 2). The cause of excessive heats at low fillings are protons, with which n-heptane reacts by means of induction effect. The total number of protons is much greater (0.52 mmol/g, according to n-heptane adsorption, which a little bit less than in case of CO_2 adsorption), however a significant contribution to the total energy of absorption is made with the protons possessing the greatest acidity.

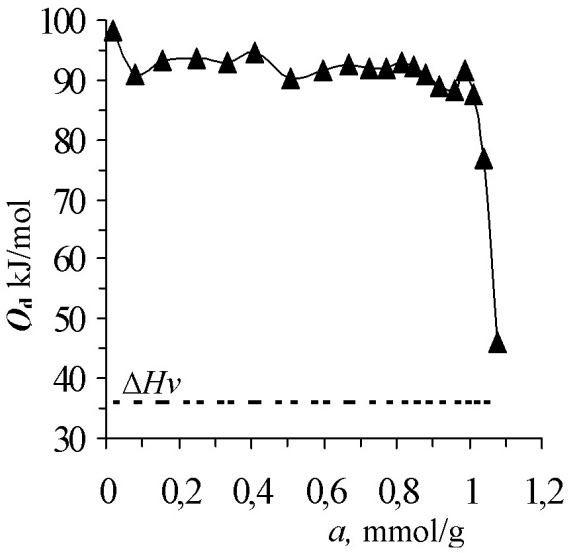

Figure 2 – Differential heats of adsorption of n- heptane in zeolite H3,25ZSM-5 at 303 K. The horizontal dashed line – the heat of condensation

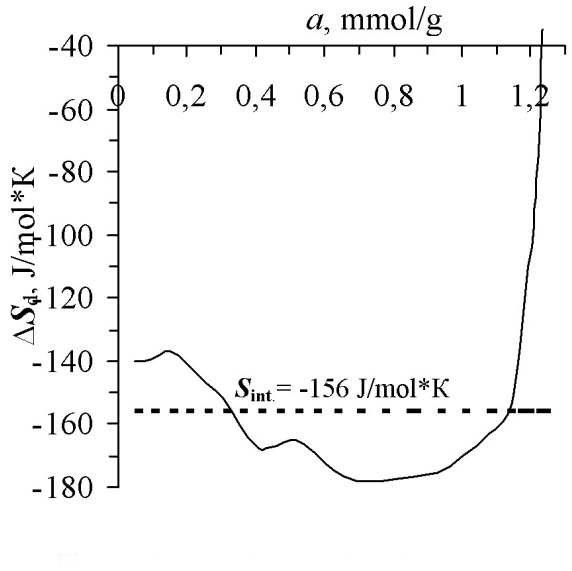

Figure 3 – Differential molar entropy of adsorption of n-heptane in zeolite H3,25ZSM-5 at 303 K. The entropy of liquid n-heptane is chosen for zero. The horizontal dashed line – is integral mean molar entropy

The heat of adsorption of n-heptane in silicalite being a pure silica analogue of ZSM-5 at the zero filling is ~ 80 kJ/mol [12], which is ~ 10kJ/mol is lower than a heat of adsorption in $H_{3,25}$ZSM-5, if one takes the overall level of the curve Q_d. Contribution to the total energy of absorption gives the dispersion component of interaction energy with the protons. In the adsorption of relatively small molecules of n-hydrocarbons it is observed an increase in the heat of adsorption due to the collective interaction between the adsorbed hydrocarbon molecules (adsorbate-adsorbate) [12]. In the case of n-heptane, as a whole, we are seeing the constancy of heat almost at the entire area of fillings (changes occur within 2–3 kJ/mol). Apparently, n-heptane molecules from the beginning of the filling are tightly packed into the zeolite channels in energetically favorable positions without remarkable interaction adsorbate-adsorbate. At the end of the process the adsorption heat abruptly drops to the heat of condensation of n-heptane.

The adsorption isotherm of n-heptane in the zeolite $H_{3,25}$ZSM-5 was investigated at a temperature of 303 K. At low coverage the equilibrium is established at a relative pressure $P/P^o=7\cdot10^{-6}$, but the saturation the adsorption comes to 1.14 mmol/g at a relative pressure P/P^o=0,58 (44.46 mm Hg). Isotherm increases linearly at a predetermined gradient to a = 0.52 mmol/g, which close to the number of protons in the unit cell, and then wave-like approaches toward the axis of adsorption. If we assume the density of n-heptane in the zeolite being the same as in normal liquid at the experimental temperature (303 K) and if we calculate the volume occupied by a molecule of n-heptane at saturation, we find that the n-heptane takes ~0.16 cm^3/g of the sorption volume of $H_{3,25}$ZSM-5 zeolite that is ~11% less than the real volume (0.18 cm^3/g). This

result indicates the presence of amorphous phase.The adsorption isotherm of n-heptane in the zeolite $H_{3,25}$ZSM-5 is described by the three-term equation VMOT [11]:

$$a = 0.633\exp[-(A/26.72)^9] + 0.337\exp[-(A/0.337)^5] + 0.351\exp[-(A/2.44)],$$

where a — is adsorption mmol/g, $A = RT\ln(P°/P)$ — is a transfer work for 1 mmol gas from the surface (pressure P°) in the gas phase equilibrium (pressure P).

Differential molar entropy of adsorption of n-heptane in the zeolite $H_{3,25}$ZSM-5 is presented in Figure 3. Curve ΔS_d throughout the region of filling the zeolite channels by n-heptane is less than the entropy of the liquid n-heptane and has a very low negative values. Entropy being less than 0.52 mmol/g, which corresponds to the number of protons attributable to unit cell of $H_{3,25}$ZSM-5, does not change much with the filling and, on average, is at the level of ~ –132 J/mol·K. This confirms the thesis put forward earlier that from the process' beginning the molecule are tightly localized likely at the intersection of straight and zig zag channels, where the protons are located. However, the length of the intersection is 0.54 nm, and the length of n-heptane is 1.15 nm, therefore part of n-heptane should go to straight or zig zag channel sections. The length of the straight channel and the intersection is 0.99 nm, and a zig zag and intersection is 1.21 nm. Given that the molecule of n-heptane in the zig zag channel is more tightly constricted by the framework atoms than the molecule in the straight channel [13], it can be assumed that the adsorption is initially take place in the intersections and zig zag channels, then in the intersections and the straight channels.

Time of adsorption equilibrium of n-heptane in the zig zag channels and intersections zeolite $H_{3,25}$ZSM-5 (up to a = ~ 0.52 mmol/g) is too slow. It is reduced from more than 8 hours down to ~4 hours. At this stage the adsorption takes place in the zig zag channels and intersections. In the final stage of adsorption it is installed in less than 1 hour.

Conclusion. The adsorption isotherms of carbon dioxide and n-pentane in $H_{3.25}$ZSM-5 satisfactorily is described by the equations VMOT. CO_2 and n-heptane's heat of adsorption in $H_{3.25}$ZSM-5 at zero filling are 60 and 91 kJ/mol, respectively. The differential heats of adsorption of CO_2 have two segments corresponding to the formation of two types of adsorption complexes with one and two molecules of carbon dioxide on average. The wavelike nature of the heat of adsorption is due to the imposition of heat of interaction of adsorbate-adsorbate on the general background of heat of adsorption of adsorbate-adsorbent. Condition of n-heptane in the zeolite matrix is solidlike but condition of carbon dioxide is closer to gaseous one. The heat of adsorption of n-heptane varies little with filling and is in average equal to ~ 91 kJ/mol. Induction component contribution to the total energy is about 12 kJ/mol. Adsorption of n-heptane in the channels is greatly slowed.

Adsorbent for ~ 11% consists of an amorphous phase.

References:

1. Rakhmatkariev G. U., Kurbanov S. D. Adsorption of Water Vapors on NaZSM-5 Zeolite//Uzb. Khim. Zh. – 2007. – №. 6. – P. 10–31.
2. Boddenberg B., Rakhmatkariev G. U., Viets J. Thermodynamics and Statistical Mechanics of Ammonia in Zeolite NaZSM-5//Ber.Bunsenges Phys. Chem. – 1998. – V. 102, – P. 177–182.
3. Boddenberg B., Rakhmatkariev G. U., Greth R. Statistical Thermodynamics of Methanol and Ethanol Adsorption in Zeolite NaZSM-5//J. Phys. Chem. B. – 1997. – V. 101. – P. 1634–1640.
4. Mentzen B. F., Rakhmatkariev G. U. Host/Guest Interactions in Zeolitic Nonostructured MFI Type Materials: Complementarity of X-ray Powder Diffraction, NMR Spectroscopy, Adsorption Calorimetry and Computer Simulations//Uzb. Khim. Zh. – 2007. – № 6. – C. 10–31.
5. Bonelli B., Onida B., Fubini B., Arean Otero C., Garrone E. Vibrational and Thermodynamic Study of the Adsorption of Carbon Dioxide on the Zeolite NaZSM-5//Langmuir – 2000. – № 11, – V. 16, – P. 4976–4983.
6. Bas Delphine., Goursot Annick., Weber Jacques., Wesolowski Tomasz. Theoretical Study of the Adsorption of Carbon Dioxide on the Alkali Metal Exchanged ZSM5 Zeolite Using Orbital-Free Embedding Formalism//Chimia – 2004, – V. 58. – № 7–8. – P. 47.
7. Harlick P. J. E., Tezel F. H. Adsorption of Carbon Dioxide, Methane, and Nitrogen: Pure and Binary Mixture Adsorption by ZSM-5 with SiO [2]/Al [2]O [3] Ratio of 30//Separ. Sci. and Technol. – 2002. – №. 1. – V. 37. – P. 33–60.
8. Mentzen B. F., Rakhmatkariev G. U. Host/Guest Interactions in Zeolitic Nanostructured MFI Type Materials: Complementarity of X-ray Powder Diffraction, NMR Spectroscopy, Adsorption Calorimetry and Computer Simulations//Uzb. Khim. Zh. – 2007. – № 6. – P. 10–31.

9. Rakhmatkariev G. U. Mechanism of Adsorption of Water Vapor by Muscovite: A Model Based on Adsorption Calorimetry//Clays and Clay Minerals. – 2006. – Vol. 54. – P. 423–430.
10. Dubinin M. M., Rakhmatkariev G. U., Isirikyan A. A. Heats of Adsorption of CO_2 on High-silicon Zeolites ZSM-5 and Silicalite//Izv. AN SSSR, Ser. Chem. –1989. – № 11. – P. 2636–2638.
11. Rakhmatkariev, G. U., Isirikyan, A. A. Complete Description of the Adsorption Isotherm by the Equations of the Volumetric Micropore Occupancy Theory//Izv. AN SSSR, Ser. chem. – 1988. – № 11, – P. 2644–2645.
12. Dubinin M. M., Rakhmatkariev G. U., Isirikyan A. A. Adsorption Energetics of Hydrocarbons on Silicalite//Izv. AN SSSR, Ser. Chem. – 1989. – № 10. – C. 2333–2335.
13. van Koningsveld, H., Tuinstra, F. The Location of p-Xylene in a Single Crystal of Zeolite H-ZSM-5 with a New, Sorbate-Induced, Orthorhombic Framework Symmetry. – 1989. – V 45 – P. 423–431.

Contents